Understanding the Sf9 – Baculovirus Expression Vector System: Exploring the Metabolic Basis of the Cell Density Effect through Nuclear Magnetic Resonance Spectroscopy and Flow Cytometry Analysis of Fluorescent Protein Accumulation

by

Alexander Pritchard-Oh

A thesis

presented to the University of Waterloo

in fulfilment of the

thesis requirement for the degree of

Master of Applied Science

in

Chemical Engineering

Waterloo, Ontario, Canada, 2020

Author's Declaration

I hereby declare that I am the sole author of this thesis. This is a true copy of the thesis, including any required final revisions, as accepted by my examiners.

I understand that my thesis may be made electronically available to the public.

Abstract

It is well established that the baculovirus expression vector system (BEVS) can serve as an important, effective production system for various biologicals. Knowing that the cells can serve as a production platform is useful, but there are still gaps in the knowledge of how best to manipulate this platform. There is room for improvement in both the upstream (in the design of the viral vector) and the downstream (in the optimization of the operating conditions of the growth culture) portions of the process. This thesis aimed to look at the latter group. In particular, this thesis was aimed to assess some gaps in the knowledge of the metabolic requirements of the cells as they grow and are infected.

It was found that higher growth was easily achievable, but growth rate drops beyond a certain cell density regardless of frequency of media exchange. Cell density could be extended to 44 x 10^6 cells/mL, up from the 12 x 10^6 cells/mL achieved in batch culture, but that cell growth rate would drop beyond 15 x 10^6 cells/mL, regardless of the frequency of media replacement. Exploring this idea, it was determined that oxygenation did not appear to be the limiting condition here, as growth rate did not drop in a separate experiment wherein the cells were intentionally deprived of oxygen, down to less than a third of the concentration in the control culture.

By using Proton Nuclear Magnetic Resonance (^{1}H-NMR) spectroscopy to measure metabolite levels, eight compounds not studied in the literature were identified to drastically vary over the culture. Fructose, fumarate, hypoxanthine, and succinate all accumulated in the culture while choline, inosine, uracil, and uridine were depleted. While these compounds also did not seem to perfectly correlate with the drop in growth rate, it was hypothesized that they may be important for supporting growth and productivity.

Fluorescent proteins were used to give a simple analogue for the productivity of the cells. However, a methodology for quantifying the productivity was needed. As an initial test, ^{1}H-NMR revealed that the composition of the baculovirus stocks were very similar to normal spent media, and with

the volumes of baculovirus stock required for addition to the culture will have minimal impact on bulk culture composition (although this does not rule out the influence of minor compounds undetectable via ^{1}H-NMR). However, only the GFP virus was deemed to be useable based on the characteristics of its fluorescence.

It was found that as a standard infection progressed, two distinct populations appeared. Testing found that these populations corresponded to healthy and compromised cells, respectively. The average fluorescence of only the healthy population increased with time whereas the average fluorescence of the compromised population was centered on a comparatively low value. Averaged together, this was a net 20% decrease in average fluorescence between 48 and 72 hpi. Individually, however, the healthy cells had roughly 60% higher fluorescence at 72 hpi than at 48 hpi. Therefore, a proposed "improved" gating method was chosen, where only the healthy population was looked at as a reporter for the progression of the infection. Overall, it was deemed that this would provide more useful information about the quality of the infection.

Lastly, the goal was to improve the productivity of cell cultures under practical conditions. To this end, baselines for the production of a fluorescent protein were established, and then the methodology developed was used to assess the effect that the compounds of interest identified would have on the productivity of cells infected under suboptimal conditions. It was found that, as expected, the average fluorescence of a culture decreased when moving from low cell-density infection to high cell-density infection conditions (a 50% decrease). Interestingly, at low cell-density, media replacement was detrimental to fluorescent protein production (a 20% decrease) while at high cell-density, media replacement was beneficial (a 33% increase). An experiment was set up according to Placket-Burman design in order to effectively probe the effect of the 8 compounds of interest, and it revealed succinate to have an overwhelmingly negative impact on fluorescent protein production. However, it was suggested that the majority of this effect seemed to have come from pH change rather than inherently from succinate itself.

Acknowledgements

I would like to thank Marco Quattrochocchi and Emma Dare for their assistance in learning the best practices for NMR profiling. I would also like to thank Mark Bruder for his thorough help with learning to carry out the infection and flow cytometry processes. I also owe a major thank you to Dr. Marc Aucoin for his patience and valuable insights on insect cell culture and the baculovirus production platform.

Table of Contents

List of Figures

List of Tables

List of Abbreviations

AcMNPV – *Autographica californica* Multiple Polynucloehedrovirus

ANOVA – Analysis of Variance

BEVS – Baculovirus Expression Vector System

CHO – Chinese Hamster Ovary

CSI – Chemical Shape Indicator

DSS -4,4-dimethyl-4-silapentane-1-sulfonic acid

FSC – Forward Scatter

GFP – Green Fluorescent Protein

HPI – hours post-infection

^{1}H-NMR – Proton Nuclear Magnetic Resonance

MOI – Multiplicity of Infection

MR – Media Replacement

PB – Placket-Burman

PBS – Phosphate-buffered saline

PFA – Paraformaldehyde

PI – Propidium Iodide

Sf9 – *Spodoptera frugiperda* cell-line 9

SFM – Serum-Free Media

SSC – Side Scatter

TCA – Tricarboxylic Acid

TOI – Time of Infection

Chapter 1 – Introduction

The research described in this thesis is about trying to overcome the cell density effect. That is, when infected at high cell densities, the cells become less productive than at low cell densities. Feeding is the general approach to bypass the cell density effect, and it has seen good results in the literature. However, there is often a lack of specificity in the feeding regimes described. It is known that some of the macro molecules in media are useful to feed to mitigate the cell density effect– glucose, for example. Others groups have had high success with yeastolate. A common concern, however, is that yeastolate is poorly defined. As such, a more targeted feeding approach would be more favourable. This thesis will aim to identify compounds of interest and determine their efficacy in alleviating the cell density effect.

Section 1.1 – Background

Insect cells have become an important platform for the production of biologics because of the versatility of the system. Insect cells may be infected with a recombinant baculovirus carrying foreign genes, and in this manner a culture of growing insect cells may be readily induced to begin production of a product of interest under controlled conditions and time frames. Usually, this insect cell – baculovirus expression vector system (BEVS) will make use of two powerful promoters, polh and p10, to drive very high levels of expression of the gene of interest (George et al., 2015).

From *Spodoptera frugiperda* ovaries, two main cell lines have been derived: Sf9 and Sf21. These cells are easy to work with, grow to moderately high densities in batch cultures when using commercial media, and are very susceptible to infection by *Autographa californica* Multiple Nucleopolyhedrovirus (AcMNPV), of the baculovirus family (Kwang et al., 2016; Sandhu et al., 2007). Furthermore, these cell lines will innately carry out a degree of glycosylation in proteins produced using BEVS (Demain et al., 2011). This is a point of interest for many recombinant proteins since they need to carry a specific glycosylation pattern in order to produce a therapeutic product with a high activity, stability, and efficacy. While the innate glycosylation machinery present in these insect cell lines may not quite be on the level of

complexity of some other mammalian hosts, it is far more developed than that found in unmodified prokaryotic cell lines (Demain et al., 2011). As such, for proteins requiring a more humanized glycosylation pattern, fewer auxiliary genes will need to be introduced to promote the desired glycosylation pathway than would be required for prokaryotic lines.

While the insect cell system is attractive, it is not without drawbacks. It has been commonly observed since the development of the system that the so-called "cell-density effect" plays a major role in limiting the system's efficiency. This principle dictates that when cultures beyond a certain cell density are infected with baculovirus, the amount of product that each cell will individually output decreases (Bock et al., 2011; Huynh et al., 2013; Radford et al., 1997). This is also known as the specific productivity. As such, with regards to the overall titer, there exists a breakeven point beyond which the positive effect of increasing the number of productive cells is unable to outweigh the negative effect of having each cell be less efficient individually.

Due to the low production efficiencies exhibited at high cell-densities in this system, it may be that the metabolites that would have been consumed for the formation of product were instead redirected to increase the number of suboptimally-performing cells. It has been reported in literature that this effect can be alleviated to a certain degree by "feeding" the cells with supplemental blends of essential nutrients and substrates (Bock et al., 2011; Huynh et al., 2013; Klöppinger et al., 1990; Radford et al., 1997). Apart from simple sugars and amino acids, studies so far have not determined any other recognizable targets in cell media that may be contributing to this effect, which is why there is a need to deepen our understanding of the nutrient requirements.

In recent years, Nuclear Magnetic Resonance (NMR) has been increasingly utilized as a means of gaining information not typically reported on profiles of metabolite consumption or production (Mulukutla et al., 2017; Petiot et al., 2015; Sokolenko et al., 2013; Weljie et al., 2006). ^{1}H-NMR specifically can be used for identification and quantification of sugars, amino acids, and a number of other

compounds of moderate complexity, while $^{13}C/^{15}N$-NMR can be used in the tracking of labelled specific carbon/nitrogen compounds through a cell's metabolic pathways (Drews et al., 2000; Sokolenko et al., 2014; Weljie et al., 2006). On the other hand, most reports on systems using Sf9 cells have made use of traditional metabolite analyzers such as a YSI Biochemical Analyzer System, which is simple to use but is limited to the quantification of glucose, glutamine, glutamate, and lactate (Bernal et al., 2009; Klöppinger et al., 1990; Mendonça et al., 1999; Rodrigues et al., 2013). Others have made use of chromatography for analysis of amino acid concentrations (Bernal et al., 2009; Doverskog et al., 1998; Radford et al., 1997). On the whole however, these methods are rather limited in scope and alternatives should be explored to broaden the set of compounds that can be studied. For example, Monteiro et al. used liquid chromatography-mass spectrometry to analyze a large set of 63 uncommon internal metabolites (Monteiro et al., 2014). Similarly, Mulukutla et al. used liquid chromatography-mass spectrometry, gas chromatography-mass spectrometry, and ^{1}H-NMR together to identify 18 accumulating compounds, 9 of which were further studied as inhibitors of cell growth that had not been studied previously (Mulukutla et al., 2017). Recent advancements in the analytical tools available provide an important opportunity to revisit the consumption and production patterns of a wider variety of metabolites. By identifying additional nutrient limitations of the Sf9 system, more effective strategies for feeding and media formulation can be developed. This will support production at increasingly high cell densities to generate higher overall titers. In addition, this will reduce the size of reactor vessels that will be needed to meet production demands, resulting in cost savings.

Section 1.2 – Literature Review

Section 1.2.1 – Cell Culture – Modes of Operation

Batch growth is the most common method of running any cell culture. Cells are added to a growth media and allowed to utilize the available nutrients as required. While this method is simple, it also means that in terms of production, the results may not be optimal, depending on the goals set for the process. In comparison, feeding strategies allow for improved cell densities and increased production of

recombinant proteins by supplying nutrients which are being depleted. Feeding strategies for cell cultures typically take on one of two forms: fed-batch or perfusion (Butler, 2005; Tapia et al., 2016).

In a fed-batch culture, a concentrated solution of essential components is added to the batch culture. This may be done in a pulse format (i.e. a spike of the feed concentrate) or in a continuous format (i.e. a slow and steady pumping of feed into the bioreactor). Fed-batch is a method that is convenient in its simplicity; nutrient levels are either measured or predicted based on models, and when specific, key components are close to depletion, the feed is added to replenish their levels in the culture (Butler, 2005).

In the Sf9 system, the power of fed-batch culture was realized early on. For a baseline, typical growth of Sf9 cells in commercial Sf-900 III media will give a maximum cell density of 12-14 x 10^6 cells/mL. In a stable Sf9 cell line, Jardin et al. (2006) found that fed-batch culture could push the cells to 28 x 10^6 cells/mL and roughly double the product yield compared to batch culture. Elias et al. (2000) also found a massive increase in cell density due to feeding, pushing cells to a maximum density 52 x 10^6 cells/mL and were able to maintain the specific productivity of the β-galactosidase up until a density of 14 x 10^6 cells/mL. Chan et al. found that a fed-batch culture will allow for a productive infection up to 7 x 10^6 cells/mL and results in a 2-3 times increase in product yield (Chan et al., 1998). In a bovine kidney cell system, a fed-batch strategy was found to improve productivity 40-fold (Pohlscheidt et al., 2008). For other examples, a review by Tapia et al. covers a number of other cases in which fed-batch cultures lead to significant improvements in final product yields (Tapia et al., 2016).

However, there are also several drawbacks to the fed-batch cultivation method. Firstly, the culture volume necessarily increases as the feed is added. This can end up causing sizing limitations based on the bioreactor being used, its mixing capabilities, and its oxygenation capabilities. Secondly, since a concentrate is added in this feeding method, the osmolality of the solution will increase. If the osmolality is not taken into account, the conditions may quickly become unfavorable towards cell growth

(Chan et al., 1998; Ikonomou et al., 2003). Thirdly, a fed-batch culture can run into difficulties if there is accumulation of inhibitory by-products. In general, lactate and ammonia are the most common examples of metabolites of concern that accumulate during cultivation. In Sf9 cultures, neither of these compounds tends to reach inhibitory levels (Ikonomou et al., 2003). However, there may be other accumulating inhibitory compounds that have not yet been identified (Mulukutla et al., 2017). Lastly, fed-batch cultures have limitations in the production of certain types of recombinant proteins. If the target product is particularly unstable, it may tend to degrade if it is kept within the bioreactor for extended periods of time (Butler, 2005; Jardin et al., 2006; Maranga et al., 2003). Since the contents of a fed-batch reactor would not be collected and purified until the very end, this could result in very significant levels of product loss.

Rather than batch culturing, continuous methods of feeding such as perfusion may be a more effective alternative. Perfusion systems involve the continuous addition of feed to the bioreactor as well as a continuous flow of spent media out of the bioreactor, while cells are retained within the reactor. Perfusion cultures are advantageous in that the cells are maintained at fairly consistent conditions, and product can be separated from the outlet media continuously (Butler, 2005; Kretzmer, 2002). Extraordinarily high cell densities are also achievable in perfusion systems, far outreaching the limits of batch cultures. In a Chinese Hamster Ovary (CHO) cell system, for instance, a perfusion set-up allowed the cell-density to reach in excess of 200 x 10^6 cells/mL (Clincke et al., 2013(a); Clincke et al., 2013(b)). In the Sf9 system, Klöppinger et al. (1990) also observed an improvement when using perfusion, measuring 23% more baculovirus production compared to a control batch culture infection.

It is noteworthy that there exists an alternative method of production using insect cells than BEVS as described prior to this. In BEVS, the cells are infected with baculovirus and subsequently die, releasing the product of interest alongside new copies of the baculovirus. This is a transient infection system. As an alternative however, a new, stable cell line can be established by transfecting and inserting the genes of interest directly into the genome. In this case, the cells do not die as a consequence of

replicating the inserted genes. This allows the culture to continue far beyond the typical three-day productive period observed with BEVS, since in this case the bioreactor may be operated such that cells are maintained at a constant density (Butler, 2005; Jardin et al., 2006). For stably expressing cell lines, perfusion allows for great potential compared to what might be observed in a standard BEVS culture. For comparison, in a stably expressing Sf9 system, Jardin et al. (2000) found that perfusion was able to maintain a productive culture for 43 days, to be overall 8 times more productive than a fed-batch system, and to be 22 times more productive than a standard batch system.

In summary, perfusion is beneficial for its ability to generate very high product yields. However, while perfusion allows for a much better control of the cellular environment, it also adds a layer of complexity to the process. To achieve extremely high densities, a cell-separation device is required to ensure that cells are retained within the bioreactor (Clincke et al., 2013(a); Clincke et al., 2013(b); Tapia et al., 2016). While this would reduce the amount of resources wasted in generating additional biomass, further effort would be required to ensure that the separation device does not become blocked or fouled during operation (Clincke et al., 2013(a); Clincke et al., 2013(b); Tapia et al., 2016). As well, the perfusion rate must be carefully controlled to follow the changes in cell density in the bioreactor (Bock et al., 2011).

There are a few other limitations to consider when operating a cell culture in a perfusion mode. Typically, the perfusion system will be more difficult to operate than a comparable fed-batch system, and will be much more equipment-intensive in its nature. As a consequence of this, the set-up and monitoring required in a perfusion system make it difficult to run multiple experiments in parallel. Therefore, fed-batch systems are highly effective for exploratory work in testing the response of a cell culture to different conditions, while perfusion systems have the potential to be more effective once a set of optimal operating conditions has been found.

Section 1.2.2 – History of Insect Cell Media Formulation

In 1956, Wyatt developed an insect cell media similar to the composition of the natural blood of insects, proposing that this would adequately address the metabolic requirements of the cell culture (Wyatt, 1956). In 1962, Grace developed an insect cell media as a modified version of Wyatt's media (Grace, 1962). Since then, Grace's media has been the starting point from which many of the other commercially available insect cell media have been developed. IPL-41 (Weiss et al., 1981), TNM-FH (Hink, 1970), and Sf-900 II are all examples of improved medias that were formulated in order to boost either the growth or productivity of their cell cultures. More recent formulation projects have tried to refine the media, aiming for blends that are both serum-free and, more challengingly, are of a more consistent, chemically-defined composition. Serum-free media are desirable because they remove a portion of the cost from production, and because they do not require animal products which can lead to potential regulatory issues. While the non-chemically-defined blends are effective at promoting cell growth, the drawback is that they can experience variability between lots (Quattrociocchi, 2017). Sf-900 III is one of the current standard media used in an academic setting, and is used in the experiments in this thesis. However, while this formulation is serum-free, it still contain a chemically-undefined yeastolate as a component. Therefore, there is a strong interest in trying to identify the unknown compounds contained in the yeastolate blend that make it beneficial to use as a media additive (Quattrociocchi, 2017).

Besides the issues with identifying the key components needed in media to effectively promote the growth of cells, one other challenge has to do with the osmolality of the media. The base media must not contain metabolites at too high of a total concentration or else the conditions may end up outside of the tolerable range of the cells. Similar to the case for mammalian cells, osmotic stress is important to consider for Sf9 cells and acts as a constraint on the media formulations that can successfully be used. Fortunately, Sf9 cells are more resistant than mammalian cells; they prefer conditions around 320 mOsm and can tolerate conditions in excess of 400 mOsm. Outside of their tolerated range they can be drastically hindered in terms of growth and viability (Agathos et al., 1990; Ikonomou et al., 2003). Sf-

900 II media is observed to have an osmolality of 360 mOsm, and over the course of a standard batch culture this will drop to 290 mOsm (Rosinski et al., 2000). This is beneficial as it allows for some degree of feeding without overshooting the tolerable range in which the cells can function effectively.

Section 1.2.3 – Insect cell metabolism

Besides the ideal composition of the starting media, in order to develop effective feeding strategies for improved production, many groups have had an interest in the metabolic consumption patterns of the insect cell culture. Very early on, it was established that glucose and glutamine were key carbon sources for the culture, and feeding of these two compounds could drastically improve productivity (Wang et al., 1993). Besides these two metabolites, however, the metabolic requirements of insect cells were not well understood at first.

Both Bédard et al. and Chan et al. performed screening experiments, and collectively found that yeastolate, a broad mixture of amino acids, and a lipid emulsion could be used together for supporting cell growth (Bedard et al., 1994; Chan et al., 1998). This was a good starting point, but the undefined nature of these blends led to an interest in determining which specific components were necessary for growth.

Bédard et al. looked at several other carbohydrates that could potentially be used to feed the cells as well as some of the organic acids involved in the TCA cycle (Bédard et al., 1993). They found that Sf9 cells preferentially grow on glucose, and can be supported by fructose or maltose, but not sucrose (Bédard et al., 1993). Mendonça et al. tested several feeding strategies and discovered that glucose depletion causes the cells to switch to consuming fructose and lactate, but this pathway was inefficient, reducing cell growth rate (Mendonça et al., 1999). Additionally, they found that glutamine levels need to be carefully controlled. Depletion of glutamine can reduce the cell growth rate and maximum cell density achieved, however, an excess of glutamine can also cause the same effects if glucose is not present in similar levels of excess (Mendonça et al., 1999). As well, two amino acids, methionine and tyrosine, can be fed to delay the onset of cell death (Mendonça et al., 1999). Maranga et al., (2003) once again found

that the depletion of glutamine was linked to cessation of cell growth. Doverskog et al., (1998) found in Sf9 cells that cysteine, another amino acid, was important in preventing cell death, but that it could also be biosynthesized from methionine if enough is present in the media. They observed that this pathway appeared to shut off in cultures that were near the end of the exponential growth phase. Jardin et al. tracked glucose and amino acid levels during the production phase both by a baculovirus infection of Sf9 cells and by a stably-producing Sf9 line, and found noteworthy differences in metabolism between the two production methods (Jardin et al., 2006). All amino acids except for alanine were consumed to varying degrees, but the stable cell line consumed aspartate at half the rate of the BEVS culture, and was noted to liberate a small amount of glutamate from glutamine towards the end of culture (Jardin et al., 2006).

Expanding on these studies and attempting to do something more complex, Bhatia et al., (1997) attempted to generate a metabolic flux analysis model to describe Sf9 metabolism, measuring 27 extracellular metabolites to predict 45 internal fluxes. They predicted that an excess of nutrients in the starting media leads to a lower efficiency in generating cell biomass, with their low amino-acid content media generating approximately 2.7-fold more biomass for the amount of carbon-containing compounds consumed (Bhatia et al., 1997). As a noteworthy limitation of this study however, Bhatia et al. did state that the inclusion of yeastolate in both of their media formulations provides small amounts of numerous compounds such as nucleotide derivatives, and that if these were incorporated into their simulation it could potentially switch the direction of some predicted metabolic flows (Bhatia et al., 1997). Similarly, Bernal et al. attempted to use metabolic flux analysis to describe 52 internal metabolites based on 24 external metabolite measurements (Bernal et al., 2009). Interestingly, they predicted that as the cells enter the early stationary phase of their growth, the TCA cycle slows to approximately 50% of that during the exponential growth phase (Bernal et al., 2009). They observed that this did not correlate with depletion of any amino acids or fed sugars, and predicted that it could be related to a combination of oxygen limitations and pyruvate consumption for the formation of alanine (Bernal et al., 2009). Later,

Bernal et al. additionally looked at enzyme and metabolite levels related to the energy carriers generated throughout their metabolic pathways, and noted that the cells enter a state of lower energy metabolism with the onset of the cell-density effect, and that pyruvate and α-ketoglutarate supplementation can help cells maintain a highly energetic state required for effective baculovirus replication (Bernal et al., 2010).

Interestingly, beyond compounds that act as simple building blocks, Ikonomou et al. suggested that the Sf9 cells themselves may additionally secrete growth factors while the cells multiply, and these can enhance cell growth (Ikonomou et al., 2004). Isolating and using these inherent growth factors would provide an endogenous pathway to improve growth without using exogenous, undefined blends of growth factors such as fetal bovine serum (FBS) that were frequently favored in early media formulations.

Section 1.2.4 – Infection Parameters

While the insect cell – baculovirus expression vector system (IC-BEVS) presents an extremely powerful tool for the production of recombinant proteins, it has many complex parameters that need to be considered for optimal performance. When infecting, one must consider the multiplicity of infection (MOI), time of infection (TOI), peak cell density, oxygen demand, and nutrient uptake demands (Klöppinger et al., 1990; Maranga et al., 2003; Shabram & Aguilar-Cordova., 2000; Tapia et al., 2016; Wang et al., 1993; Wong et al., 1994).

MOI, TOI, and peak cell density are all closely tied together. The MOI describes the ratio of baculovirus particles needed to fully infect the cells in the culture, and is described in terms of infectious particles per cell. However, an MOI of 1 does not necessarily indicate that each cell will be infected by a single viral particle. Rather, each cell is capable of being infected by multiple different viral particles and a Poisson distribution will describe the likelihood that each cell is infected one or more times (Shabram & Aguilar-Cordova., 2000). As such, to ensure a >95% infection rate (that is, ensure that at least 95% of cells receive at least one infectious particle), an MOI of at least 3 is required (Shabram & Aguilar-Cordova., 2000).

TOI is the point during the growth phase at which cells are infected. Because of the cell density effect, this is an issue of critical importance. The cell density effect is a condition that appears in a number of different systems. This term describes the observed effect that when cells are infected above a certain density, the specific productivity of the cells decreases (Bock et al., 2011). As such, even though the number of cells present in the culture can be pushed higher, increasing the density may in fact result in a net loss in total amount of product since each cell produces less. In a batch culture of Sf9 cells, the onset of the cell density effect appears to be dependent on the culture conditions. Radford et al. reported that the cell density effect begins at 5×10^6 cells/mL in Sf-900 II media, whereas the onset is at 2×10^6 cells/mL in IPL-41 media (Radford et al., 1997). Huynh et al. on the other hand observed that the onset of the cell density effect begin as early as 1×10^6 cells/mL (Huynh et al., 2013). Taken together, this suggests that the quality of the growth media plays a very important role in maintaining a productive culture. If the culture is seeded at especially low cell densities or if less-rich initial media (IPL-41, for instance) is used, then the onset of the cell density effect can be expected to occur at low cell densities.

Peak cell density is a result of both MOI and TOI. Due to the nature of the baculovirus infection, once a cell is infected it will become unable to divide. As such, when cells are infected at a high MOI, they all rapidly become incapable of further division and the cell density peaks soon after. This is termed a synchronous infection. However, if cells are infected at a low MOI instead, it is termed an asynchronous infection since the baculovirus only stops the growth of a few cells initially while the remainder continue to grow freely. Then, once the initial batch of infected cells finish replicating baculovirus and release them, this second wave of virus will infect a greater portion of the cells. In this manner, the peak cell density achieved before division ceases will be considerably higher than if a high MOI had been used at the same TOI (Maranga et al., 2003). There are advantages to using this sort of approach. As was found by Mena et al., by infecting at a low MOI and moderate TOI, the end protein titer can be increased relative to a high MOI and high TOI infection (Mena et al., 2010). Additionally, there is less concern about the amount of baculovirus stock that needs to be added to carry out the

infection. This makes scaling up considerably easier, reduces the concern that the addition of the baculovirus stock may be diluting the media and hindering the cells in that manner, and cuts down on the number of defective baculovirus particles produced (Maranga et al., 2003).

Oxygenation is important during the cell growth phase and it becomes even more critical during infection to ensure high productivity. It has been reported that during infection the oxygen demand of the cells will significantly increase (Wong et al., 1994). It has also been found that if the cells are deprived of oxygen, the productivity of the infection will decline. In one paper, it was found that if oxygen tension dropped below 20%, virus production would drop by more than 50% (Klöppinger et al., 1990). Looking at the problem from the other direction, Wang et al. demonstrated a 200% improvement in volumetric yield simply by maintaining >35% oxygen tension (Wang et al., 1993), and Scott et al. demonstrated drastic differences in both cell growth and recombinant protein production when spinner flask stirring rate (and consequently oxygen transfer) was changed from 30 to 80 rev/min (Scott et al., 1992). In another experiment by Jäger and Kobold, it was demonstrated when Sf9 cells were inoculated with virus under conditions of insufficient surface aeration, they had little to no productivity (Jäger & Kobold, 1995). They proposed that the low oxygen state may prevent the virus from replicating or may prevent its entry into the cell, though they did not further delve into the specific mechanisms involved (Jäger & Kobold, 1995).

Regarding the consumption of nutrients after infection, the requirements seem to vary from case to case. It is generally accepted that the cell density effect is dependent on the levels of various nutrients in the culture because media replacement or similar feeding strategies can mitigate a large portion of the cell density effect (Bock et al., 2011; Huynh et al., 2013; Klöppinger et al., 1990; Radford et al., 1997). For instance, carrying out media replacement before infection, Klöppinger et al. observed a 28% increase in baculovirus production relative to the control (Klöppinger et al., 1990). Similarly, Radford et al. observed that complete media replacement eliminates cell density effect up to 10×10^6 cells/mL in Sf-900 III media, or 6×10^6 cells/mL in IPL-41 media (Radford et al., 1997). The exact impact of nutrient

depletion and restoration on the cells is not fully characterized, but Huynh et al. suggest that it may tie into mRNA and viral DNA replication (Huynh et al., 2013; Huynh et al., 2014). Interestingly, once cells reach their maximum density and enter the stationary phase, they seem incapable of a productive infection even if metabolites are replenished (Maranga et al., 2003). In a large industrial-scale culture however, media replacement is not as easy as in a lab-scale cultures. In this case, perfusion would act as a more straightforward method than the work-intensive centrifugation and manual media replacement strategies that might be adapted for small cultures. The amount of product produced appears to vary for different viral constructs (Bock et al., 2011).

In designing any system for production using BEVS, all of these parameters must be carefully optimized to ensure that the operation proceeds efficiently. MOI and TOI must be chosen based on the goals and constraints of the system. The balance between the two parameters determines the volume of virus required to start the infection, the synchronicity of the infection, and the peak cell density that the culture will achieve. Hence, the selection made can have a major impact on the extent of the cell-density effect experienced by the culture. Oxygenation can become an extremely limiting factor, particularly in the case of large-scale cultures. In a research environment at bench-scale, this may not cause problems, but can severely limit the efficiency of the production based on the physical constraints of the bioreactor used. Lastly, the feeding strategy must be optimized based on the other conditions. Several choices must be made about which metabolites to add, at what time they should be added, and whether they should be added continuously or in spikes. These decisions must also take into account the effect that it will have on the culture with respect to the osmolality, and should also assess the monetary cost associated with adding these additional feed streams. Together, this presents a very complex issue where some of the goals compete against one another.

Section 1.3 – Hypothesis

There are three main hypotheses for this thesis, and one will be explored in each of the three results chapters. The first hypothesis is that the cell growth is limited by metabolites besides the sugars and amino acids reported in literature, and that restoring or removing these metabolites will have large impacts on the maximum cell density achievable.

The second hypothesis is that fluorescent proteins will be able to serve as an effective reporter of cell productivity after infection. In order to address this hypothesis, the second results chapter will aim to establish a methodology for effectively tracking the production of fluorescent proteins in Sf9 cells.

The final hypothesis is that the metabolites that are not reported on in literature will serve as key components related to the cell density effect, and that the replenishment or removal of these compounds can drastically help (or hinder) the specific productivity of an infected Sf9 culture.

Section 1.4 – Research Objectives

The work described in this thesis will aim to address the hypothesis by focussing on two main areas of study. The first set of experiments will aim to better understand the insect cell system alone. That is, the system will first be studied without any infection. ^{1}H-NMR characterization of spent media will support the evaluation of a feeding strategy to improve the maximum growth that can be achieved with a standard media formulation, and to determine the factors that lead to the cessation of cell growth.

The second area of study will consider the insect cells when used together with baculovirus as a production platform. In this case, ^{1}H-NMR will again be used to identify any metabolites that are consumed or produced at exceptional rates. These will then be used as targets to attempt to work around when running the infection. The goal in this case will be to establish the baselines that are to be expected of the cell-density effect, and then to attempt to exceed the performance of these baselines through a targeted feeding strategy.

Chapter 2 – General Methods

Section 2.1 – Sf9 Cells

For all experiments, Sf9 cells were used. Stocks of the cells were stored in liquid nitrogen and were less than 20 passages old, and maintenance flasks were only kept until the cells reached passage 40. To prevent contamination, the cultures were maintained in a sterile environment until their time of disposal. Whenever a new culture was thawed, it was passaged at least twice before being used in experiments. This was done to allow for the components used in the freezing media (dimethyl sulfoxide and fetal bovine serum) to be diluted out of the culture, as they could potentially confound any experimental findings.

Section 2.2 – Media

Cells were grown in the commercial media Sf-900 III (ThermoFisher Scientific, Gibco ™ Sf-900™ III SFM, Catalog number: 12658019). This is a serum-free formulation developed for insect cells with Sf9 cells being the primary target, and it requires addition of no additional components before use. Cell cultures typically grew to densities around 12 x 10^6 cells/mL if seeded at 0.5 x 10^6 cells/mL in this media.

Section 2.3 – Culture Conditions

Cells were grown in suspension cultures in shake-flasks. These flask cultures were stored in an incubator set to 27^{o}C and 130 RPM. The incubator was not supplied with any enriched oxygen environment. Typically, maintenance cultures were grown in 125 mL shake-flasks. These cultures had a working volume of 25-35 mL and were split each time the cell density reached roughly 3 x 10^6 cells/mL. Each new passage of the culture was seeded at 0.5-0.6 cells/mL in fresh Sf-900 III media, warmed to 27^{o}C. For a healthy culture in this media, approximately three days were required between passages.

When setting up for experiments, flasks were seeded at 0.6 x 10^6 cells/mL in 125 mL flasks. To ensure that there was enough culture volume to allow for the collection of samples without harming the health of the culture, a 30-35 mL working volume was used unless there was an inadequate volume of culture to seed from. These flasks were always seeded from the same mother culture. The mother flask used was typically the ongoing maintenance flask. In general however, if six or more flasks were required for the experiment, a larger culture would be grown to seed these new flasks instead of the usual maintenance flask. These larger seed cultures were grown in a 250 mL shake flask with the working volume kept around 60 mL. As before, the new flasks were all seeded from this mother flask once the culture reached a cell-density of roughly 3 x 10^6 cells/mL.

Section 2.4 – Cell Counts and Viability Analysis

Any time that the cell density and viability of a culture was analyzed, a small sample of cell culture was withdrawn from its flask. Under most circumstances, if the cells were only to be counted, a 500 µL sample was withdrawn and placed into a 1.5 mL tube. Otherwise, if the sample was to be further analyzed via ^{1}H-NMR or flow cytometry, a 1 mL sample was withdrawn instead. The tube was inverted a few times to ensure the cells were well-distributed throughout, and 100 µL of the cell suspension was transferred to one well of a 96-well plate. An additional 100 µL of a 0.5% solution of Trypan Blue dye in a phosphate-buffered saline (PBS) was added to this well and then mixed by pipetting up and down repeatedly. A 10 µL sample of this cell and dye mixture was removed and pipetted into one side of a glass hemocytometer slide. The same process was repeated for the other side of the slide. The slide was then inserted into a Countess II automated cell counter (ThermoFisher Scientific, Cataologue Number: AMQAX1000), the field was moved to an area free of any bubbles or obvious slide contaminants, and the automated count was performed. The cell density and viability measures from this slide were recorded, and then the same counting process was performed on the other side of the slide. The results from the two sides of the slide were averaged and recorded. The slide was then washed with water, sprayed with ethanol, and left to dry. If the two counts were ever extremely different from one another, the tube of

cells was then mixed again by inverting, a new well of the 96-well plate was loaded with cells, and the process from that point was repeated.

Section 2.5 – Baculovirus Constructs

There were two different baculovirus constructs used for carrying out infections. Both constructs were designed to produce different fluorescent proteins. The first construct produced eGFP, a green fluorescent protein, while the other construct produced mKate2, a red fluorescent protein. These two proteins have been shown to have emission spectra that are substantially different, having little overlap at their respective peak emission wavelengths (Haimovich, 2012)

Section 2.6 – Virus Amplification

Cells were grown in a large flask seeded at 0.5 x 10^6 cells/mL in Sf-900 III media. The flask was incubated for approximately 3 days, until the culture reached a cell-density around 3 x 10^6 cells/mL. The culture was then split equally into two 50 mL Falcon tubes (VWR International, Falcon® Centrifuge Tubes, Polypropylene, Sterile, Corning®, Catalogue number: CA21008-940) and centrifuged with a relative centrifugal force (RCF) of 120 for 10 minutes to pellet the cells. The suggested target for infection was a culture at 1.5 x 10^6 cells/mL in 75% fresh media. Therefore, the cells and media from one tube were discarded entirely, and half of the supernatant media in the other tube was also discarded. The cells in the remaining tube were pipetted gently to re-suspend in the spent media and were then transferred back into the culture flask. Fresh media with a volume three times that of the remaining cell suspension was then also added into this flask and mixed gently. Lastly, a small volume of the chosen virus was then added to the culture, and the culture was returned to the incubator for several days. Past experience of lab members using the P1 virus stocks suggested a ratio of 100 µL of virus stock per 30 mL of culture was sufficient to ensure a low MOI infection for effective viral amplification.

Note that here, P1 refers to a first-passage amplification stock of baculovirus. In this stock, an initial viral isolate is amplified to a usable volume. In this way, the P1 stock becomes much more usable, allowing for numerous infections with the same viral construct. Similarly, the stock generated as described by the method in this section would be a P2 stock, or a second-passage amplification. Generating a P2 stock allows for a large volume of the virus to be used across many different infections. However, it comes with the drawback of accruing mutations over the course of the amplifications, leading to a potential deviation from the original viral isolate.

The culture was assessed for cell viability over the next several days. When the viability dropped below 80%, the virus was collected. The culture was centrifuged at 800 RCF for 10 minutes to pellet as much of the cellular debris as possible. The debris of the cell pellet was discarded and the remaining baculovirus-containing supernatant was-filtered by passing it through a 0.45 μm filter (VWR International, VWR Syringe Filters, Catalogue number: 28145-505). This P2 baculovirus stock was stored in a clean Falcon tube and stored in a darkened fridge at 4^{o}C until use.

Section 2.7 – Endpoint Dilution Assay

After generating a batch of P2 baculovirus stock, a fresh batch of cells was grown in a flask. Cells were collected at a cell density of roughly 2 x 10^6 cells/mL and were then diluted in fresh media to a cell-density of 2 x 10^5 cells/mL. 100 μL of cell suspension were added to each well in 11 rows of a 96 well plate. The final row of the plate was instead filled with plain Sf-900 III media instead. Cells were given time to adhere to the plate by placing the plate in a humid box inside an incubator, free of agitation. During the time while the cells were adhering, successive 10-fold dilutions of virus stock were prepared in 1 mL volumes. The first dilution (10^{-2}) was prepared by adding 10 μL of virus stock to 990 μL of fresh media. The second dilution (10^{-4}) was prepared by taking 10 μL from the first dilution (10^{-2}) and adding it to 990 μL of fresh media. In sequence, each of the following dilutions (from 10^{-5} to 10^{-10}) were

prepared by taking of 100 µL of the previous dilution and adding it to 900 µL of fresh media. An example of this serial dilution process is demonstrated in Figure 1.

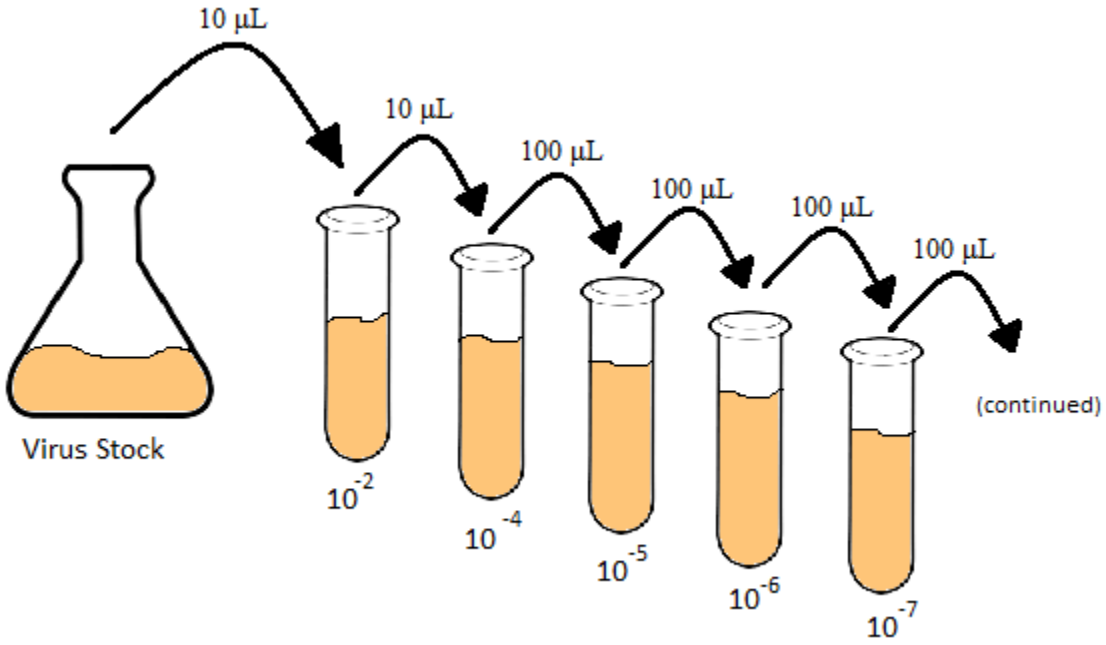

Figure 1: Serial dilutions of virus stock for endpoint dilution assay.

After these dilutions were prepared, the 96-well plate was removed from the incubator. Each of the prepared dilutions was assigned to one row of wells (i.e. 12 wells), and for each dilution (skipping the 10^{-2} dilution), 10 µL of the virus stock was added to each well in the row. The plate was then returned to the humidified box in the incubator for 5 days. After the 5 day incubation period, the cells were then examined under a fluorescent microscope to detect the occurrence of infection in cells. For each dilution (i.e. one row), the number of wells containing at least one fluorescent cell was recorded. These results were then used to compute the "Tissue Culture Infective Dose" (TCID50), a measure of the dosage of virus required to effectively infect half of the cultures.

The TCID50 is interpolated from the proportional distance (PD) between two dilutions bounding the 50% infection point. This is based on the formula:

$$PD = (A - 50)/(A - B) \quad (1)$$

Where A is the percentage of cells infected in the more concentrated virus stock, and B is the percentage of cells infected by the more diluted sample of virus stock. PD represents the distance between these two points and the 50% infection mark.

$$log_{10}(TCID50) = log_{10}(Dilution\ A) - PD \quad (2)$$

The viral titer is calculated based on the volume of virus dilution added to the well, and is given as:

$$titer = (1/TCID50)/0.01\ mL \quad (3)$$

This gives the titer on a per mL basis. The TCID50 does not have units, as it is instead itself reflective of the dosage that would be expected to infect half of the cultures it is introduced to. That is, the titer is reported in TCID50 units/mL. However, it is more useful to consider the adjusted titer based on the number of plaque-forming units (pfu) per mL, which is in turn based on the Poisson distribution chance of a viral particle to infect a single cell. The Poisson distribution is given by the equation:

$$P(k\ events) = \frac{\lambda^k * e^{-\lambda}}{k!} \quad (4)$$

Where P is the probability of the event occurring, k is the number of events occurring, and λ is the average number of events that are expected to occur. Again, the TCID50 is reflective of a dose that should, statistically, infect half of the cells that it is introduced to. Examined another way, it is also equivalent to the probability for a cell to not receive any viral particles upon infection. In the Poisson probability model, this titer can be defined as P(>0) = P(0) = 0.5. The number of events of interest is 0 because that is easy to work with, and as such the equation becomes:

$$P(0\ events) = \frac{\lambda^0 * e^{-\lambda}}{0!} = \frac{1 * e^{-\lambda}}{1} = 0.5 \quad (5)$$

Rearranging the formula and solving for λ:

$$\lambda = -\ln(0.5) \approx 0.69 \quad (6)$$

Considered in another way, this indicates that by multiplying the TCID50 by 0.69, would give the number of plaque forming units per mL. If the stock is diluted and added to multiple cultures, the λ = 0.69 means that roughly half of cultures will be infected (with some receiving no viral particles, some receiving one particle, and others more than one particle). In a single culture, however, each cell would receive an average of 0.69 viral particles; the cells that do receive virus become able to form the plaques, hence the term plaque-forming units.

$$titer\ [pfu/mL] = 0.69 * TCID50 \quad (7)$$

Section 2.8 – Standard Infection Protocol

For most experiments, the infection was performed similarly with slight changes to the culture conditions. Cells were seeded into shake flasks, each with a working volume of 30-35 mL, at 0.5 x 10^6 cells/mL. The cells were grown until the desired cell-density (chosen based on the criteria desired for each specific experiment), and then the virus of choice was added. An MOI of 5 was used in all experiments to ensure a synchronous infection. In all cases, the infection was tracked once per day for the next three days. At the same time each day, a 1 mL sample was collected to assess the cell-density and viability of the culture. The remainder of the sample would then be prepared for analysis by flow cytometry and ^{1}H-NMR, as outlined in the following sections.

Section 2.9 – Flow Cytometry – Methods, Setting, Type

The flow cytometer used was a BD FACScalibur Flow Cytometer (BD Biosciences, Mississauga, ON, Canada). To analyze each sample of baculovirus-infected cells, 1 mL samples of infected cells were

centrifuged at 100 RPM for 10 minutes. The supernatant media was pipetted off of the cell pellets and frozen at -80^{o}C for later analysis by ^{1}H-NMR. The media removed from the cell pellet was replaced with 1 mL of a 2% solution of paraformaldehyde (PFA) in PBS. The cells were re-suspended in this PFA solution and kept in a dark, tinfoil-covered box for 15-30 minutes. Because each sample of cells was typically from cultures grown to relatively high cell densities, each sample of cells was then diluted by adding another 4 mL of PBS and transferred into a flow cytometer tube. For cells infected at low cell-densities, a 1:1 dilution in PBS was sufficient, instead. These samples were then taken over to the flow cytometer for analysis. For analysis of cells, four parameters were recorded. Forward scatter (FSC) and Side scatter (SSC) were of interest for all samples, and the fluorescent channel of interest depended on the baculovirus construct being used. FSC is commonly associated with the size of the measured cells, and SSC is commonly associated with the granularity of the cells, or how much the laser is reflected off of particulates within the cell. In the FL1 channel (530 nm wavelength), eGFP fluorescence was expected to be visible. Similarly, in the FL3 channel (670 nm wavelength), mKate2 was expected to be visible. The voltage settings used for all experiments are shown below in Table 1. The samples were all run using the machine's high flowrate setting, and the acquisition was set to collect 10000 events (instances of detectable signals). If the number of events recorded per second exceeded 1000, either the flowrate would be adjusted or the dilution would be increased by adding more PBS to the sample, and the acquisition was rerun using the new conditions. The number of events recorded per second was limited in this manner to reduce the occurrence of coincidental readings.

Table 1: Flow cytometer settings

Parameter	**Voltage**
FSC [Lin-scale]	E1 [Gain = 6.55]
SSC [Lin-scale]	300 [Gain = 1]
FL1 [Log-scale]	258
FL2 [Log-scale]	258
FL3 [Log-scale]	304

After data acquisition, the samples were interpreted and gated using FlowJo software (Treestar Inc., Ashland, OR, United States). The default outputs of the software are histograms when only one of the measured parameters is selected, and density plots when two different parameters are assigned to the x and y-axes. All gating was performed manually in the software, and was done by arbitrarily drawing in a gate over of one of the histograms or density plots that would effectively capture the densest area (or areas) of detected events. For gating in the FSC vs. SSC density plots, events in the bottom left corner (low FSC and low SSC) were excluded from the gate due to their high likelihood of being noise inherent to the flow cytometer. For consistency, when a gate was created, the same gate was applied to all samples that would be compared within a group, and its shape was iteratively adjusted by hand until it was adequately suitable for all of the samples it was applied to.

Section 2.10 – ^{1}H-NMR Methods

^{1}H-HMR spectroscopy for metabolite analysis has been previously described (Sokolenko et al., 2013, 2014). Briefly, to prepare each sample for analysis, 630 µL of the media of interest was gently mixed with 70 µL of a DSS (4,4-dimethyl-4-silapentane-1-sulfonic acid) internal standard in D_2O and loaded into a 5 mm NMR tube (New Era Enterprises Inc., Catalogue number: NE-UL5-7). These NMR tubes were checked for scratches or cracks in the glass prior to loading, especially in the lower portion of the tube. If significant damage was found, the tube was not used as these scratches may interfere with the data acquisition. After an experiment was completed, all tubes were washed out and dried to be reused.

These samples were run individually on a Bruker Avance 600 MHz spectrometer with 1D-NOESY pulse sequence, 1 s pre-saturation pulse, 100 ms mixing time, and 4 s acquisition. The sample wobb and water suppression were carried out manually, but the 1D and 3D gradient shimming were run automatically. Each sample scanned via ^{1}H-NMR was later analyzed using NMR Suite 8.4 (Chenomx Inc., Edmonton, Canada). Baseline and phase correction were performed automatically in the package,

and were checked for the fit manually. The chemical shape indicator (CSI) needed to be adjusted manually to get an effective fit of the DSS internal standard peak. When fitting these DSS peaks, the peak around the 0.60 ppm region was assigned the highest priority followed by the peak at 0.00 ppm, and the CSI was adjusted until both of these peaks fit reasonably well with a concentration value of 0.490-0.510 mM. For the analysis, 43 metabolites were selected for profiling. The software was used to attempt an automatic fitting of these selected metabolites, and was generally capable of attempting to fit roughly half of them. The remainder were fit manually, and the automatically fit ones also required a second, manual pass to be checked for accuracy.

Chapter 3 – Factors Limiting High Cell-Density Culture Growth

^{1}H-NMR spectroscopy can be used as a fingerprint, but in conjunction with a database of known compounds spectra, it can also be used to track many specific compounds. Sf-900 III is an excellent media that supports growth and infection of insect cells, and is known to contain undefined constituents including yeastolate. When Sf-900 III was subjected to ^{1}H-NMR and the spectra examined using Chenomx NMR Suite 8.4, 43 compounds were identifiable.

Section 3.1 – Deconvolution of the ^{1}H-NMR spectra

In previous work dealing with CHO or Sf9 cultures, the Aucoin lab grouped compounds based on their ability to be profiled. Every compound in the database has a specific set of peaks corresponding to its structure. Some of these sets of peaks appear in areas of very low convolution. That is, the peaks in that window all correspond to a single compound. An example of this is shown in Figure 2.

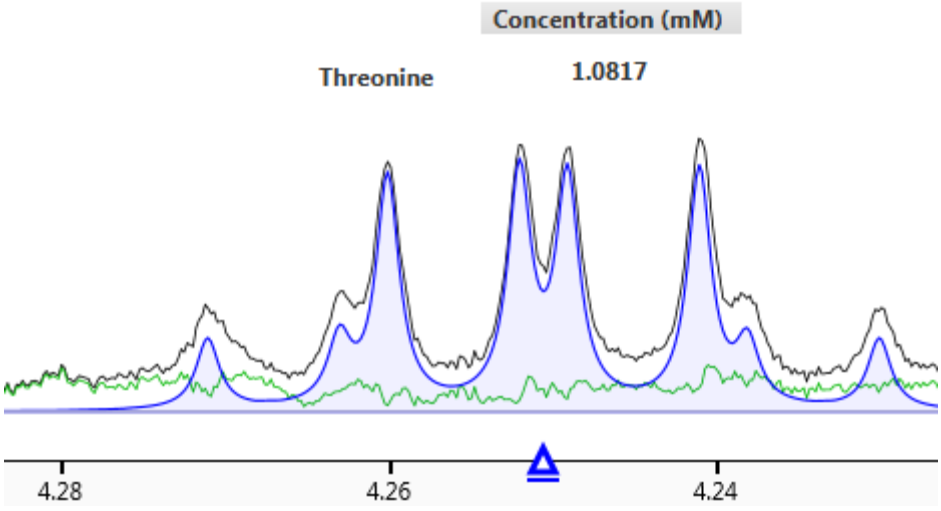

Figure 2: ^{1}H-NMR profile of a non-convoluted peak cluster (The black line is the original scan output from the ^{1}H-NMR. The blue area is the peak shape of the compound loaded from the database after adjusting the scaling for concentration. The green line is the result of subtracting the profiled compounds from the original scan. Compounds are fit sequentially in order to try to make the resultant green subtraction line flat.)

The areas featuring only a single compound in one space are prioritized first when profiling. In other areas however, the profiling is not as simple due to the convolution of peaks from multiple different compounds. While the fitting is more difficult in these areas, the goal remains the same: to fit compounds in a manner that gives the flattest subtraction line, or in other words, to establish the compound concentrations that would have been able to generate that particular set of ^{1}H-NMR peaks. Typically, for each compound this involves choosing the least convoluted of all peaks in its spectra, fitting the phase-shift (leftwards or rightwards drift) based on those first, and then making subsequent adjustments to the concentrations (size of the peaks) afterwards as required. An example of a highly convoluted peak cluster is shown in Figure 3.

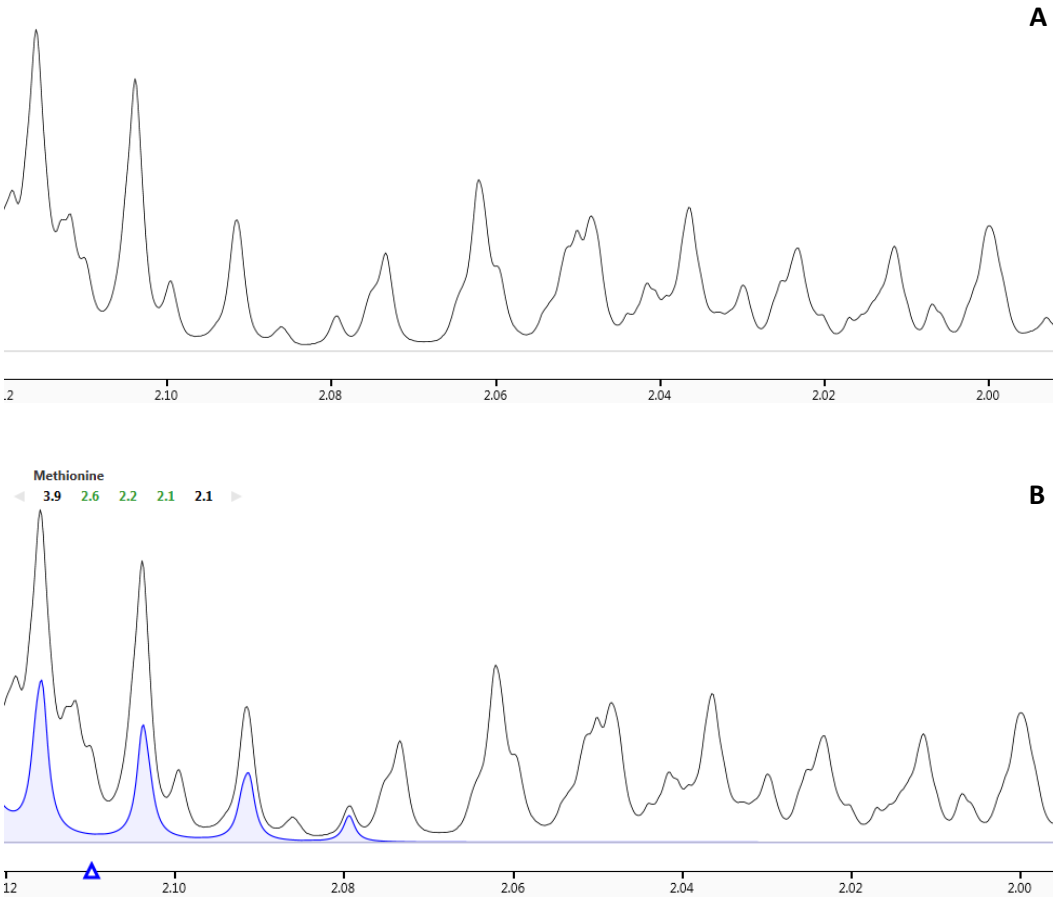

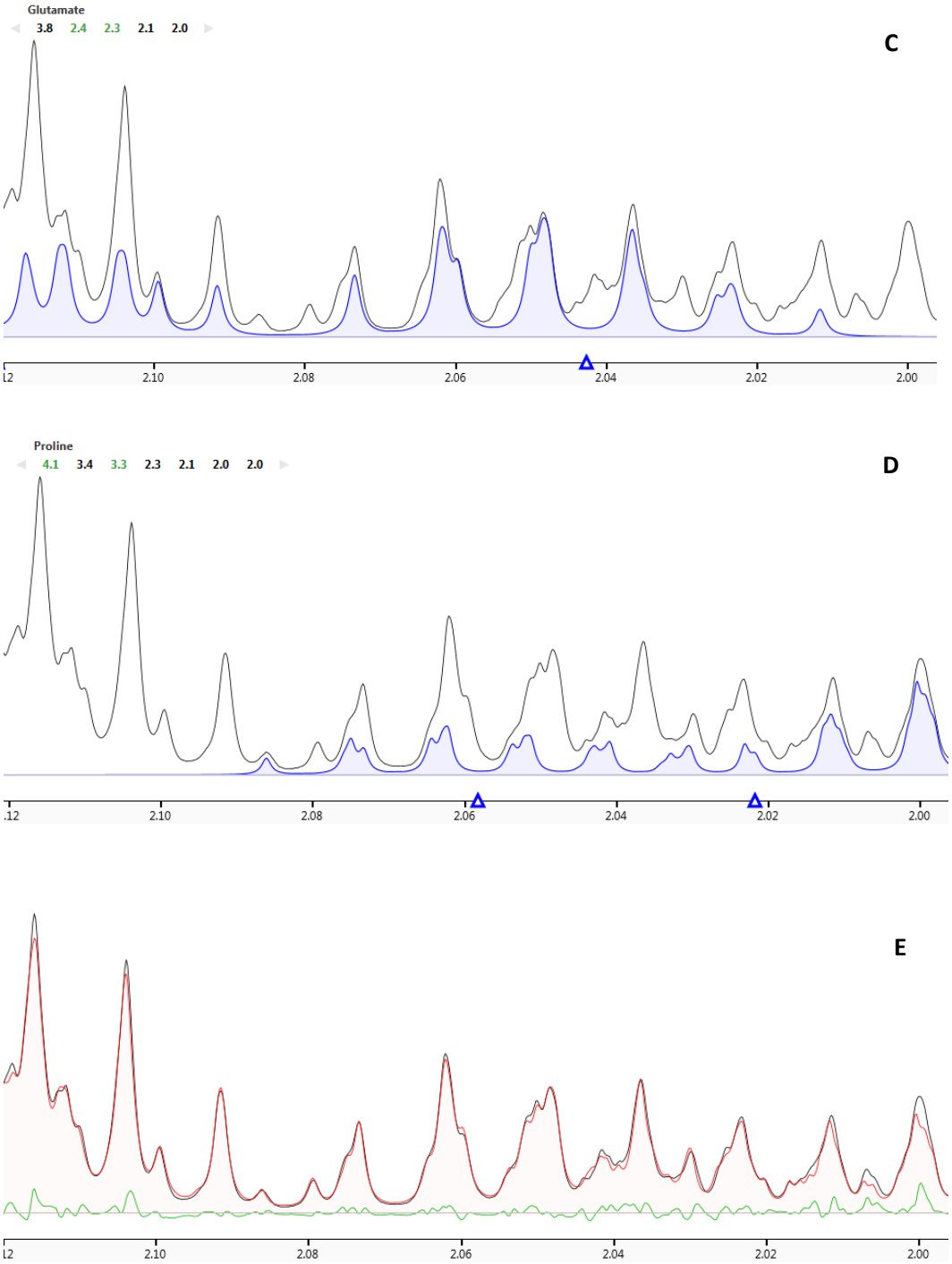

Figure 3: ^{1}H-NMR profile of a convoluted peak cluster at different stages of peak fitting. **A)** The original output prior to profiling. **B)** Fitting of methionine peaks. **C)** Fitting of glutamate peaks. **D)** Fitting of proline peaks. **E)** The final profile after all fitting is completed. (The black line is the original scan output from the ^{1}H-NMR. The blue area is the peak shape of the compound loaded from the database after adjusting the scaling for concentration. The red area is the sum of the all of the fitted peaks. The green line is the result of subtracting the profiled compounds from the original scan. Compounds are fit sequentially in order to try to make the resultant green subtraction line flat.)

This chapter aimed to use ^{1}H-NMR to characterize shake flask cultures of Sf9 cells grown to high cell densities and to contrast them with cultures grown to more typical cell densities. Additionally, ^{1}H-NMR was used to see if cells that experience stressful conditions could be identified via certain metabolites in the culture.

Section 3.2 – Methods

Section 3.2.1 – High Cell Density Experiment

Six shake flasks, each with a working volume of 30 mL, were seeded as described in Section 2.3. For the first three days (i.e. up to 2-3 x 10^6 cells/mL), all six flasks were operated identically in batch mode. After this point, media replacement began in three of the cultures while the others were used as controls. To replace the media, the flasks were emptied into separate 50 mL falcon tubes and centrifuged at 100 RCF for 10 minutes. Taking care to keep the cell pellet intact, as much of the spent media as possible was removed, and 5 mL of fresh media warmed to 27 ^{o}C was added. The media was pipetted up and down gently so as to break up the pellet, and then more media was added to bring the cell suspension back up to a total of 25 mL. Cell counts and ^{1}H-NMR samples were taken once per day, just before exchanging the media. In the first high cell-density experiment, this process was repeated every 24 hours. In the second high cell-density experiment, this was initially repeated every 24 hours. However, after the cultures exceeded a cell density of 10 x 10^6 cells/mL, the frequency of the media replacement was increased to once every 12 hours. This was done for one day (i.e. two media exchanges), then the frequency of media replacement was further increased to once every 8 hours.

Section 3.2.2 – Sealed Flask Experiment

Cells were seeded in a similar fashion to the high cell-density experiment, in four different flasks. The cells were allowed to grow as normal until they reached 2 x 10^6 cells, after which the lids of all flasks were sealed to cause a slow depletion of the oxygen concentration in the flask. Because the sealed flasks

could not be opened for cell counts without disturbing the oxygenation conditions, a control, non-sealed flask was run in parallel to approximate the cell-density instead. In the final four days of the control culture duration as it approached the end of the exponential growth phase, one sealed flask was sacrificed per day. In each of these sacrifices, the flask was unsealed and the dissolved oxygen content of the media was immediately measured by using a dissolved oxygen probe (Sper Scientific, product code 850045). The cell-density and viability were then recorded via the cell counter as usual.

Section 3.3 – Results – High Cell-Density Culture Growth and Limitations

Section 3.3.1 – High Cell-Density Growth Profiles

The cell growth curves of this first experiment are shown in Figure 4. Daily media replacements improved the duration of culture, with a maximum cell density of 44 x 10^6 cells/mL. Moreover, it also extended the duration of the exponential growth phase. Above roughly 15 x 10^6 cells/mL, media replacement was insufficient to maintain a constant growth rate (to the right of the dotted lines there was a significant change in slope indicating cells exited the exponential growth phase; see also Appendix Figure A1a and A1b). A follow-up experiment was performed in which the frequency of media replacement was increased shortly before the drop in growth rate was expected. In this case, when the cells passed 10 x 10^6 cells/mL, the time between media replacements was reduced to 12 hours. Then, one day after the cells exceeded 10 x 10^6 cells/mL, the time between media replacements was further reduced to 8 hours. There was no difference between this experiment and the first experiment (24hr media replacement), and the cells experienced a very similar drop in growth rate at 15 x 10^6 cells/mL. Because no positive effect was observed, the work intensive nature of an even more frequent media exchange regime was not explored.

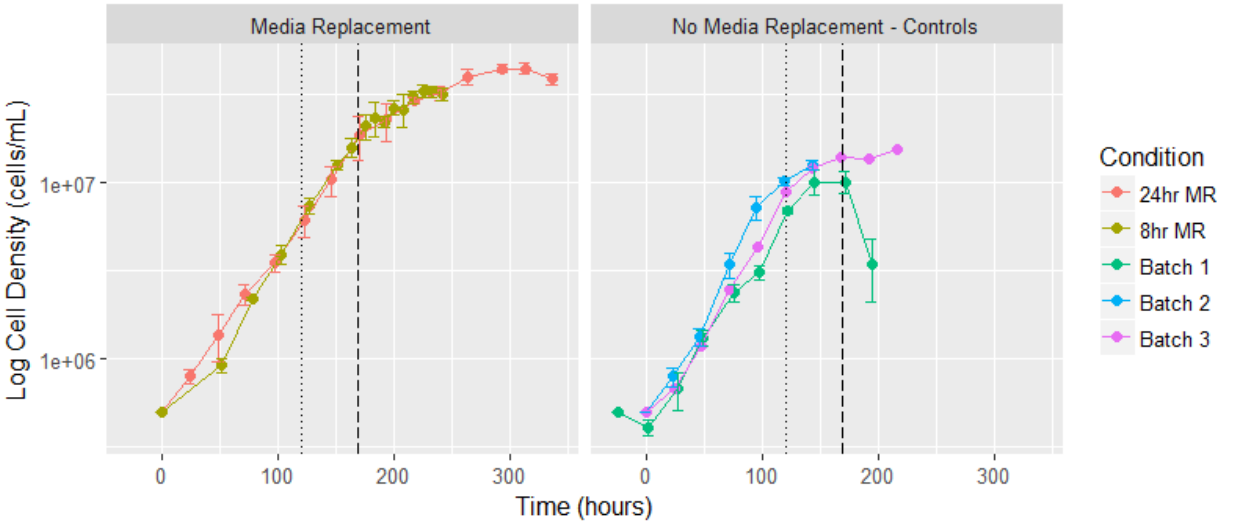

Figure 4: High cell-density experiment growth curves (The dotted line marks the drop in batch growth rate, and the dashed line marks drop in high density growth rate. MR designates the number of hours between media replacements in the experiment shown. n = 3 replicates, with the exception of "Batch 3", which consisted of a single flask. Error bars = 1σ.)

As seen in Figure 4, the increased supply of nutrients in the media did not alleviate the drop in growth rate. This raised concerns over the oxygenation requirements of the culture. It was proposed that when the cell-density exceeds a certain level, the shake flask system could become insufficient to allow for sufficient oxygen transfer. Therefore, an experiment was carried out to see what changes, if any, occur when the culture is deprived of oxygen. This experiment is described in the Methods of this chapter, Section 3.2.2

Comparing oxygen content of sealed flasks to the control culture, a difference was observed. In the sealed flasks, the oxygen concentration steadily dropped to a final value of 1.7mg/L on day 8. In contrast, in the unsealed control flask, on the final day the dissolved oxygen had reached a concentration of 6.2mg/L, a 3.6-fold difference. For comparison, it was found that if air was bubbled through the media, the maximum dissolved oxygen concentration was 8.2 mg/L, meaning that these end-point DO concentrations were equivalent to 20.7% and 75.6% saturation, respectively. The growth curves of these cultures are shown in Figure 5. Despite this difference in oxygen levels, there was no appreciable

difference between the sealed flasks and the control flask in terms of growth rate. This suggested that while the sealed flasks had significantly lower oxygen levels, it was not to the degree that it could negatively affect growth. An even lower level of oxygen may have resulted in decreased cell growth, however. The first sealed flask, (opened five days after seeding) had an average growth rate of 0.0232 h^{-1} compared to the collective 0.0225 h^{-1} average growth rate in the control, non-sealed flask over the first 5 days. The growth rates then sharply dropped in both sets of cultures. The average growth rates can be found in the Appendix Figure A2.

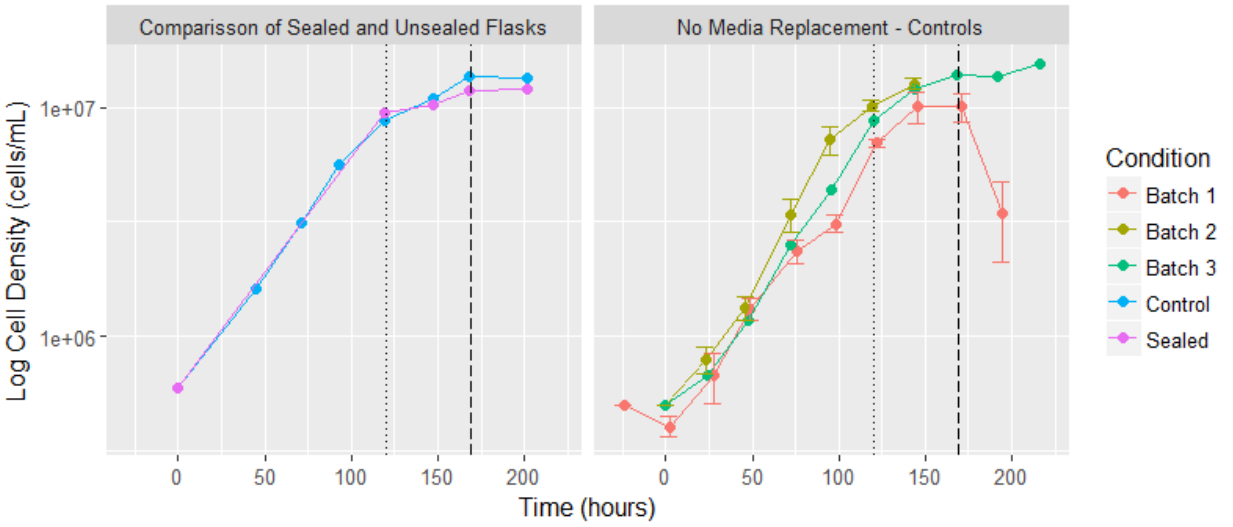

Figure 5: Sealed flask experiment growth curves (Cell density is on a log-scale. The "No Media Replacement – Control" cultures are the same ones presented in Figure 4, shown here as a point of comparison. Error bars = 1σ. No error bars are presented for the "Sealed Flask" or "Non-Sealed Flask", since the data points each corresponded to measurements taken from a single flask. The dotted line marks the drop in batch growth rate, and the dashed line marks drop in high density growth rate.)

Daily samples taken from both of these sets of experiments were analyzed by ^{1}H-NMR. Forty-one compounds were analyzed, and the full set of profiles can be found in the Appendix, Figure B1. Inspection of the time profiles for these two sets of experiments revealed several compounds that tended to increase with time (be produced) or to decrease with time (be consumed). Comparing these ^{1}H-NMR results to those in literature allowed for them to be classified as either being typical (i.e. compounds that

are well established already in the literature) or atypical (i.e. compounds that have usually been ignored in prior reports).

In the majority of the literature, the only accumulating compounds tracked in Sf9 cultures are alanine, lactate, and ammonia. Ammonia is a compound that is undetectable by ^{1}H-NMR, but it has been observed to be of negligible importance in Sf9 cells compared to the other two metabolites due to the presence of alternative pathways to handle the nitrogen load (Bédard et al., 1993; Ikonomou et al., 2003). Consequently, of these three compounds, only alanine and lactate were examined within this thesis. The profiles of alanine and lactate are shown in Figure 6, with the top row representing batch culture (control), the middle representing cultures with media replacement, and the bottom row representing the sealed flask cultures. Besides alanine and lactate, the other metabolites that were produced and detected included fructose, fumarate, hypoxanthine, and succinate. These profiles are shown in Figure 7.

Sugars and amino acids have all been studied in literature. Glucose, glutamine, serine, and cystine were the sugars and amino acids that experienced the greatest degrees of consumption. Therefore, these were chosen to be representative of the trend in typically consumed metabolites. These four profiles are all shown in Figure 8. In terms of rarely or not reported compounds, choline, inosine, uracil, and uridine were all detected and depleted in a rapid manner. The profiles of these compounds are shown in Figure 9. For clarity in the presentation of the data, the daily effect of media replacement is not shown in any of these four plots. It is important to note, however, that the reality of the situation is that the media replacement causes the concentration of the metabolites in the culture to return to the initial concentration (i.e. the 0 hour time point) after every replacement.

Section 3.3.2 – ^{1}H-NMR: Typically Measured Compounds, Accumulating

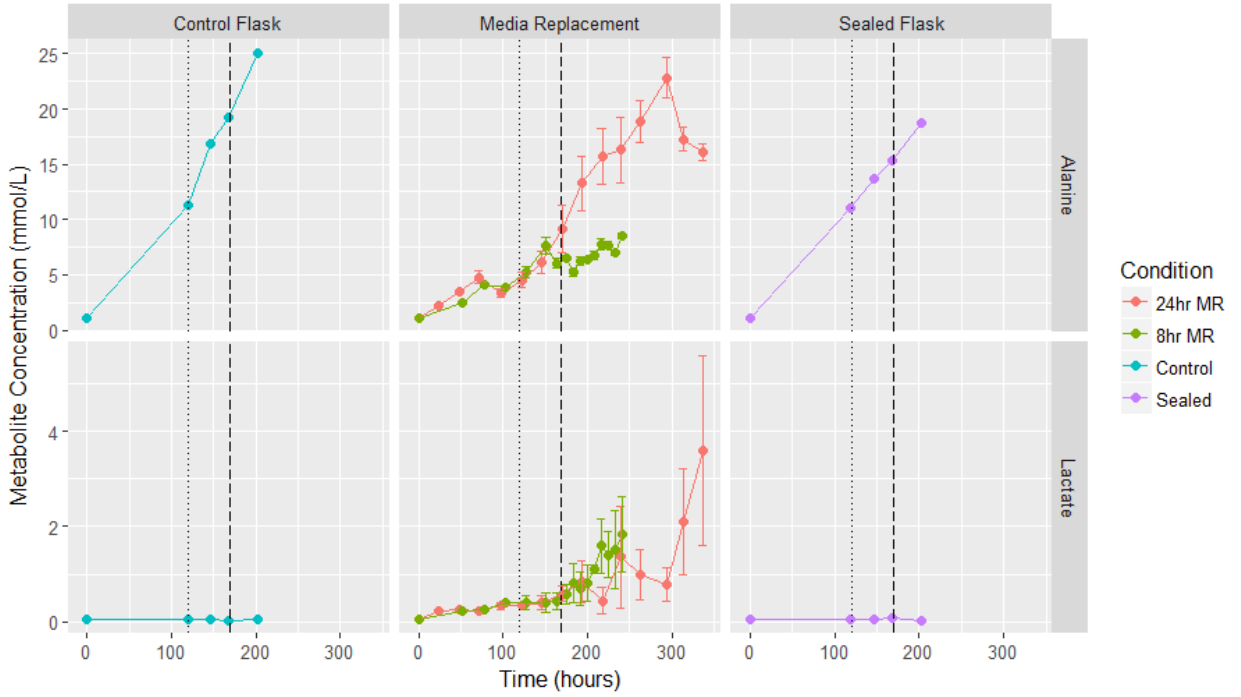

Figure 6: Typically profiled metabolites produced during culture (increasing trends). (n = 3 and error bars = 1σ for the media replacement condition. Error bars were only placed on the media replacement conditions, because the sealed flask and control flask conditions each only had samples taken from one flask at each time point. The dotted vertical line marks the drop in batch growth rate, and the dashed vertical line marks drop in high density growth rate. MR designates the number of hours between media replacements in the experiment shown.)

As the culture progressed, a substantial amount of alanine was produced in every experiment. In the sealed flask experiment, only about 80% as much alanine accumulated when compared to the control. Production was comparable in the media replacement experiment when the cell-densities were similar, and as expected the rate increased as the cell-density increased. After 300 hours, once the cells started to die, the production rate also started to decrease. On the other hand, lactate did not exceed baseline levels in the sealed or control cultures at the time points examined, and only started to accumulate in notable amounts later in the cultures with media replacement. It is important to remember, however, that the compounds were only profiled for the late part of the culture in the sealed flasks. As such, it cannot be

ruled out that lactate experienced a large jump in concentration soon after the flask was sealed, and then declined back to baseline levels around the time that the culture entered the stationary phase. In order to better address this point, additional ^{1}H-NMR samples should be taken from sealed flasks in the early growth phase.

Section 3.3.3 – ^{1}H-NMR: Atypically Measured Compounds, Accumulating

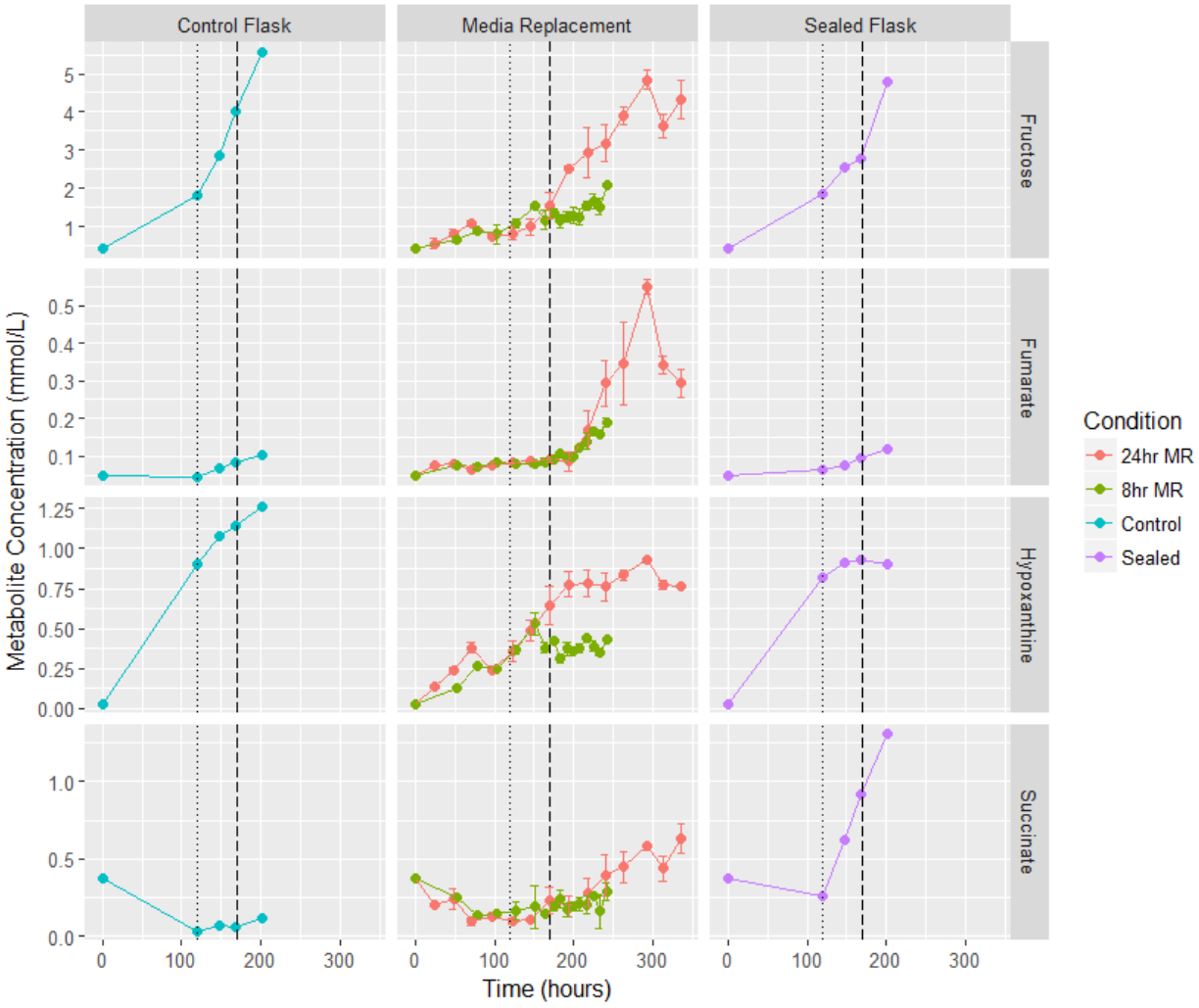

Figure 7: Atypically profiled metabolites produced during culture (increasing trends). (n = 3 and error bars = 1σ for the media replacement condition. Error bars were only placed on the media replacement conditions, because the sealed flask and control flask conditions each only had samples taken from one flask at each time point. The dotted vertical line marks the drop in batch growth rate, and the dashed vertical line marks drop in high density growth rate. MR designates the number of hours between media replacements in the experiment shown.)

A very noteworthy amount of fructose accumulated in the cultures, up to approximately 5.5 mM in the control. Compared to the 60 mM of glucose in the initial media, this is a sizable fraction of the total sugar content present. For both fructose and hypoxanthine, as was the case with alanine, production in the sealed flask only amounted to roughly 80% of the levels in the control flask. On the other hand, fumarate levels were roughly 10% higher, and the succinate levels followed an opposing trend, increasing in the sealed flask while decreasing in the control flask. In the media replacement experiment, the fumarate production rate increased until cell death began and then dropped rapidly. Hypoxanthine showed a trend of increasing with cell density, but only for the first 192 hours, after which it seemed to stabilize at a constant daily amount of production despite changes in cell-density. Succinate followed alternating trends in different phases; early on, it was mostly consumed like in the control, but after 250 hours in culture it was produced like in the sealed flask.

Section 3.3.4 – ^{1}H-NMR: Typically Measured Compounds, Depleting

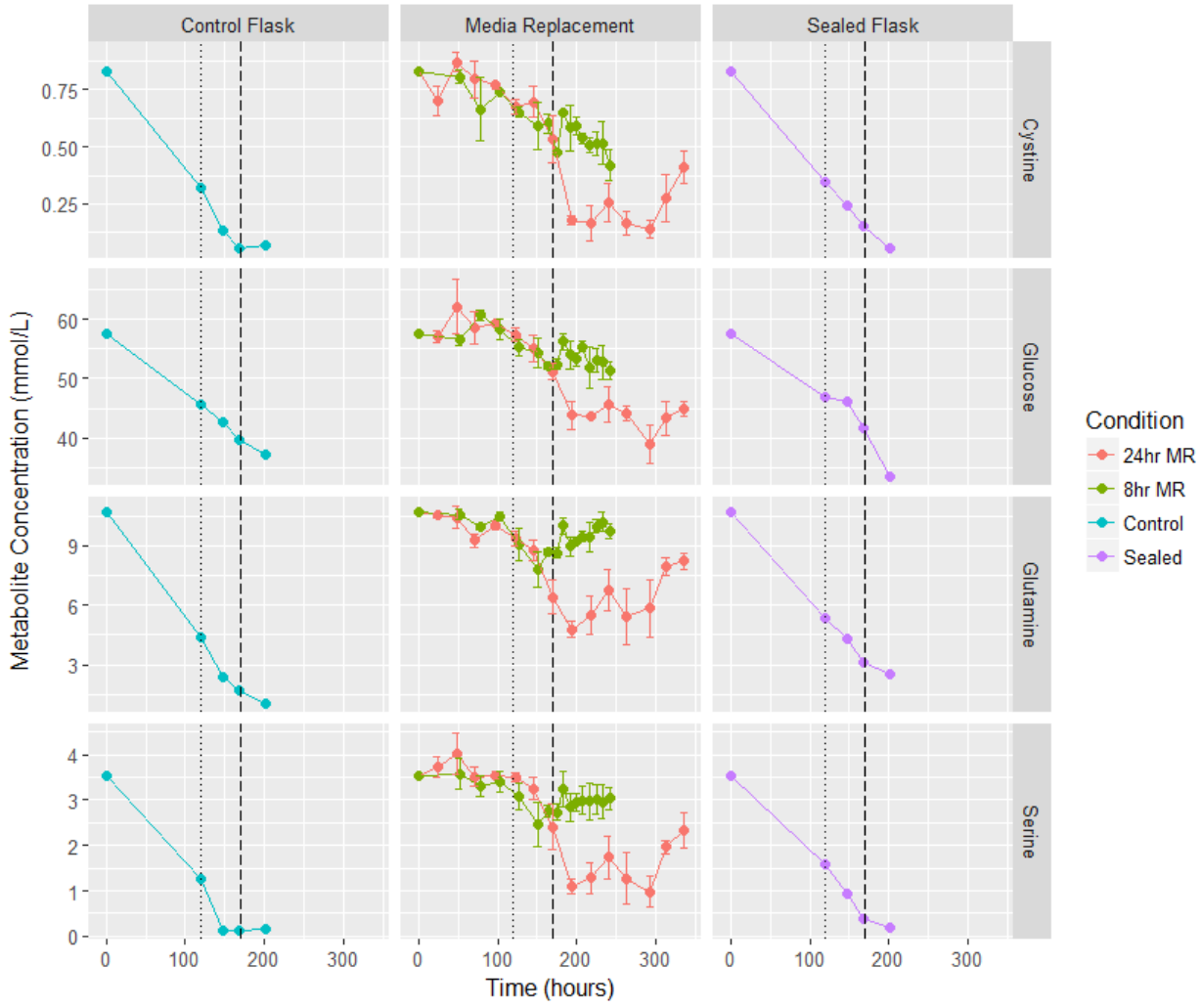

Figure 8: Typically profiled metabolites consumed during culture (decreasing trends). (n = 3 and error bars = 1σ for the media replacement condition. Error bars were only placed on the media replacement conditions, because the sealed flask and control flask conditions each only had samples taken from one flask at each time point. The dotted vertical line marks the drop in batch growth rate, and the dashed vertical line marks drop in high density growth rate. MR designates the number of hours between media replacements in the experiment shown.)

In the sealed flask, cystine consumption was slightly slower than in the control, requiring an extra 24 hours to reach the minimum of 0.05 mM. Glucose, glutamine, and serine consumption were all similarly slower in the sealed flask when compared to the control flask. Serine was also completely

depleted 24 hours before the cell density peaked in the control flask. These compounds were all depleted quite quickly in the case of the media replacement experiment, with around 25% of the glucose being consumed every 24 hours, and for the other three compounds more than 50% of what was available in the media being consumed every 24 hours.

Section 3.3.5 – ^{1}H-NMR: Atypically Measured Compounds, Depleting

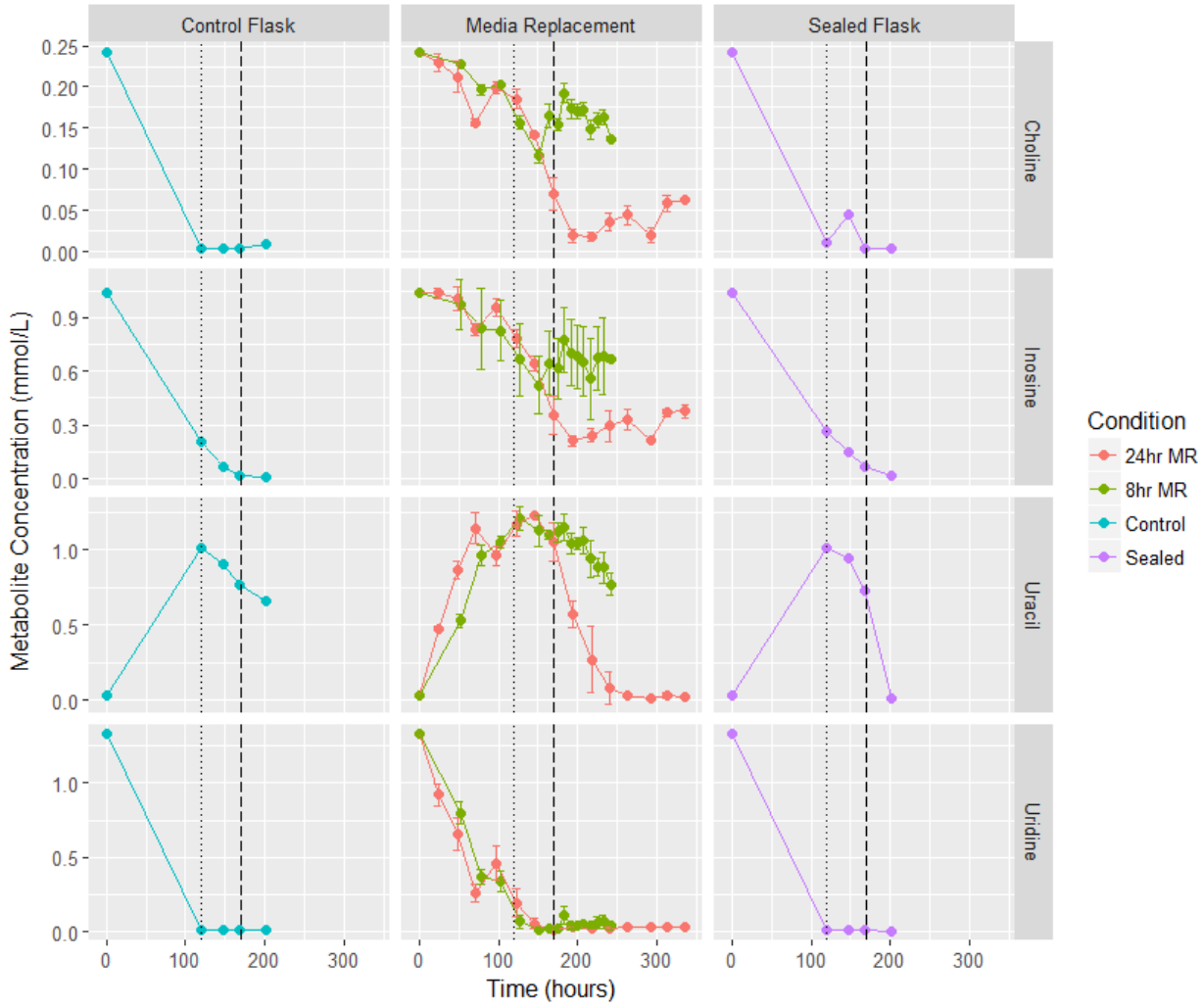

Figure 9: Atypically profiled metabolites consumed during culture (decreasing trends). (n = 3 and error bars = 1σ for the media replacement condition. Error bars were only placed on the media replacement conditions, because the sealed flask and control flask conditions each only had samples taken from one flask at each time point. The dotted vertical line marks the drop in batch growth rate, and the dashed vertical line marks drop in high density growth rate. MR designates the number of hours between media replacements in the experiment shown.)

In both the control and the sealed flasks, choline and uridine were completely depleted before the first time point measured. While this is notable, the ^{1}H-NMR data are only currently available starting from this 100 hr point and it is uncertain how soon before this time that total depletion of the choline or uridine would have occurred. As such, there is currently no indication in this experiment as to whether or not the depletion of either choline or uridine was related to the slowing of cell growth, and this will require further investigation. Inosine was consumed slightly slower in the sealed flask, requiring another 24 hours to be completely depleted than the control. In the case of uracil, the opposite trend was observed, with its concentration peaking likely somewhere slightly greater than 1 mM at a time point slightly before the first one recorded (at 120 hours in culture). Projecting based on the first three days of the media replacement experiment (before media replacement was started), the peak looks to be expected in the range of 1.25-1.5 mM, roughly 96 hours after seeding. After reaching the peak, uracil is steadily consumed. In the media replacement experiment, these compounds were all depleted to a greater extent on a daily basis than the typical compounds shown in Figure 8. Inosine reached a daily rate of nearly 80% consumption, and the other three compounds all reached near 100% consumption in every media exchange. This degree of depletion raised the question of just how important these compounds are for supporting Sf9 cell growth.

Section 3.4 – Discussion

Section 3.4.1 – Effects of Media Replacement

There is ample capacity for the commercial media formulation to support cell growth. A paper by Clincke et al. (2013) suggests that with highly focused perfusion bioreactors, the cell-density can be pushed close to the very limits based the physical size of each cell. For CHO cells, this is equivalent to roughly 146 x 10^{6} cells/mL when allowing for a healthy 2 μm gap between cells, and this was

demonstrated in their paper (Marie Francoise Clincke et al., 2013). Similarly, for an average 15 µm Sf9 cell, this suggests that in theory a maximum cell-density of approximately 204 x 10^6 cells/mL should be achievable under perfect conditions (Marie Françoise Clincke et al., 2013). In general, the trend shown is that, typically, the more intensive the feeding method that is used, the higher the cell density can be forced. The cell density effect seems to always appear far below the maximum density limits, however, hindering the practicality of such systems. The maximum density achieved in Figure 4, roughly 44 x 10^6 cells/mL, was much lower than the value achieved by Clincke et al. However, it is still several-fold higher than the usual 12-14 x 10^6 cells/mL attained in a standard batch culture, illustrating the benefit of the turnover of the spent media. While not the ultimate goal of the experiments to come in this thesis, in order to further improve the maximum cell density achieved, the media replacement strategy could likely be refined further. Ideally, the media replacements could be spaced longer than 24 hours apart in the beginning of culture when cell densities (and nutrient demands) are still low, and then be spaced more closely in the later stages of the culture as the cell density increases. Interestingly, both uracil and uridine were fully consumed every 24 hours during the last four days of culture. This also coincided with the cell density starting to plateau. It would be interesting to see at that point if a more frequent media replacement could restore the culture to an exponential growth state.

Section 3.4.2 – Metabolism

Because perfusion is required to reach such extremely high cell-densities, it supports the theory that various metabolites play a role in limiting or supporting cell growth. Most obviously, the depletion of metabolites should limit the growth of the cells. However, less commonly, some metabolites may accumulate and have an inhibitory effect on the cells. Specifically for the Sf9 cell line, the metabolites studied in this thesis can be sorted into one of four categories. Firstly are the commonly studied accumulating compounds. Alanine and lactate are the only two in this category when using the ^{1}H-NMR technique. Secondly are the accumulating compounds that are rarely or never covered in the literature. In this category are fructose, fumarate, hypoxanthine, and succinate. The third category is the compounds

that are identified in literature as being limiting for cell growth. Specifically, this typically includes glucose, glutamine, cystine, and serine. Lastly, the compounds newly identified in this thesis that are in limited supply (and consequently are suspected to be important for allowing continued cell growth) are choline, inosine, uracil, and uridine.

Section 3.4.2.1 – Accumulation of Typical Metabolites

Alanine is well studied in Sf9. According to Ikonomou et al., alanine is produced instead of ammonia as an alternative nitrogen sink (Ikonomou et al., 2003). This reaction is also thought to rely on pyruvate and glutamate, suggesting it may fail to proceed under glutamine/glutamate depletion (Ikonomou et al., 2003). As seen in Figure 6, alanine is produced to a very high degree in all cultures. By the final time point, it is slightly lower in the sealed flask than in the control flask. It is uncertain if this is due to the slightly lower cell density or if it is as a result of the oxygen concentration affecting cell metabolism. Lactate presents an interesting trend here that is in contrast with expectations. In the literature, production of lactate is associated to a depletion of oxygen in the culture. The lactate produced in both the sealed flask and the control flask is effectively zero, despite the measured differences in dissolved oxygen content between the flasks. On the other hand, it does appear to be produced at a reasonably high rate in the media replacement experiments, particularly towards the end of culture (i.e. when cell densities are very high). This trend will be of interest in future experiments as it may indicate oxygen limitations when cells get to high cell densities. Future experiments should further delve into the metabolites produced under oxygen deprivation by reducing the amount of headspace in shake flasks (i.e. increasing the working volume in the shake flasks).

Section 3.4.2.2 – Accumulation of Atypical Metabolites

Amongst the atypical compounds, fructose, fumarate, and succinate can all be tied to the glycolysis pathway. Fructose (i.e. fructose-1,6-biphosphate) is an intermediate of glucose as it is converted to pyruvate for entry into the TCA cycle. Both forms are of interest, but it should be noted,

however, that due to the physical limitations of ^{1}H-NMR (i.e. relying on the detection of protons), this method is unable to detect the presence of phosphate groups. As such, it is uncertain whether or not the extracellular fructose detected in the ^{1}H-NMR analysis here has been phosphorylated. It is a small distinction, but one that could have significant implications.

Following the reaction of pyruvate with citrate in the TCA cycle, fumarate and succinate exist as intermediates of citrate as it is converted to other forms. The profile of succinate is especially interesting in the case of the sealed flask experiment. Unlike lactate which did not appear to be produced despite the lowered oxygen concentration, succinate was produced at a substantial rate compared to the control flask. Since it was also produced at the end of the high density culture experiment, it suggests that there may be a threshold level of dissolved oxygen below which succinate is produced and released into the media. Studies in other organisms further support this possibility; *S. cerevisiae* and *E. coli* have been shown to produce succinate under anaerobic conditions, as have numerous bacterial species (Ahn et al., 2016). Fumarate and succinate also both appear as markers during ischaemic injury (Haas et al., 2016), supporting the thought that they may be appearing as the cells attain higher densities and oxygenation becomes potentially limiting.

Section 3.4.2.3 – Depletion of Typical Metabolites

Glucose is widely used as the primary sugar source for Sf9 cells. The cells have no issues with metabolising it, and it is consumed at a steady rate. Glutamine is the second-most frequently profiled metabolite and is also well understood to be crucial for supporting the growth of the cells. Most other amino acids are consumed as well, but often to a lesser degree. Serine and cystine were the closest to being depleted in the media replacement experiments, and were in fact fully depleted in the sealed flask experiment. As such, they were also selected to be shown in Figure 8 as typical trends. Most of the other amino acids follow similar trends.

Section 3.4.2.4 – Depletion of Atypical Metabolites

Lastly, the remaining atypical profiles include choline as a vitamin as well as inosine, uracil, and uridine as nucleic acid-related compounds. Choline was the only vitamin found in the Sf-900 III media at measurable levels. It has been observed in other systems to have an important role in cell membrane formation, so it would be reasonable for its concentration to change appreciably over the course of the culture, especially during the exponential growth phase (Plagemaen, 1971; Plagemann, 1969). In one study, its consumption rate was observed to drop to 20% when the cells entered into the stationary phase (Plagemann, 1969).

Regarding the nucleic acid compounds, uracil can be paired with uridine, as can inosine with hypoxanthine (from the atypical compounds that were produced, shown in Figure 7). Hypoxanthine and uracil are both their respective compounds without an attached ribose ring (nucleobase), while inosine and uridine are the compounds with the ribose ring in place (nucleoside). Regarding the trends in Figures 5 and 7, the nucleoside appears to be steadily converted to the nucleobase form. The two reactions here can be described as:

$$Inosine \xrightarrow[enzyme]{} Hypoxanthine + Ribose \tag{8}$$

$$Uridine \xrightarrow[enzyme]{} Uracil + Ribose \tag{9}$$

This reaction appears to occur much faster than the cells actually need to make use of the compounds. Early on in the culture, the sums of concentrations for the sets of nucleoside/nucleobase pairs are relatively stable; this is indicative that little overall consumption of the nucleic acid compounds occurs at the beginning of the culture, and that the conversion is driven much more by the consumption of ribose than by the demand for either of the nucleobases. However, it is of note that the rate for uridine-uracil conversion is significantly faster than that of inosine-hypoxanthine conversion. The cellular demand for hypoxanthine also appears to be much lower than that of uracil, as uracil levels steadily drop

in the later stages of the culture unlike hypoxanthine. For this reason, uracil is the nucleic acid of the greatest interest, and is followed by hypoxanthine (due to the seemingly low overall demand for the compound + inosine). Inosine and uridine should be considered as important still, but it will be important to separate the effect that they have from the effect of ribose alone. These trends seem similar to what has been observed previously in our lab (Quattrociocchi, 2017).

Interestingly, the ^{1}H-NMR profiling revealed a number of nucleic-acid-related compounds in the media. However, with the great deal of overlap between their peaks, it makes it difficult to distinguish between them effectively. Therefore, there are drawbacks to using ^{1}H-NMR to look for these compounds. In particular, many of the nucleosides are confounded around 5.90 ppm, where they share peaks describing the carbon where the nucleobase joins to the ribose ring. Furthermore, early on in cultures, these peaks would initially be overshadowed to an extreme degree by uridine. Moreover, some of the predicted profiles for these compounds in the library do not exactly fit with the peaks that were actually observed. The best example would be inosine and adenosine which are closely related. In the Chenomx library, inosine fits nearly all peaks perfectly, while adenosine is just slightly off. However, inosine's library entry has a small peak at 4.76 ppm where none exists in the profiled sample, and this peak is also absent from adenosine's library entry. This difference seems to exist due to the shift, broadening, or overlap of certain peaks when the compound is not measured under ideal conditions. In generating the profiles available in the library, everything was tested using pure samples of the compounds at a pH of exactly 7. As such, when the pH is shifted and when other compounds are introduced that can interact with the compound of interest in some way, the actual response to the ^{1}H-NMR can differ from the expected "ideal" response. For this reason, an alternative method to ^{1}H-NMR will be required to adequately distinguish the different nucleic acid compounds.

Section 3.4.3 - Oxygenation and Other Concerns

This is reassuring and confirms that, in Figure 4, the drop in growth rate in the high cell-density media replacement cultures is a phenomenon related to the inherent characteristics of the culture. However, the downfall of the media replacement experiment is that there is a limiting constraint occurring as the cells cross the critical density of around 15 x 10^6 cells/mL, and it is not well understood. The ^{1}H-NMR data does not reveal any especially noteworthy compounds being depleted at that point, and the study on oxygenation suggests that in the case of an oxygen limitation a higher level of succinate would possibly be observed. Although this was a rather crude method of testing for the oxygenation, it is unusual that it revealed different trends for the batch cultures as opposed to the cultures undergoing media replacement. Specifically, in the low oxygen batch culture condition, succinate accumulated and no lactate was observed. The media replacement culture on the other hand observed an increase in lactate before succinate made the switch from being consumed to being produced. It would seem that the metabolic pathways at play are related, but exactly what the threshold is that triggers their switching is not currently known.

For this reason, it would be of great interest to try testing the high cell density media replacement experiment in a setting other than shake flasks. Specifically, it would be informative to study the system under conditions where the dissolved oxygen levels can be maintained at high levels and actively monitored. A controlled bioreactor, for instance, would serve well for this purpose. Presently, it is merely speculation that it was not an oxygenation issue that led to the drop in cell growth rate in the media replacement experiment, as evidenced by the dissimilarity between the media replacement ^{1}H-NMR profiles and those of the sealed flasks. The sealed flasks produced succinate and saw no reduction in growth rate, but the media replacement flasks only saw succinate accumulation a few days after the drop in growth rate. Testing in an oxygen controlled environment would allow for the effects to be cleanly separated.

Besides oxygenation, there are alternative theories that could also explain the drop in growth rate. For instance, a shift in gene expression as a result of the cell's environmental conditions would not be covered by the methods used here, unless it were to simultaneously cause a drastic shift in the metabolic requirements of the cell that it could be correlated to. Such a thing could be caused by a variety of small protein-type signalling molecules or growth factors. Because ^{1}H-NMR as a technique cannot pick up on the complex chemical signature of proteins well, their presence would be invisible to this study. In fact, it has been shown in the literature that there are some small, secreted signalling molecules present in culture that do have an effect on the cells. For instance, Ikonomou et al. showed that by carrying out a partial media replacement, their cultures had a higher productivity than in the case of a full media replacement (Ikonomou et al., 2004). While they demonstrated a beneficial effect at the densities they tested, it is equally possible that at higher densities, different growth-inhibiting factors could be secreted.

With this in mind, the infections in the next chapters would need to be designed such that this does not become an issue. In studying the cell density effect, the goal is not to increase the cell density achievable by the culture, but rather to increase the specific productivity of the cells, or otherwise to increase the cell density up to which specific productivity is maintained. Because the drop in growth rate and the possible oxygen limitation issue occurs at 15 x 10^6 cells/mL, the high cell-density condition for infection would need to be chosen well below this point. Given that the peak cell-density in the batch culture is in the range of 12-14 x 10^6 cells/mL, selecting a cell-density of 10 x 10^6 cells/mL should effectively keep the culture in the safe range.

Chapter 4 – Adaptation of Flow Cytometry Methodology

Ultimately, increasing cell growth is not the goal when using Sf9 cells. Sf9 cells are grown so that they can be infected with a recombinant virus that forces the Sf9 cells to produce a product of interest. Although not of high interest themselves as a product, fluorescent proteins can be used as surrogates for ease of tracking, and for refinement of the culturing process. Furthermore, using fluorescent proteins enables the use of flow cytometry, a technique that can quickly examine cells individually for how they scatter light and how they emit fluorescence.

Section 4.1 – Flow Cytometry for the Monitoring of Infection

Typically, cells are first characterized by how they scatter light in terms of forward scatter (FSC) and side scatter (SSC), correlating with cell size and granularity respectively. Healthy, uninfected insect cells typically form a population as seen in Figure 10.

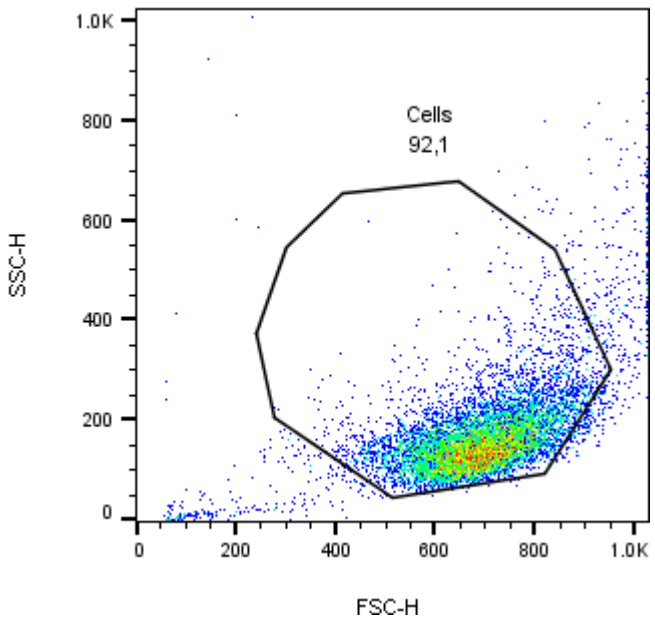

Figure 10: Appearance of healthy, non-infected cells in the FSC versus SSC channel. The plot is coloured in accordance with the density of events (areas with high event frequency are in red, while low event frequency areas are shown in blue). An arbitrary gate has been drawn to capture the majority of non-noise events, and the number above it is the percentage of events captured by the gate.

After infection, cells increase in diameter and then decrease in diameter as they die. When infection occurs synchronously, the movement of the population usually follow that of a simple population. This is shown in Fig 10A and B

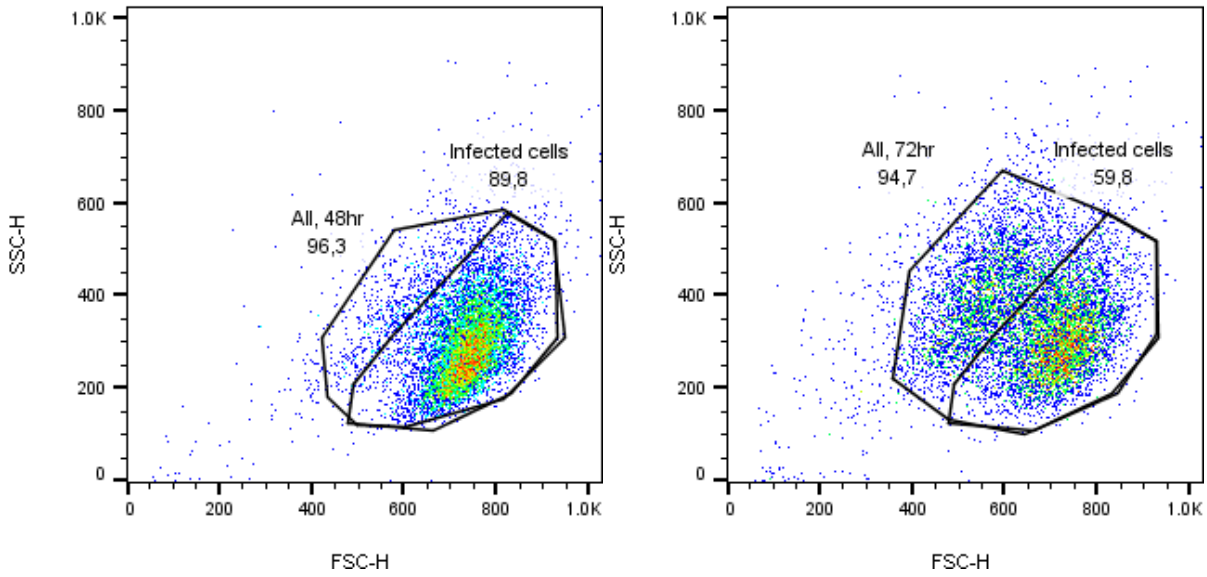

Figure 11: Transition of healthy, living cells after infection in the FSC versus SSC channel. Both plots show a smaller gate within a larger gate. The smaller gate (labelled as infected cells) is identical in both images. This is also the only gate used to capture the cells in samples at 24 hours post-infection. **A)** The figure on the left shows a normal infection at 48 hours and the corresponding gate chosen to enclose the non-debris events. **B)** The figure on the right similarly shows the chosen gate to enclose the entire population of non-debris events, but for an infection at 72 hours post-infection. In both cases, the plot is coloured in accordance with the density of events (areas with high event frequency are in red, while low event frequency areas are shown in blue). The numbers above the gates are the percentages of events captured by the gates.

In this work, where high density infection is being investigated, two different recombinant viruses were used. The two recombinant viruses each coded for a different protein product, specifically two different fluorescent proteins that can be detected using two different lasers and detectors on the flow cytometer. Due to their different emission spectra, the two proteins had little overlap in the other detector's respective channel.

The goal is to make use of these convenient fluorescent proteins to easily study the cell-density effect. Presumably, a higher level of fluorescence emitted by an infected cell should correspond to a higher level of protein production. A preliminary experiment comparing a low cell-density and a high cell-density infection seemed to support this as being the case (the high density infection had a notably lower average fluorescence than the low density infection). However, while this seemed to suggest that the method was sound, it was decided that further testing of the method was required to better validate it. This chapter focuses on the choice of virus used as well as the issues and limitations in using this method as a means of assessing productivity.

Section 4.2 – Methods

Section 4.2.1 – Selection of Baculovirus Construct

Two large flasks were used to prepare baculovirus stocks, as described in the General Methods, Section 2.6. A small volume of a P1 eGFP stock was added to the first flask and a similar amount of P1 mKate stock was added to the second flask. The viral titres in these P1 stocks were not known, so a ratio of 100 µL of stock per 30mL of culture was used instead.

Cell counts were taken from both flasks every 24 hours to track the progress of the infection, and when the cell viability dropped to 80%, the cells were harvested, also as described in Section 2.6. At a later date, 1 mL samples were taken from both baculovirus stocks for analysis by ^{1}H-NMR. These ^{1}H-NMR samples were run along with samples from two lots of fresh Sf-900 III media for comparison.

Section 4.2.2 – Comparison of mKate Stocks

Prior to this experiment, two P2 stocks of mKate were prepared in similar manners, as described in section 2.6. For each of these baculovirus stocks, the same P1 stock of mKate virus was used in the amplification. The difference between the two P2 stocks was the duration they spent in the fridge prior to

being used in experiments. The new P2 stock of mKate was prepared approximately three months after the old P2 stock, and all testing on it was done within days of its preparation. Additionally, only 10 μL of the P1 baculovirus was added per 30 mL of culture, rather than the 100 μL of P1 baculovirus used in the preparation of the aged P2 baculovirus stock). These baculovirus stocks were stored in the same fridge until use, roughly one week after the newer baculovirus stock was collected.

In the subsequent infection experiment, only two flasks were cultured. When the cell-densities in these flasks reached 2 x 10^6 cells/mL, these flasks were infected in accordance with the protocol outlined in the General Methods, Section 2.8. The first culture was infected with the old baculovirus stock, and the second was infected with the new baculovirus stock. The new mKate stock had an unknown titre (as the end-point dilution assay had not yet been performed), but based on the manner in which the amplification progressed, it was assumed to have a similar titre to the old baculovirus stock. With this assumption, both viruses were added in volumes sufficient to achieve an MOI of 5.

The cell cultures were tracked for three days post-infection. Once every 24 hours, a sample was taken from each flask and assessed for cell-density and viability. The remainders of the samples were further assessed by flow cytometry and ^{1}H-NMR, as described in the General Methods, Sections 2.9 and 2.10.

Section.4.2.3 – Propidium Iodide Cell Viability Analysis

Propidium Iodide (PI) (Sigma-Aldritch, Catalogue number: P4170-10MG) was prepared at a concentration of 1 mg/mL by dissolving one 10 mg vial of solids into 10 mL of PBS (i.e. a 1 mg/mL propidium iodide solution). This solution was then transferred to a 15 mL Falcon tube, wrapped in tinfoil, and stored in a darkend fridge at 4^{o}C until use. The solution was pipetted up and down to mix initially, and was similarly mixed prior to any use. This was done in an attempt to prevent any suspended solids from settling out of solution.

Section 4.2.3.1 – Viability Analysis

Cells were seeded from the maintenance flask at a density of 0.6 x 10^6 cells/mL into flasks with 25 mL culture volumes. Cells were left to grow for two days to reach a cell density of 2 x 10^6 cells/mL and were then infected with an MOI of 5 using the GFP baculovirus. One sample was taken from each flask every 24 hours for a 72 hour period, counted on the hemocytometer, and then prepared for analysis by flow cytometry. As before, each sample of cells was fixed with PFA for 5 minutes and then diluted into PBS. However, in this experiment, each sample of cells was then split into two separate tubes and PI was added to one. A report in which Sf9 cells were studied as the organism of interest suggested that propidium iodide be added to give a final concentration of 50 μg/mL (Sandhu et al., 2007). A more general methodology suggested that a 50 μg/mL solution of propidium iodide be added to cells at a ratio of 1 mL per 10^6 cells (Deitch et al., 1982). In this work, 0.1 mL of propidium iodide solution (1 mg/mL) per 10^6 cells/mL was used, essentially doubling the final concentration of propidium iodide added.

Section 4.2.3.2 – Propidium Iodide Concentration Assessment

To determine that the PI was not the cause of cell death observed, multiple concentrations of PI were tested to confirm that it was not having an effect. The infection was tested only at low cell density (2 x 10^6 cells/mL), but was otherwise set up exactly as in the above method (section 5.1.3.1). Four samples were taken from the flask and PI was added to each in four different concentrations. 250 μL, 190 μL, 130 μL, and 60 μL were added to yield samples with roughly 100%, 75%, 50%, and 25% of the PI concentration used in the first set of experiments, respectively.

Section 4.2.3.3 – Flow Cytometry Sample preparation Assessment

As an additional experiment to assess the cause of cell death (as suggested by high-intensity PI staining observed to occur in even the uninfected samples), the samples prepared for flow cytometry were assessed on a more fundamental level. An infection was prepared just as in section 5.1.3.1, and four

samples were taken. However, rather than fixing all samples with PFA for 5 minutes, only half of the cell samples were re-suspended in PFA. For the remainder of the cell samples, this step was skipped and the cell pellets were immediately re-suspended in PBS after the spent media supernatant was removed. PI was then added to half of all samples to give four different combinations of components (no PFA and no PI; no PFA and PI; PFA and no P; and PFA and PI). Flow cytometry was then run on all of these samples as usual.

Section 4.2.4 – Flow Cytometry Gating

As described in Section 2.9, any 2-dimensional gating performed in this section (i.e. gating of FSC vs. SSC) was performed arbitrarily. That is, the gate was drawn in by hand to avoid the bottom left corner of the plot, where events are primarily background noise. The gate was then applied to all samples in the set being compared, and subsequently adjusted to ensure a reasonable fit for all samples being compared. Whenever fluorescence cut offs were used (to distinguish fluorescent cells from non-fluorescent cells), and FL1 value of 0.5 was used and applied directly to the FL1 histograms.

Section 4.3 – Results – Selection of Baculovirus Construct

Initially, two different baculovirus constructs coding for similarly sized fluorescent proteins were tested. The first baculovirus construct coded for green fluorescent protein (GFP) while the second coded for a red fluorescent protein known as mKate2. For simplicity, henceforth, these two constructs will be referred to as the GFP baculovirus and the mKate baculovirus. Similarly, the cultures infected with either of these constructs will be referred to as a GFP culture or an mKate culture. In creating the viral stocks used for the experiments in this work, a small amount of each was taken from a P1 stock and separately amplified as described in the methods section.

Cells were infected during their mid-exponential growth phase, and the infection was allowed to progress until the cell viability fell to 80%. This occurred at approximately 90 hours post-infection (hpi). As can be seen in Figure 12, because a low MOI was used, cell growth continued until around 72 hpi. However, while the two cultures were infected at the same time and at the same density, the two had somewhat different growth profiles over the course of the next several days. The shapes were similar, but the mKate2 culture grew to nearly twice the cell density compared to the GFP culture. This may suggest that the P1 stock of GFP virus used was at a higher titre, and therefore more cells were infected during the initial stage of the amplification. For this reason, fewer cells would be available to continue dividing during the first 24 hpi in the GFP culture.

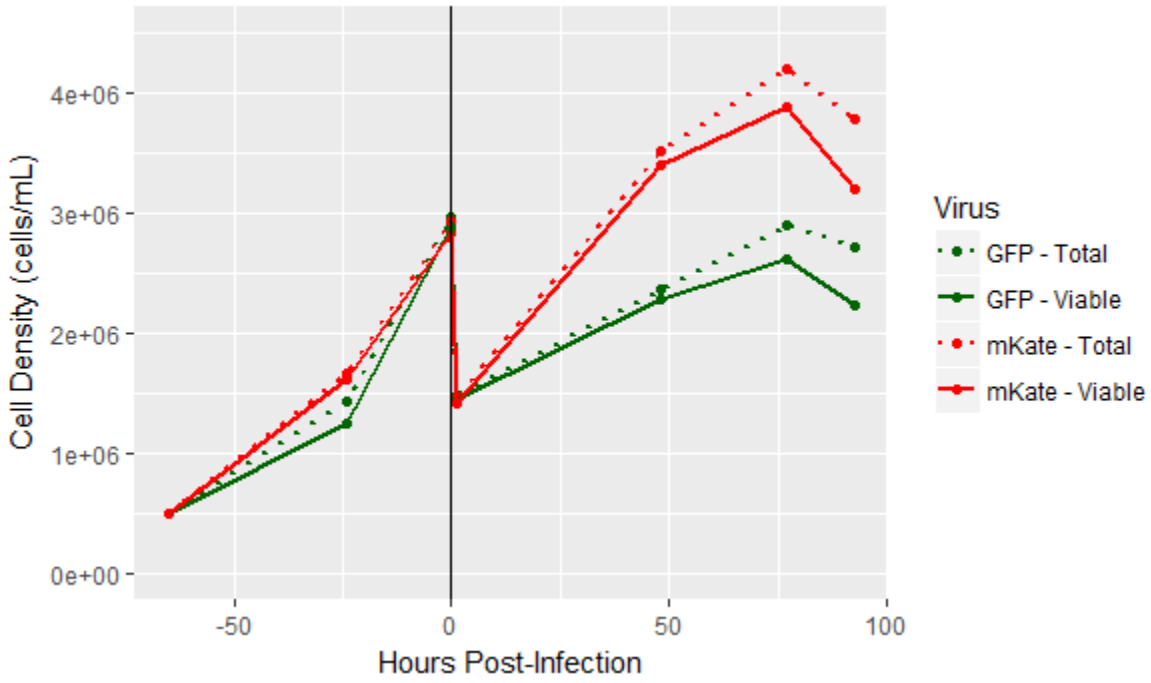

Figure 12: Growth curve of cells infected with 2 different baculovirus constructs. (The vertical line at 0 hpi denotes media replacement and time of virus addition.)

The average growth rates of the cells in the two cultures were calculated assuming exponential growth between each of the time points, and these results are shown below in Figure 13. While the

growth rate appears relatively steady prior to infection, assessing the average growth rate of the cells post-infection reveals a steady drop in growth rate after infection by the baculovirus. Again, the drop in growth rate seems to have occurred faster in the GFP stock, suggesting that it is at a higher titre and was able to infect a higher portion of the cells initially. Interestingly, the cells seem to behave comparably in the following stage of the infection when the second wave of virus causes infection of the remaining cells (i.e. around 72 hpi). At that point, it would seem that nearly all cells in the culture are infected and growth is effectively halted.

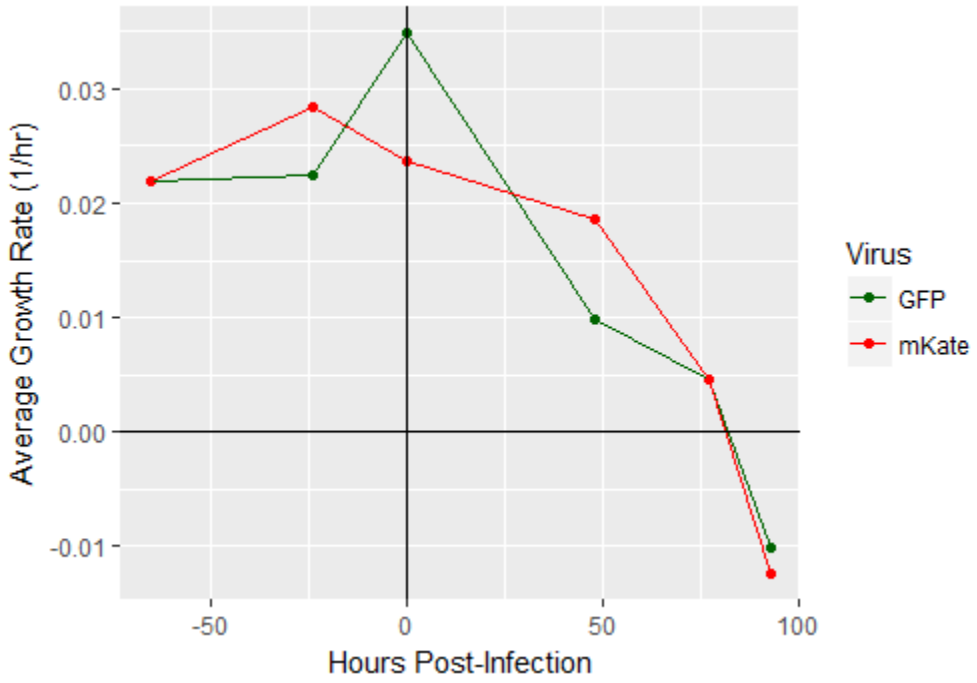

Figure 13: Average growth rate of cell cultures over the duration of the infection. (The vertical line denotes media replacement and time of virus addition.)

After harvesting the two batches of virus, the endpoint dilution assay was run as described in the General Methods, Section 2.7. Both stocks of virus were found to have similar titres. The GFP stock was found to have a titre of 4.97×10^8 pfu/mL, and mKate2 stock was found to have a titre of 6.90×10^8 pfu/mL. This concentration of baculovirus was deemed sufficiently high for use in the infection

experiments. To infect a culture of cells at 10 x 10^6 cells/mL (which Chapter 4 demonstrated is slightly below the maximum cell density achievable in this media without feeding), a multiplicity of infection of 5 would only require that virus be added in a volume equal to 10% of the culture volume for the GFP stock, or slightly less in the case of the mKate2 stock. In this way, dilution of the starting media is inconsequential at low cell-densities and should be mostly negligible at high cell-densities.

To better understand how the culture will change in composition at the time of virus addition, ^{1}H-NMR analysis was carried out on the two baculovirus stocks. Samples of two batches of fresh Sf-900 III media that were previously scanned were included as a point of comparison ("Media Stock 1" and "Media Stock 2"). These two batches were from different lot numbers, and were recorded separately to give a sense of the degree of lot-to-lot variability versus the variability between the two baculovirus stocks that were collected. When compared to the initial media, the concentrations of several compounds were noted to have changed drastically. The concentrations of these selected compounds are shown in Figure 14. The complete set of compounds profiled can be found in the Appendix Figure D1.

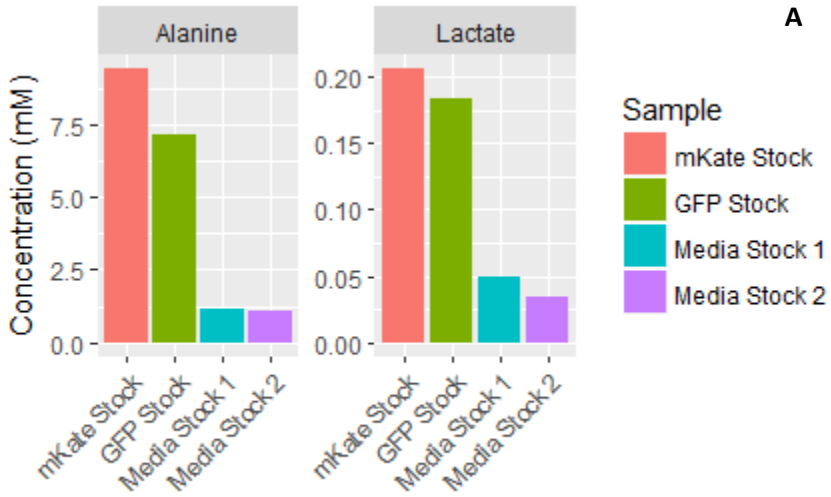

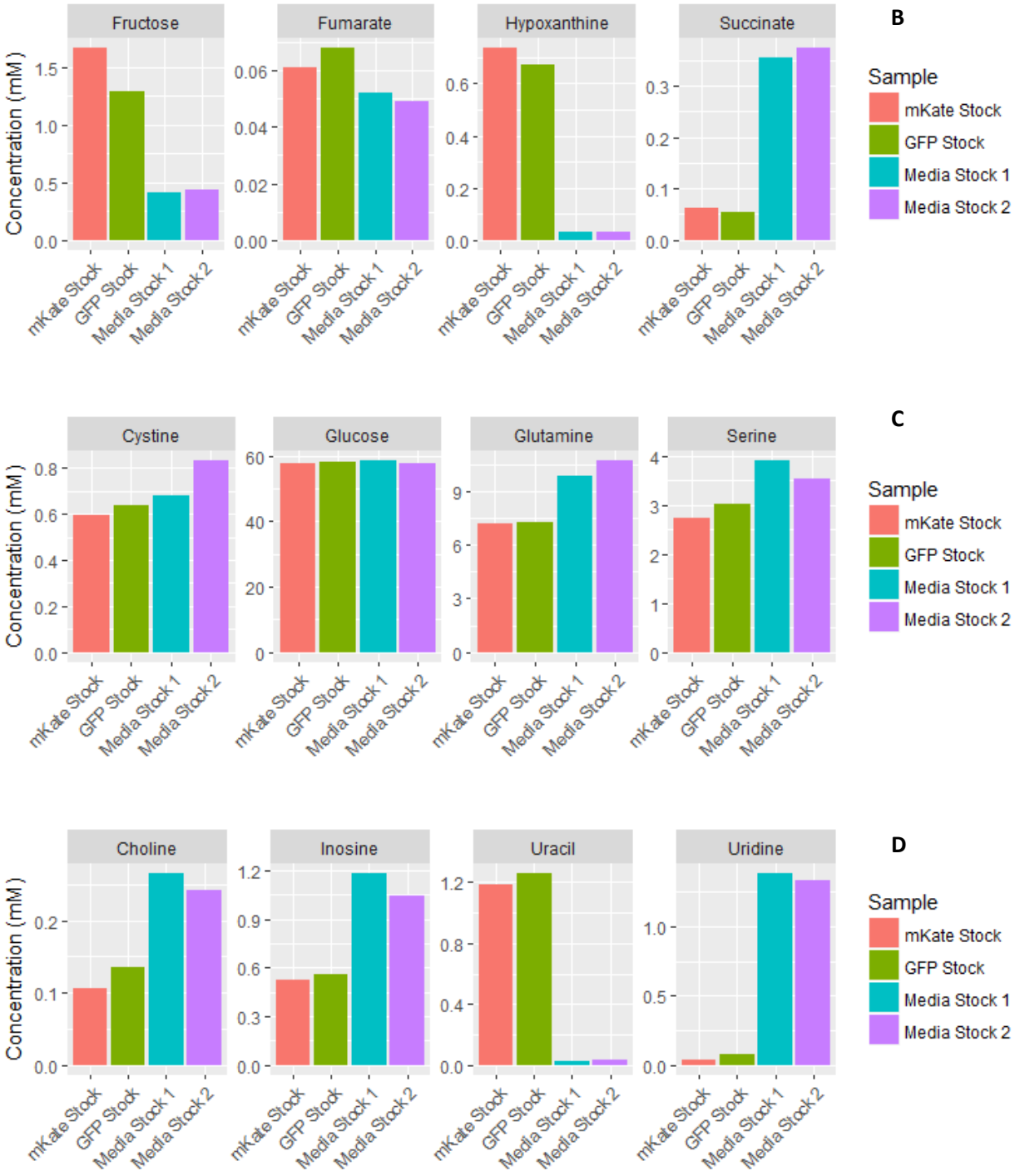

Figure 14: Selected metabolite concentrations determined by ^{1}H-NMR **A)** Increasing, common compounds. **B)** Increasing, uncommon compounds. **C)** Decreasing, common compounds. **D)** Decreasing, uncommon compounds.

The results observed here are similar to the trends observed in the previous high cell-density experiments. Because these baculovirus stocks correspond to 4 day-old spent media from cell cultures, this result is not very surprising. In all of the profiles shown here, the concentrations of compounds in the mKate2 cultures are slightly different from those in the GFP cultures. Almost all accumulating compounds in the mKate stock are at slightly higher levels than in the GFP stock, and almost all consumed compounds are at slightly lower levels. This can likely be attributed to the difference in the final cell densities of the two cultures leading to higher metabolic demands for the mKate culture.

Section 4.4 – Results – Comparison of mKate Stocks

In a preliminary experiment to test that both viruses were working properly, several cultures were infected at low cell-densities with one of the two constructs and tracked via flow cytometry. The results were examined and it was found that in a plot of the FL1 vs FL3 signals, some spectral overlap appears when the intensity of the signal increases beyond a certain threshold. Previous literature suggests that this is within expectations, because while the two fluorescent proteins have peak emission intensities at wavelengths corresponding to their respective detectors, the peaks are wide enough that they will contribute a small amount of signal at a wavelength measured by the opposite detector (Haimovich, 2012). For instance, Haimovich suggests that if 100% of the GFP signal is detectable at a wavelength of 509 nm, then roughly 5% of the signal would be detectable at a wavelength of 605 nm (Haimovich, 2012). A comparison of the two constructs in their respective detector channels at 48 hpi is shown below in Figure 15. In this figure, GFP begins being detected in the FL3 channel after the FL1 signal reaches a value approximately 50, and mKate begins being detected in the FL1 channel after the FL3 signal reaches a value of approximately 20. These numbers would vary depending on the parameters input used when setting up the flow cytometer, but nonetheless demonstrate that there is a small degree of overlap in the emission spectra.

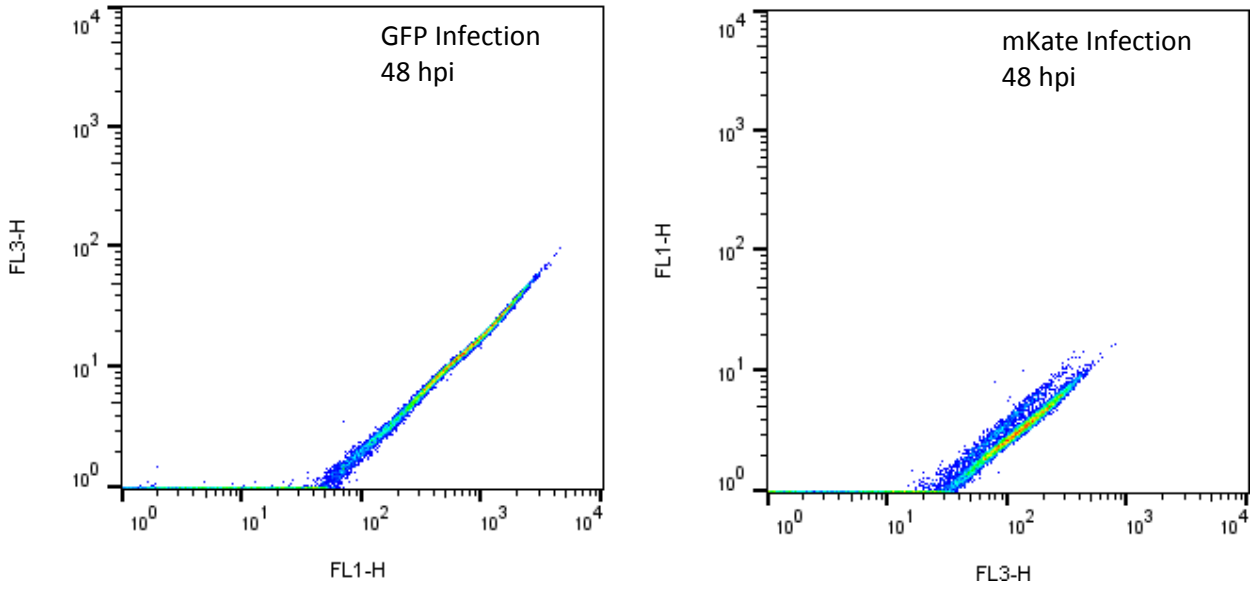

Figure 15: Comparison of 48 hpi samples from cultures infected with GFP (left side) or mKate (right side) to illustrate the apparent dual population present during infection with mKate.

Interestingly, while the GFP construct had FL1 and FL3 signals that increased linearly from 24 hpi to 72 hpi, in the mKate samples the signal separated at the 48 hpi time point into two distinct populations. Oddly, at 72 hpi, the two populations had merged back together. This could be due to maturation of the protein, but it is uncertain. The protein matures extremely fast at 37 ^{o}C, taking less than 20 minutes to achieve its final conformation(Shcherbo et al., 2010). However, it may mature much slower at the 27 ^{o}C temperature used for Sf9 cell cultures. For the mKate baculovirus construct, this split in the fluorescence of cells did not have any correlated trends in forward or side scatter. Rather, in the forward and side scatter domains, the two fluorescent populations fully overlap.

As a first possibility, it was hypothesized that the splitting of the population may have been caused by a poor quality of baculovirus stock leading to the formation of defective virus. To test this theory, in the experiment described in this section, two cell cultures were each infected at low cell

densities with one of two different stocks of mKate baculovirus. The first stock of baculovirus, the one used in the preliminary experiments, was prepared roughly 3 months prior to the experiments in this section. The second stock of baculovirus tested was prepared one week prior to running the set of experiments described in this section. The growth profile of the culture used to generate this new baculovirus stock is not shown here, but proceeded similarly to the profile demonstrated by the old stock in Figure 13.

Section 4.4.1 – Cell Growth and Viability of Infected Cultures (mKate)

The titer of the new stock of baculovirus was not measured, but was assumed to be similar to the titer of the old baculovirus stock due to the similarity of the conditions used in its amplification. Having tracked the cultures after infecting one flask with the old stock and one flask with the new stock, both infections progressed in a comparable manner. The cell densities and viabilities for both flasks are shown in Figures 16.

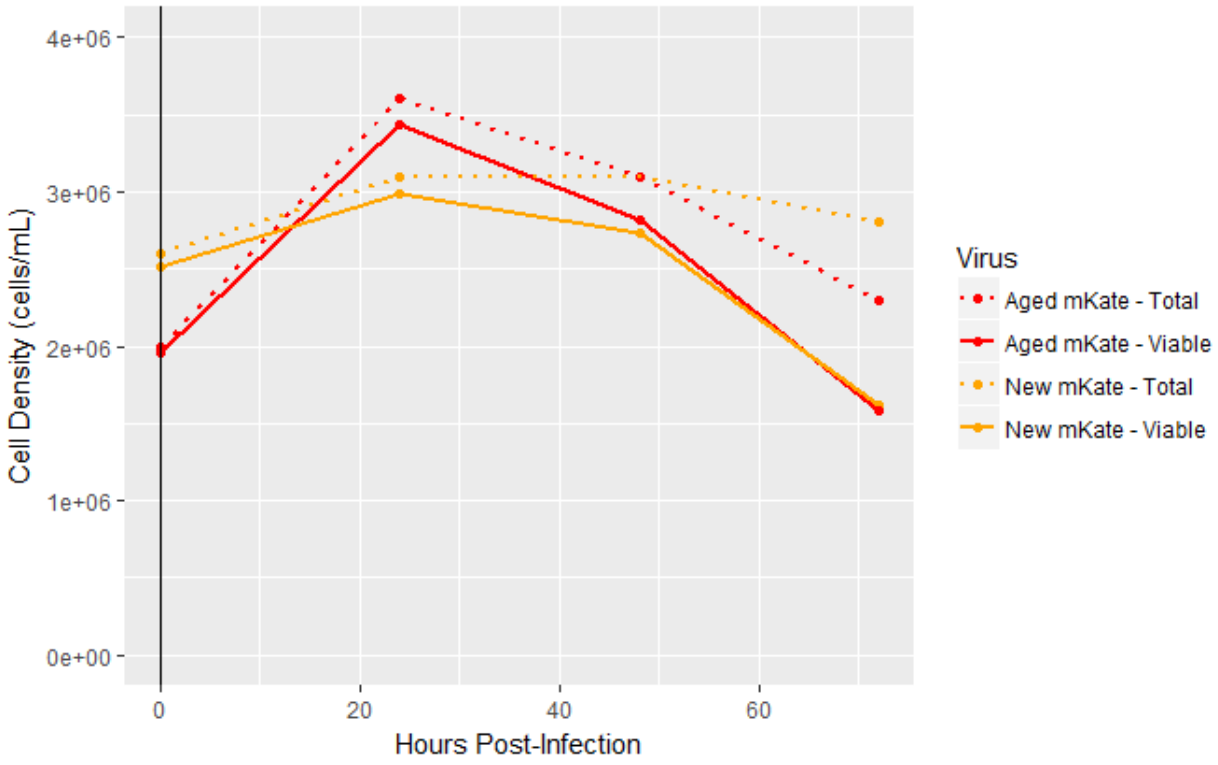

Figure 16: Cell density over the course of infection for new and aged stocks of mKate

Only two flasks were infected, each getting one of the two stocks of virus. Statistical significance cannot be determined due to the lack of replicates, but just from the numbers, the two infections seemed to proceed similarly. The infection with old baculovirus reached a slightly higher peak cell density (3.6 x 10^6 cells/mL vs. 3.1 x 10^6 cells/mL), despite starting from a slightly lower initial cell density. Additionally, the culture infected with old baculovirus saw a sizable drop in overall cell density from 24 to 48 hpi. The drop in total density in this period likely indicates that the 24 hpi count overestimated the density. Despite this possible error in the density count, the cells achieved less than one complete doubling regardless of the virus used. This confirms that the titer was sufficient such that synchronous infection was achieved in both cases.

Section 4.4.2 – Flow Cytometry of Infected Cells (mKate)

Concurrently with the collecting of the above cell density and viability counts, flow cytometry was run on all samples from this infection. Figure 17 below shows the FSC versus SSC measurements that were recorded. In all cases, there were events appearing in the bottom left corner of the plots. These events were at sizes far too small to be attributed to actual cells. A gate was therefore drawn to exclude these events of "noise" and debris, and instead include only what should be actual cells. For consistency, the same gate was applied to all samples. Drawing this gate usually removed approximately 5% of the detected events in each sample. Uninfected cells are also shown as a point of comparison, and can be seen to lie in a region of very low SSC and an FSC that overlaps more closely with the 24 hpi samples than the samples at 48 or 72 hpi.

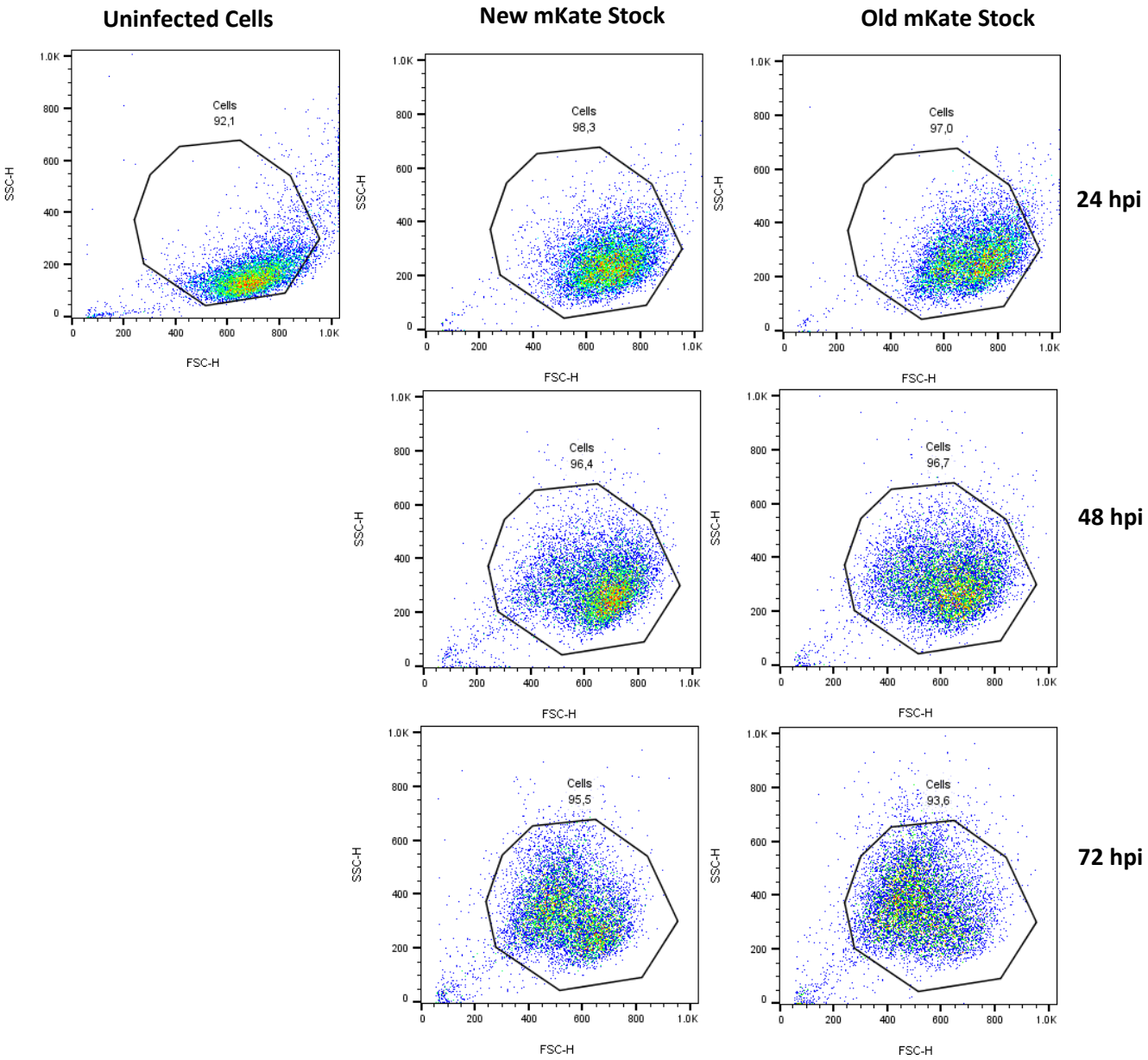

Figure 17: FSC versus SSC measurements for new versus aged mKate stocks. The plot is coloured in accordance with the density of events (areas with high event frequency are in red, while low event frequency areas are shown in blue). An arbitrary gate has been drawn to capture the majority of non-noise events, and the number above it is the percentage of events captured by the gate.

Both infections appear to proceed in a standard manner. The population of infected cells moves to the left (a steady decrease in FSC) and slightly upwards (a slight increase in SSC) in both infections. For the infection with new baculovirus stock, this transition was from an FSC of 667 at 24 hpi to an FSC of 537 at 72 hpi, and from an SSC of 242 at 24 hpi to 318 at 72 hpi. For the old baculovirus stock, this

transition was from a slightly higher initial FSC of 689 at 24 hpi to a slightly lower FSC of 506 at 72 hpi, and from a slightly higher SSC of 260 at 24 hpi to 350 at 72 hpi. As mentioned previously, this trend is the behaviour that has come to be expected in a standard baculovirus infection.

Section 4.4.3 – Fluorescence of Infected Cells (mKate)

These non-noise events were examined in the FL3 channel in Figure 18. It was observed that the two infections progressed in a nearly identical fashion despite the differences in the age of the stocks and differences in the degree of amplification (based on the original amount of P1 stock used). For comparison, the uninfected cells run as a control are shown as well. From this control, it was established that uninfected, non-productive cells can be distinguished from their fluorescent, infected counterparts based on their FL3 signal (or FL1, in the case of GFP infections). For mKate, a cut-off of FL3 < 0.5 was found to be sufficient to remove > 99.9% of events in the uninfected sample, and a cut-off of FL1 < 0.5 was similarly useful in GFP infections.

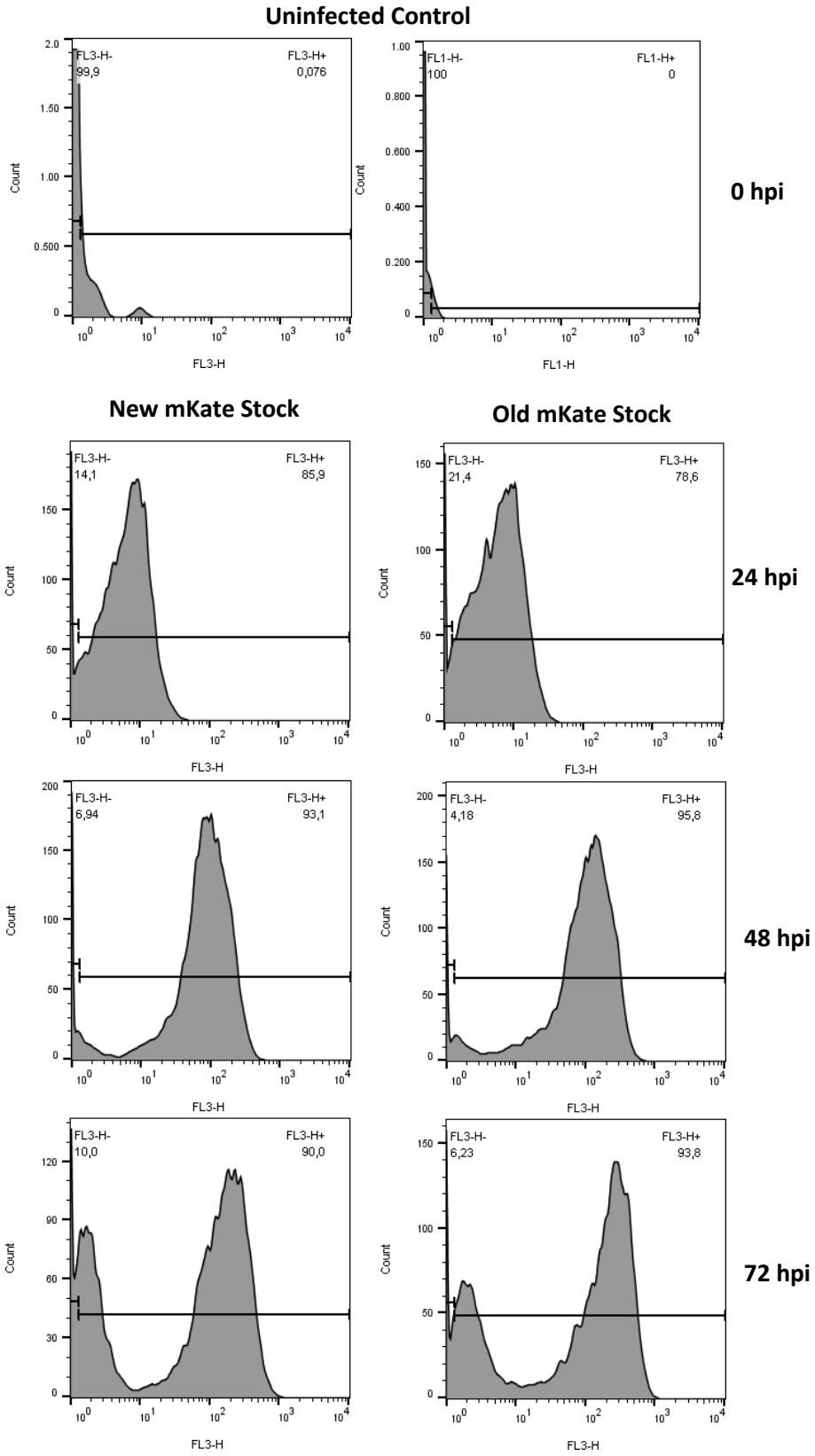

Figure 18: Histograms during the course of infection for new versus aged mKate stocks

At the 24 hpi time point, the infection with the new baculovirus stock appears to be progressing faster. At this point, 85.9% of the cells have exceeded the fluorescence threshold set to distinguish them as being productive. Comparatively, 78.6% of the cells infected with the old stock were similarly productive at this point. Interestingly in this set of histograms, at 48 hpi there are also two populations that appear. However, in contrast to the trend observed for the FL1 vs FL3 plot, the second population in this set of figures progressively grows until 72 hpi rather than merging back into the bulk of the population. Unfortunately, due to the nature of this second population that appears, it also overlaps with any potentially non-fluorescent cells remaining (i.e. those with an FL3 value below 0.5). This is highlighted by the fact that the fraction of cells to the left of the gate is at its lowest at 48 hpi, and then the number goes back up at 72 hpi. Specifically, for the new mKate stock, 6.9% of cells are below the fluorescence threshold at 48 hpi vs 10% at 72 hpi. For the old mKate stock, this is similarly 4.2% of cells at 48 hpi vs. 6.2% of cells at 72 hpi. Despite the increase in peak fluorescence as the infection progresses, the overall mean FL3 for both infections actually decreased as a result of the evolution of this secondary population. The infection with the new mKate stock had a mean FL3 of 54.7 at 48 hpi, and this subsequently dropped to 33.7 at 72 hpi, a 40% decrease. The old mKate stock similarly dropped from 69.8 at 48 hpi to 49.6 at 72 hpi, a 30% decrease. Because the low-fluorescence population continued to grow until the 72 hour time point, it seemed to be unrelated to the initial concern over the split in the fluorescent population appearing at 48 hpi in the FL1 vs FL3 plot. Instead, it was proposed that the low fluorescence population that grew in Figure 18 was as a result of cell death, and that the split population appearing in Figure 15 was as a result of a different mechanism.

The new stock and the aged stock of mKate caused similar effects in the infected cultures, so it was unclear if their fluorescent profiles would differ. Of specific interest was the aforementioned splitting of the populations at 48 hpi when examining the fluorescence in the FL1 vs FL3 plot. The FL1 vs FL3 plots for both infections are shown below in Figure 19.

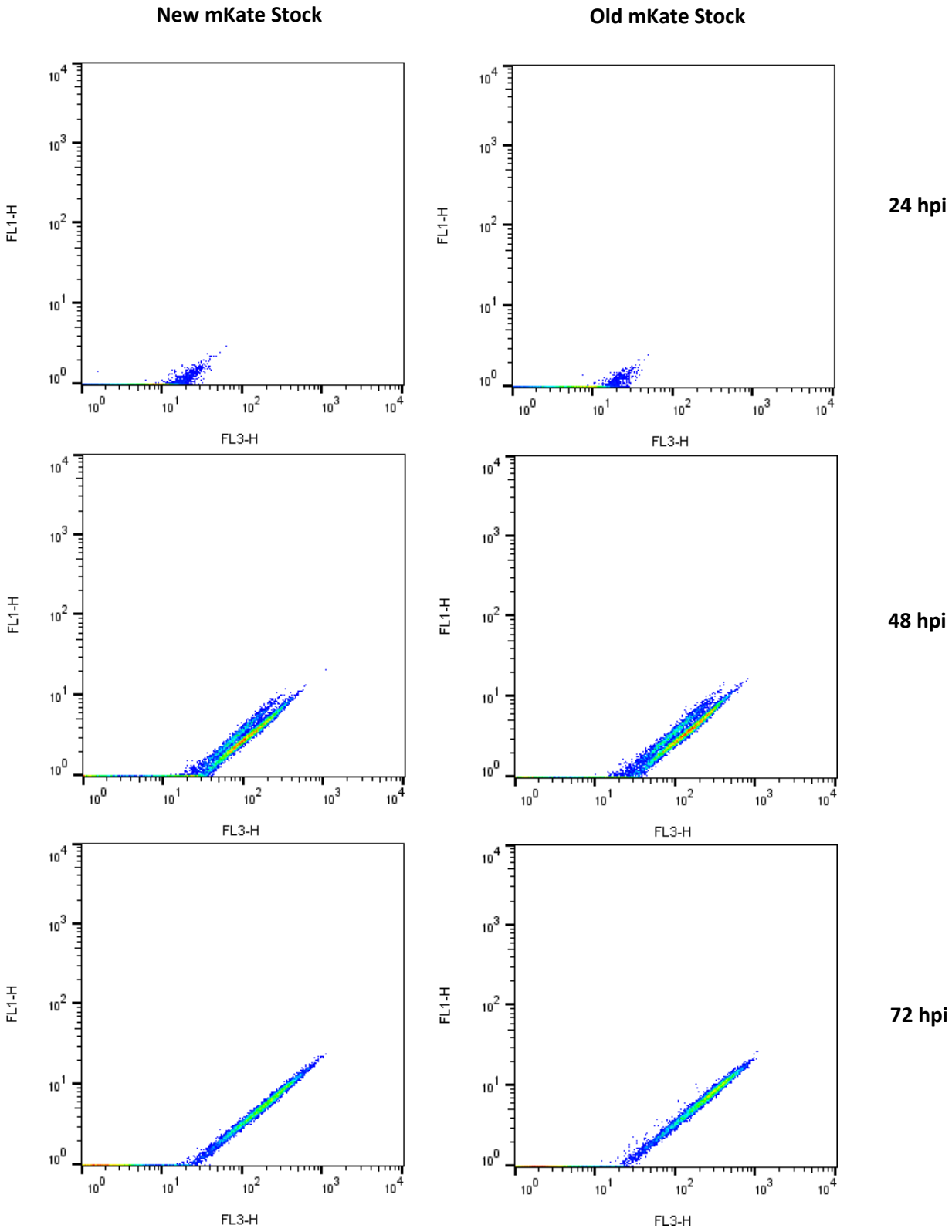

Figure 19: FL1 versus FL3 measurements for new versus aged mKate stocks

The peak FL3 of the cell population increases over the course of infection, and is slightly higher in the case of infection with aged mKate stock. However, as was the case in the preliminary experiments, the split population once again appears at 48 hpi, and is visible in both stocks of mKate. Additionally, just as was the case in the preliminary experiment, this population merges back into one single population by 72 hpi. Since this split was not dependent on the age of the stock, it was hypothesized it may instead be due to some inherent property of the protein itself, perhaps requiring a maturation period to settle into its final state. This was not investigated further in this thesis. While the shift in average fluorescence is overall rather small, because it could not be explained at this point in time and seemed so irregular, it was decided that the mKate construct would not be used in future experiments. The GFP construct gave much more consistent results in this regard, so it was the only construct tested.

Section 4.5 – Results – Cell Viability Analysis for GFP Construct

In the previous section of experiments, the population was gated in the FSC vs SSC domain to capture the majority of events that did not fall within the bottom-left corner (i.e. low FSC signal and low SSC signal) as shown back in Figure 17. The signals falling in the bottom-left corner of this domain were deemed to be a combination of background noise (which shows up even in blank samples, free of cells) and cell debris resulting from cell lysis. The remainder of the cells were analyzed all as one large population and the mean FL1 signal of this population was used as the analogue for cell productivity. This measure was then compared over the three days of the infection. An example of this was taken from one of the preliminary experiments and is shown below in Figure 20.

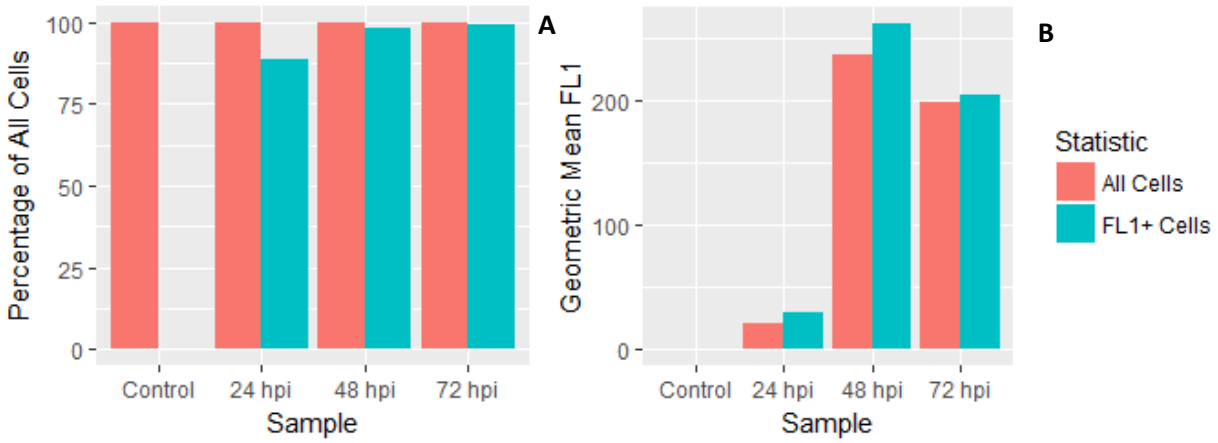

Figure 20: Flow cytometry measures of a standard, low-density infection with GFP baculovirus. **A)** Number of events detected separately from cell debris. **B)** Geometric mean fluorescence. (In both figures, fluorescent cells (FL1+) are denoted as those possessing an FL1 value of at least 0.5)

As discussed earlier, in order to distinguish productive cells from non-productive or uninfected cells, a fluorescence value of 0.5 was chosen. Figure 20A reveals that this was a highly effective infection with approximately 90% of the cells producing fluorescence at 24 hpi. This rises to nearly 100% at 48 hpi and 72 hpi. As expected, there is a corresponding increase in average fluorescence intensity from 24 hpi to 72 hpi. Notably however, the entirety of this increase happens from 24 hpi to 48 hpi. Between the 48 and 72 hour time points, the mean fluorescence tends to decrease by roughly 20% instead. Since the infection continues to progress from 48 to 72 hpi, this seems like a counterintuitive finding.

Section 4.5.1 – Fluorescent Sub-populations in Infected Cultures (GFP)

To better understand this trend, the data were re-examined to look for the cause of the drop in fluorescence. Just as was the case when the mKate stocks were compared (Figure 18), when the histogram of the FL1 channel was investigated, the emergence of two populations was detected starting from the 48 hour time point, and it became even more pronounced at the 72 hour time point. Coincidentally, in the FSC vs SSC domain, it was already known that a shift towards the upper left corner

occurs as the infection proceeds and is indicative of an effective infection. However, the significance of this was not investigated. Therefore, a gate was applied to separate the cells in the FSC vs SSC domain into an "early-stage infection" population and a "late-stage infection" population. The "early-stage infection" gate was defined based on the area the cells occupy at 24 hpi, while the "late-stage infection" gate was set to cover the remainder of the cells falling outside of the "early-stage infection" gate. As was the case with the initial gate to remove cellular debris and noise, the same "early-infection" gate and "late infection" gate was applied to all samples in this experiment. This was done for all time points, and an example of this is shown below in Figure 21 for a 72 hpi sample.

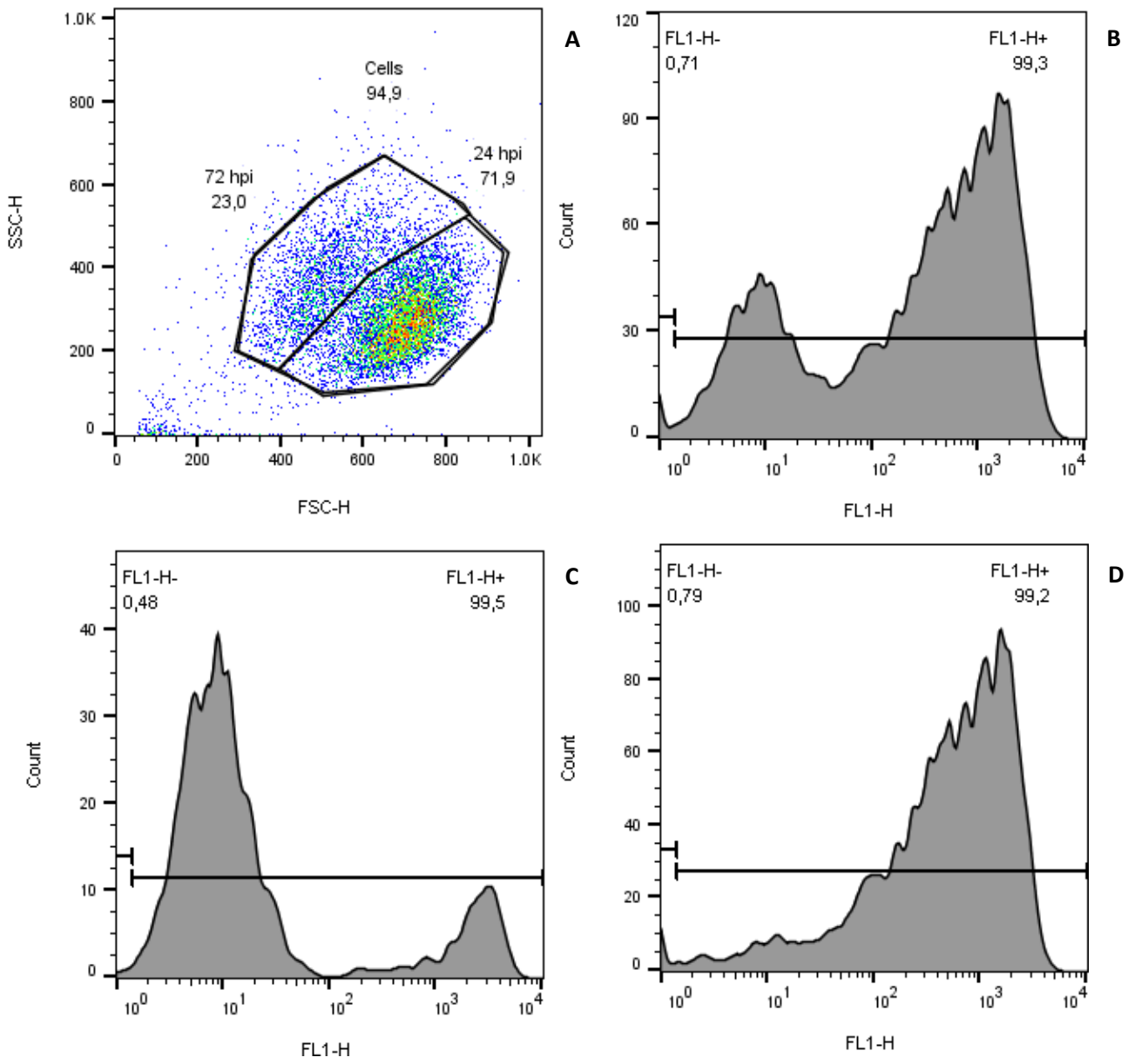

Figure 21: Flow cytometry gating at 72 hpi. **A)** Gating to separate two populations present in the FSC vs SSC domain. The plot is coloured in accordance with the density of events (areas with high event frequency are in red, while low event frequency areas are shown in blue). **B)** FL1 histogram of both gates when summed together. **C)** FL1 histogram of only cells within the leftmost gate, assumed to be dying or compromised cells. **D)** FL1 histogram of only cells within the rightmost gate, assumed to be living cells.

In this figure, there is a remarkable difference in the average fluorescence of the two populations. While some overlap in the fluorescence exists, the bulk of the events are grouped quite well. The "early-stage infection" gate, i.e. the gate set based on the 24 hpi samples, contains the bulk of the cells

expressing high intensity fluorescence, while the majority of the cells outside of this gate possessed low fluorescence. Also, in contrast to the experiment comparing the mKate stocks, it is worth noting that the GFP-expressing cells in the low-fluorescence population still exceed the lower threshold set to separate them from uninfected or non-productive cells.

Section 4.5.2 – Effect of Cell Death on Fluorescence

It was hypothesized that the events occurring outside of the 24 hpi gate might correspond to cells that are no longer in a healthy morphology, or are compromised in some way. In order to test this hypothesis, a preliminary experiment was performed wherein infected cells at 24, 48, and 72 hpi were physically lysed by using either ethanol or a fast freeze-thaw cycle. The FSC versus SSC profiles resulting from this experiment are shown in Figure 22.

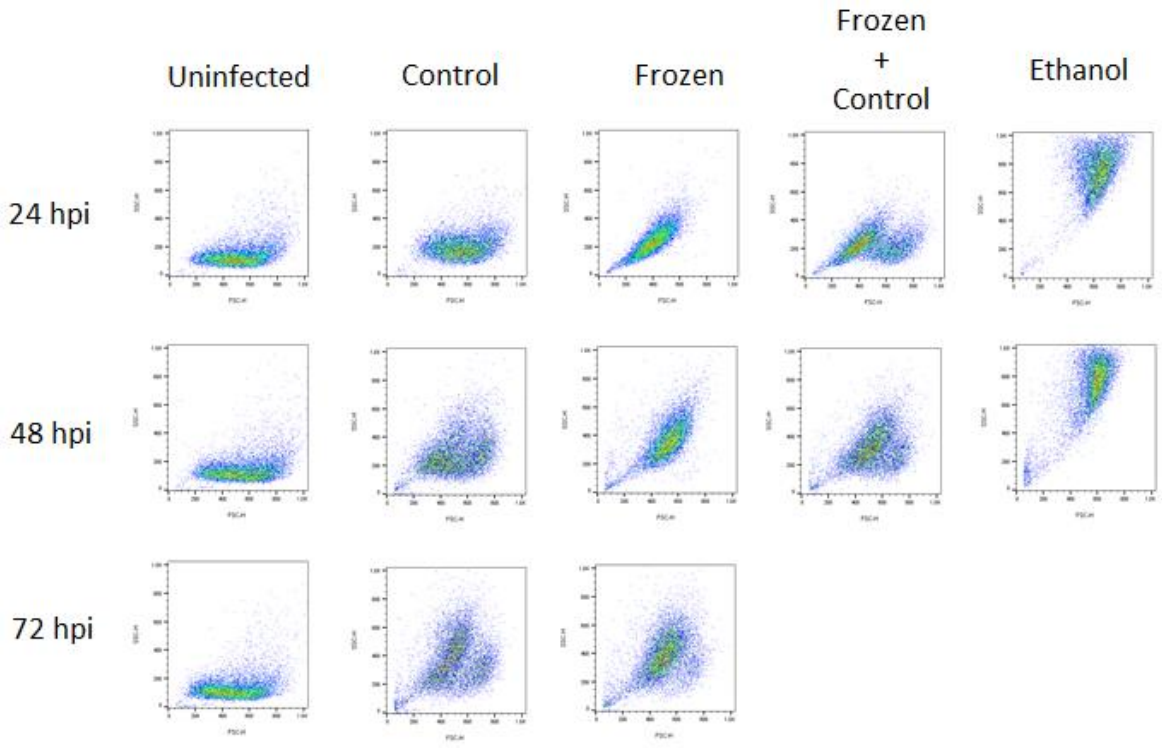

Figure 22: SSC versus FSC plot of killed and control cells. (The "Uninfected" condition corresponded to cells taken from a growing maintenance flask and prepared for flow cytometry as normal. The "Control" condition corresponded to cells taken from a flask infected at 2 x 10^6 cells/mL with the GFP baculovirus at an MOI of 5. The "Frozen" condition corresponded to cells taken from the "Control" flask, transferred to a -80^{o}C freezer for until fully solid, then rapidly thawed in a 27^{o}C waterbath and thawed. The "Frozen+Control" condition corresponded to a 50% mixture of the "Control" and "Frozen" cell cultures prepared for analysis, prepared with the intent of revealing the overlap between the two populations. The "Ethanol" condition corresponded to cells taken from the "Control" flask which were subsequently centrifuged, resuspended in 70% ethanol for 2 minutes, then prepared for flow cytometry as normal. FSC has been plotted on the x-axis, and SSC has been plotted on the y-axis.)

The ethanol-killed cells did not work as intended, as the process seemed to drastically alter the cellular morphology. This condition was therefore ignored at the 72 hpi time point. However, cells that were damaged by freezing lined up very well with the population of cells tentatively assigned the label of "compromised" in the control infection. As an additional point of interest, the fluorescence histograms of the cells exposed to these different conditions were compared in Figure 23.

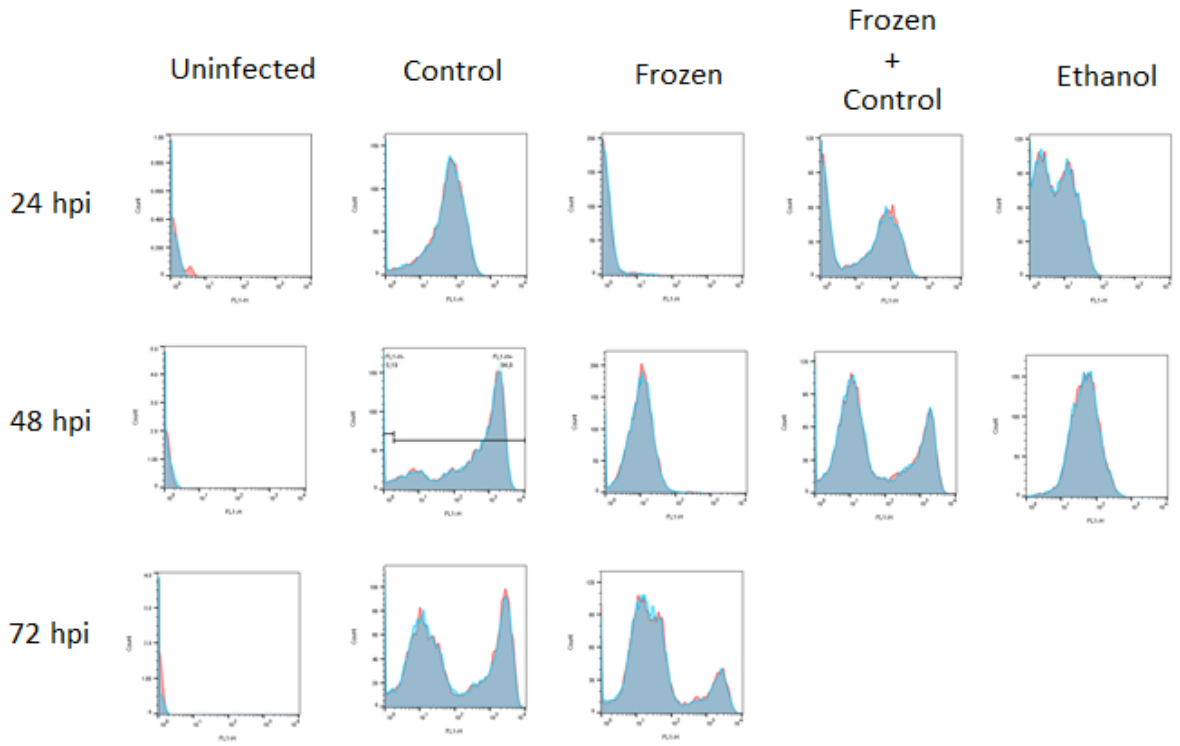

Figure 23: FL1 Histograms of cells exposed to various lethal conditions. (The "Uninfected" condition corresponded to cells taken from a growing maintenance flask and prepared for flow cytometry as normal. The "Control" condition corresponded to cells taken from a flask infected at 2 x 10^6 cells/mL with the GFP baculovirus at an MOI of 5. The "Frozen" condition corresponded to cells taken from the "Control" flask, transferred to a -80^{o}C freezer for until fully solid, then rapidly thawed in a 27^{o}C waterbath and thawed. The "Frozen+Control" condition corresponded to a 50% mixture of the "Control" and "Frozen" cell cultures prepared for analysis, prepared with the intent of revealing the overlap between the two populations. The "Ethanol" condition corresponded to cells taken from the "Control" flask which were subsequently centrifuged, resuspended in 70% ethanol for 2 minutes, then prepared for flow cytometry as normal. FL1 has been plotted on the x-axis versus the event count on the y-axis.)

The cells that were damaged (whether by freezing or by ethanol) all possessed a much lower level of fluorescence than their control counterparts. However, as was the case in Figure 22, the pattern exhibited by the frozen cells is extremely similar to the one exhibited by the control infection, as it progresses and cells die. Notably, at 48 and 72 hpi, once the infected cells have produced substantial amounts of GFP, the fluorescence does not drop all the way to 0 after the cells are freeze-killed. In particular, the similarity between the 48 hpi "Frozen+Control" sample and the 72 hpi "Control" culture was striking. The fluorescence profiles of the two cultures looked extremely similar, albeit with a

difference in the distribution between the healthy (high-fluorescence peak) and compromised (low-fluorescence peak) parts of the population. A rough comparison of the overlap between the populations and their segregation in the FSC vs. SSC domain can be found in Appendix E, Figure E1.

Section 4.5.3 – Staining for Cell Death

As a follow-up to this experiment for a more accurate confirmation of the leftward growing population corresponded to dying or compromised cells, a cell membrane-impermeant dye, propidium iodide, was introduced to samples immediately prior to flow cytometry analysis. The dye exhibits a much higher level of fluorescence upon binding with DNA and is therefore able to serve as an effective indicator of the integrity of the cell membrane. Any cell that is still alive and healthy will express only low levels of red fluorescence due to the dye sticking to the membrane, while any cell with a compromised membrane will express an intense red fluorescence.

A first experiment with the propidium iodide revealed a distinct separation of different populations in all samples. These are compared below in Figure 24. Only the 48 and 72 hpi time points were examined due to the relatively low amount of cell death appearing at 24 hpi. A contour plot was used to better illustrate the apparent differences between the populations appearing (in the low cell-density infection) and to reveal the populations appearing at the left axis (in the case of the control and high cell-density infection).

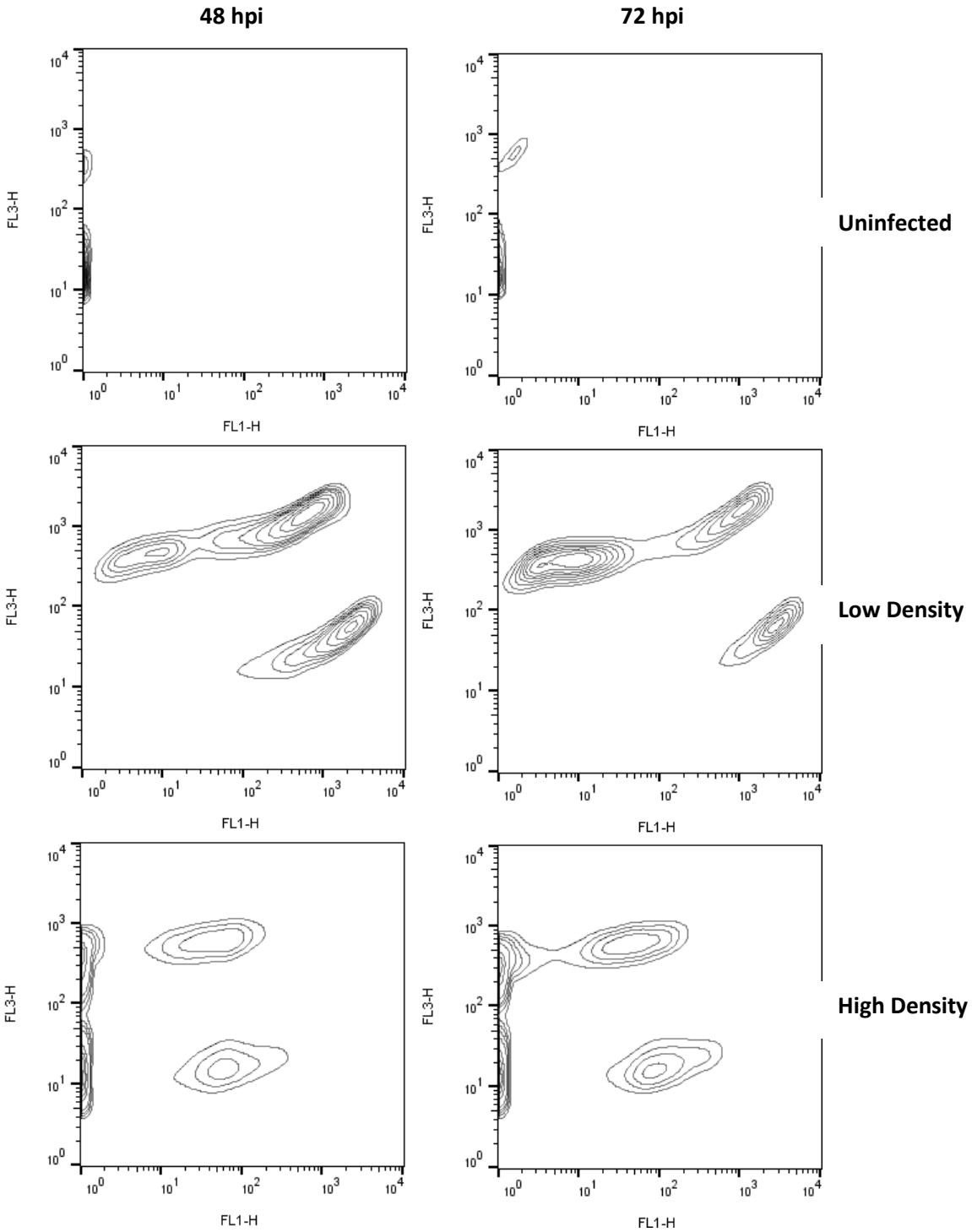

Figure 24: FL1 vs FL3 domain of cultures treated with propidium iodide. FL1 intensity, tracked on the horizontal axis, is a measure of the GFP production. FL3 intensity, tracked on the vertical axis, is an indicator of cell viability, with healthy cells possessing low FL3 values and damaged cells possessing high FL3 values. At 48 (left column) and 72 (right column) hours post-infection, a low cell-density (middle row) and high cell-density infection (bottom row) were compared alongside an uninfected, control sample taken from a maintenance flask (top row)

In Figure 24, it would appear that as many as four separate populations may be present in the samples. In the uninfected samples, only two populations are visible and neither has any significant level of green fluorescence (i.e. no reading in the FL1 channel), as expected. The majority of the cells are in the low FL3 group suggesting that the majority of the cells are still viable at the time of flow cytometry.

In the low cell-density infection shown in the second row, 3 populations are visible at both 48 and 72 hpi. The bottom right population (low FL3, high FL1) corresponds to viable, infected cells. The upper left population (high FL3, low FL1) would seem to correspond to the population identified in the preliminary experiments – cells that were productive but now have a compromised cell membrane. The last population is a new subset of the cells that was not identified previously. The high FL3 suggests that the membrane is compromised but the high FL1 suggests that there is still a lot of the GFP present within the cells. The significance of this population is not known at this time, but it could be hypothesized that it represents an intermediate stage as the cells transition from the bottom-right to upper-left population, wherein the cell retains most of its physical appearance but something occurs to the GFP contained within. That is, the disruption of the cell membrane as the infection nears its terminal stage could lead to diffusion of the GFP out through the compromised membrane, or the change in the internal pH could lead to disruption of the protein, or the cell death signal could lead to its rapid degradation.

In addition to this unusual third population, there was a fourth population that appeared in the case of the high density infection. This new population appeared in the bottom-left portion of the FL1 vs FL3 plot (low FL3, low FL1), an area that was empty in the case of the low density infection. This population would correspond to cells that are alive, but unproductive. This seems to be a population that would actually be expected, and can be interpreted as a confirmation that the cell-density effect is in effect in this culture, acting to reduce the efficiency of the infection.

Section 4.5.4 – Stability of Cell Membrane During Flow Cytometry

One issue that came up in this experiment is that far too many cells that were supposed to be alive were appearing as dead (i.e. exhibiting a high FL3 signal). In the uninfected cell samples where viability would be expected to be around 98-99%, instead 10-25% of the cells were apparently dead based on the propidium iodide stain. No concentration of PI tested appeared to have a negative impact on the health of the cells, and attempts to reduce the stress on the cells during the media removal and flow cytometry preparation steps did not have any effect on the level of cell death observed (See Appendix Figure E1). Additionally, it appeared that the level of cell death was not related to the propidium iodide itself. Decreasing the concentration used had a minimal impact on the level of fluorescence attained and had no effect on the apparent cell death. Rather than these possibilities, it seemed that the cell death was an artifact of the fixative, PFA, used before taking cells to the flow cytometer. The effect of the PFA on the cell morphology is shown below in Figure 25 as compared re-suspension in a saline solution alone.

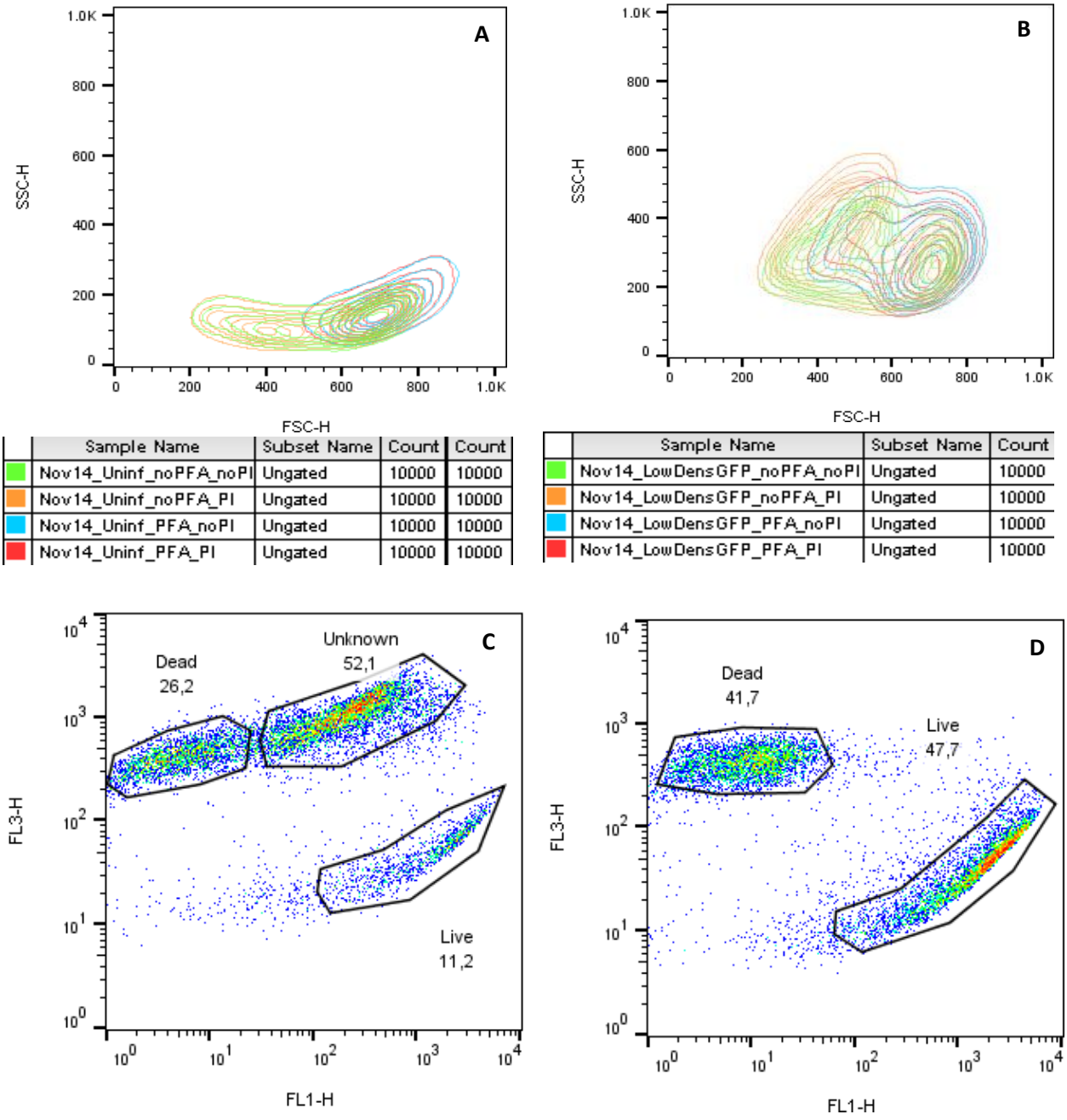

	Sample Name	Subset Name	Count	Count
	Nov14_Uninf_noPFA_noPI	Ungated	10000	10000
	Nov14_Uninf_noPFA_PI	Ungated	10000	10000
	Nov14_Uninf_PFA_noPI	Ungated	10000	10000
	Nov14_Uninf_PFA_PI	Ungated	10000	10000

	Sample Name	Subset Name	Count
	Nov14_LowDensGFP_noPFA_noPI	Ungated	10000
	Nov14_LowDensGFP_noPFA_PI	Ungated	10000
	Nov14_LowDensGFP_PFA_noPI	Ungated	10000
	Nov14_LowDensGFP_PFA_PI	Ungated	10000

Figure 25: Comparison of PFA-fixed versus non-treated populations after GFP infection. **A)** FSC vs SSC domain for uninfected cells taken from a low density maintenance flask (November 14), and treated with or without PFA and with or without PI. **B)** FSC vs SSC domain for cells taken from a low cell-density infection at the 72 hpi time point treated with or without PFA and with or without PI. **C)** FL1 vs FL3 domain for infected cells 72 hpi treated with PFA and with PI. **D)** FL1 vs FL3 domain for infected cells 72 hpi treated without PFA and with PI

In both Figure 25A and 25B, samples with or without PI overlap nearly perfectly. It can therefore be concluded that the PI solution has no effect on the cell morphology. However, there is a distinction between the samples with PFA and those without PFA. In Figures 25C and 25D, it is evident that the inclusion of PFA in the sample is the cause of the transition population with high FL1 and FL3 readings. Without PFA (Figure 25D), the cells only exist in one of two states: either alive and with a lot of GFP, or compromised and with little GFP. Additionally, there are roughly four times as many living/intact cells in the sample that was not treated with PFA than in the sample that was treated with PFA. This is an indication that the PFA is forcing cells out of the "Live" gate upwards into the "Unknown" gate instead of acting as a proper fixative and "locking" cells that are already on their way to the "Dead" gate in that state. On the other hand, the redeeming feature of the case where PFA is used is that it effectively does its job of preserving the state of the cells. In Figure 25C and D, the percentages shown below each gate are out of the total number of events. Adjusting the numbers to only account for gated events, roughly 70% of the gated events in Figure 25C do not fall in the "Dead" gate (i.e. $\frac{Live+Unknown}{Live+Dead+Unknown}$). In contrast, only 53% of the gated cells are alive in Figure 25D (i.e. $\frac{Live}{Live+Dead}$). Thus, even though PFA appears to permeabilize the membrane enough that PI is capable of entry into the cells, the process does not allow for significant degradation of the accumulated GFP. Without PFA, the cells will continue to die throughout the period of preparation for flow cytometry. Taken together, this means that the two populations observed in Figure 18 do indeed correspond to healthy and compromised cells respectively, as was hypothesized.

Section 4.6 – Discussion

Section 4.6.1 – Metabolite Composition of Baculovirus Stocks

The metabolic profiling was initially performed on the baculovirus stocks due to concerns over the quality of the stocks. An infection at a high cell-density of 10 x 10^6 cells/mL would require roughly a roughly an addition of baculovirus stock equal to roughly 10% of the culture volume. For this reason, if

there are any major differences in the metabolite profile of the baculovirus stock compared to plain media, then it is possible that the addition of the stock itself to a culture could significantly affect the conditions feeding the cells.

These baculovirus stocks were generated from infections taking place at low cell-densities and were therefore collected during the early stages of the culture. Overall, the profiles completed here suggest that there is little difference in the metabolic composition of the baculovirus stock and fresh media. As such, even when the baculovirus stock is added in a high cell-density infection at 10% of the culture volume, it should have a fairly negligible impact on the overall composition of the culture. As mentioned previously however, there are limitations to what ^{1}H-NMR is capable of detecting. The drawback is that, if small signalling molecules are released by the cells as suggested by Ikonomou et al., then they will not be detected here and any effect they have could end up being attributed to something else (Ikonomou et al., 2004)

When comparing the GFP virus stock with the mKate virus stock, there was little difference in the effect that they had on the cells. Aside from the initial titer and the channel that they cause the cells to fluoresce in, they have little impact on the metabolic conditions imposed on the cultures. Neither exhibited any obvious, unusual metabolic trends. For both sets of metabolic profiles, the consumption patterns line up with the expectation for a standard, low density batch culture that is only grown for a few days.

Section 4.6.2 – Flow Cytometry Methodology for Gating Fluorescent Cells

With regards to the decision to use flow cytometry as a method of analysis, it seems to be quite potent. With the discoveries made in the cell viability experiments of this chapter, the following can be concluded to be an improvement to the analysis method used in Figure 20. The bulk of the cell population should be gated first in the FSC vs SSC domain to remove any events corresponding to noise or debris. Next, the lower-right population of the cells (primarily visible at 24 hpi) should be gated to

separate live cells from dead cells. As cells die, their average fluorescence drops drastically and thus they should not be considered when assessing the net productivity of the infection. Lastly, for this flow cytometer setup, all gated populations should have a gate added at an FL1 value of 0.5 so as to allow for the optional separation of uninfected or non-productive cells. It should be noted that this floor value for determining the fluorescence threshold would likely need to be set to a different value on another machine depending on the baseline noise exhibited in an uninfected sample. Additionally, for any attempts made to estimate the overall productivity of the infection, the average viability of the cells determined by the trypan blue method should be used (i.e. since the flow cytometry appeared to lead to some level of cell death in the case when PFA is used). Analyzing the flow cytometry data shown in Figure 20 again under this new gating scheme, the following figure was generated.

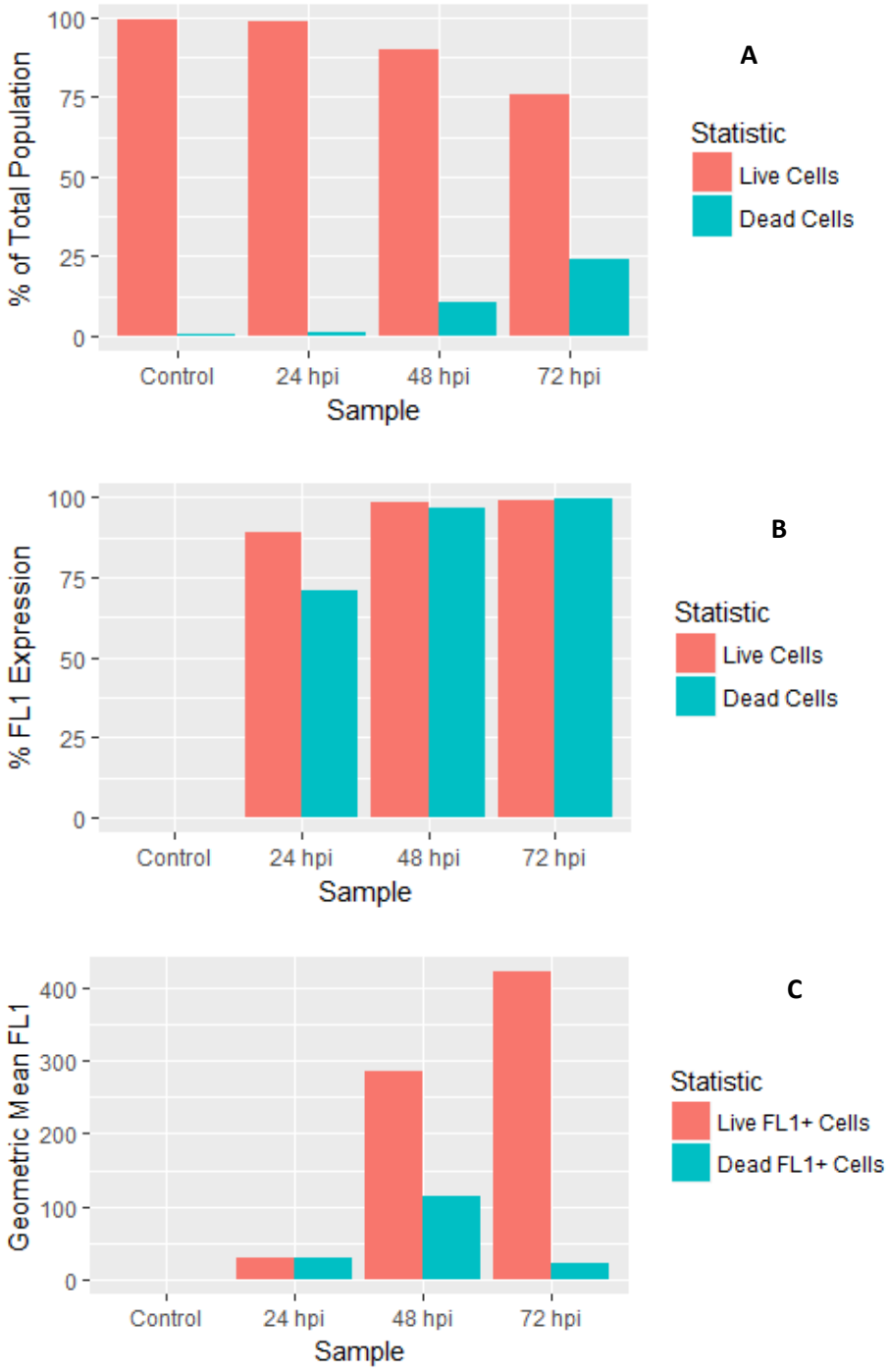

Figure 26: Re-gating the data used to construct Figure 20 **A)** Proportion of cells in the gates demonstrated in Figure 21 **B)** The prevalence of fluorescent (FL1+) cells within those populations, where fluorescence is defined as having an FL1 value > 0.5 **C)** Geometric mean FL1 fluorescence of the newly gated populations

In Figure 20, the red bar (All Cells) was at 100% at all time points, as it includes both living and dead cells. In contrast, in Figure 26A it has been broken into two separate and better reflects the change in cell viability as the infection progresses, decreasing from near 100% at 24 hpi to roughly 75% at 72 hpi. In Figure 26B, it is interesting to note that fluorescence appears in the dead cell population slightly more slowly than in the living cell population, and this is in line with the expectation that cells that die early on will not have had enough time to accumulate much GFP yet. In Figure 26C, under this new gating scheme, the 48 hpi average fluorescence is slightly higher than in the case when the entire population was gated. Additionally, from 48 hpi to 72 hpi, the average fluorescence of the living cells increases a further 60% in contrast to the overall fluorescence which was seen to decrease in Figure 20. There is a large drop in the average fluorescence of the dead cells from 48 hpi to 72 hpi. It is possible that this suggests that there may be a process of cell death occurring during this period that leads to a progression of the fluorescence decline. However, it is also important to note that the dead cells population at 48 hpi only constituted approximately 12% of the cells in the sample. In that case, if a few healthy cells spilled over out of the 24 hpi "early-stage infection" gate it could have a noticeable impact on the recorded fluorescence.

Overall, this is quite interesting. Compared to the initial analysis method proposed in Figure 20, this method of analysis provides a more nuanced view of the makeup of the infected cell culture and how the conditions used may be affecting the infection. Specifically, it is now clear that for the population of cells that are still alive (at least up to 72 hpi), the fluorescence will continue to accumulate to increasingly high levels. Furthermore, while not applicable in this particular case, this new method allows for a distinction to be made about different populations and this will be particularly useful for the Placket-Burman design to be covered in Chapter 6. For instance, at a comparable time point two samples could have a nearly equal mean overall FL1 value, but for different reasons. If one were to have a faster onset of cell death, but also a faster production of GFP, the old analysis would not be able to pick up on this

distinction whereas the new one would. Alternatively, if the fluorescence of the "Dead cells" population were to drop, the new method could distinguish a drop in infection efficacy (an increase in the percentage of cells that are dead and lack detectable fluorescence) and genuine change occurring to the dead cells (a change in the mean fluorescence of the cells that were previously alive and productive).

Contrary to the promise of this method, to mention one of its drawbacks, it should be noted that the ratios of events in the gates should be used with caution. As demonstrated in Figure 25, the inclusion or exclusion of PFA in the samples appears to have a major impact on the apparent amount of cell death. When a chemical indicator such as PI is used, the presence of PFA will greatly increase the amount of cell death reported, and conversely the absence of PFA will allow for continual cell death to occur between the time of their harvesting and the time at which they are run through the flow cytometer. Incidentally, the ratio of events in the 24 hpi gate compared to the total number of cells is somewhat reflective of the expected cell viability, but it is unreliable and tends to underestimate viabilities by upwards of 10%. As such, considering the options, it is best to rely on the initial viability readings taken by the Trypan Blue method at the hemocytometer as opposed to approximating the viability based on flow cytometry data.

Additionally, as an added drawback to this method, while it is extremely insightful about individual cell characteristics, it does a less effective job at describing the cumulative situation in the flask than other methods would. This is because other methods such as assessing β-galactosidase activity look for the protein of interest in the culture supernatant instead of inside of the cells themselves. Even in the case where GFP is the product of interest, an extracellular method of analysis would be usable if the product is released and accumulates in the spent media. Sander & Harrysson for instance made use of a fluorescent plate reader to determine the amount of GFP accumulating in the culture supernatant and the intracellular space (Sander & Harrysson, 2007).

Overall, this method does have limitations. It does not perform as well as other, previously established methods with regards to analyzing the output of the culture as a whole. However, because

this flow cytometry method allows for such an in-depth analysis by separating the culture into physiologically-different populations of cells, it provides another layer to the analysis that is not available with the older methods.

Chapter 5 – Results of Infection Studies

In this section, the methodology developed in the previous chapter was applied to an infection experiment with the intent of improving the protein productivity of the cells at high cell-densities. Initially, several infections were carried out to establish a baseline for the expected productivity levels. This was followed by a Placket-Burman design experiment wherein several different metabolites (identified in Chapter 4 as being of interest) were tested to determine their effect on productivity. A Placket-Burman was selected as the experimental design choice due to its power for separating the effects of multiple confounded factors. In this thesis, 8 different metabolites were identified as being of interest, and as such, carrying out a full factorial experimental design to determine the effects of each metabolite would require an overwhelming number of experiments. In the Placket-Burman design, however, the primary effects of these different factors can be distinguished in just 12 runs. This chapter will conclude with an analysis of the results and a discussion of areas that could continue to be explored in further work.

Section 5.1 – Methods

Section 5.1.1 – Methods – GFP Baselines

The first experiment aimed to set up baselines for the productivity of cultures infected with the GFP- baculovirus construct. Infections were carried out at either low cell-density or high cell-density. For the low cell-density condition, cells were infected near 2 x 10^6 cells/mL. For the high cell-density condition, cells were infected around 8 x 10^6 cells/mL. In all cases, cells were seeded at 0.6 x 10^6 cells/mL in flasks with a 30 mL working volume, and were allowed to grow until the target infection density. In both sets of infections, the cell cultures were either subjected to media replacement or were left untreated in their spent media. In the case of media replacement, the procedure followed was identical to the method used in previous chapters. Each experimental condition was run in triplicate, and two additional flasks were added as non-infected control cultures. As well, the first control was similarly

treated by carrying out a media replacement, while the second control remained in its spent media. In all cases, the addition of baculovirus stock corresponded to less than 10% volume addition.

During the course of the infection, the cells were tracked for three days. During this period, the cell density and cell viability were measured daily via the cell counter as usual. The samples were further analyzed by flow cytometry and ^{1}H-NMR spectroscopy in accordance with the procedure outlined in the general methods section.

Section 5.1.2 – Methods – Placket-Burman-based Metabolite Additions

In this experiment, cells were seeded into 12 flasks, each with a 30 mL working volume at a cell density of 0.6 x 10^{6} cells/mL. After seeding, the flasks and were left to grow until the target infection density. To mimic the high cell-density condition of the GFP baseline experiment, cells were infected around 8 x 10^{6} cells/mL.

In this experiment, one hour before infection, cells were each dosed with an addition of metabolites according to a Placket-Burman design. The conditions applied in each flask are shown in Table 1 below, and the concentrations chosen (as selected based on the ^{1}H-NMR profiles of standard high cell-density cultures) are shown below in Table 2. For each compound, the low concentration condition (-) corresponded to no addition of said compound, and was replaced with an equivalent volume of 1x PBS. To prepare each compound, the required amount was added to 0.5 mL of MilliQ water. However, due to solubility limitations, this was an inadequate volume to fully dissolve all compounds. Therefore, each cell culture was individually centrifuged (200 x g, 10 minutes) to pellet the cells, the majority of the supernatant was removed, and the assigned compounds were added directly to the supernatant as outlined Table 1. This spent media plus spike was then sterile filtered and re-introduced to the cells, and the pellet was re-suspended using a 5 mL pipette.

Table 2: Placket-Burman assignment of metabolite additions

	Fructose	Fumarate	Hypoxan.	Succinate	Choline	Inosine	Uracil	Uridine
Run 1	+	+	+	+	+	+	+	+
Run 2	+	+	+	+	-	-	-	+
Run 3	+	+	-	-	-	+	-	-
Run 4	+	-	+	-	+	+	+	-
Run 5	+	-	-	+	-	-	+	-
Run 6	+	-	-	-	+	-	-	+
Run 7	-	+	+	-	-	-	+	-
Run 8	-	+	-	+	+	+	-	-
Run 9	-	+	-	-	+	-	+	+
Run 10	-	-	+	+	+	-	-	-
Run 11	-	-	+	-	-	+	-	+
Run 12	-	-	-	+	-	+	+	+

Table 3: Selected concentrations for the high concentration (+) condition

Metabolite	Concentration (mM)
Fructose	10.00
Fumarate	0.20
Hypoxanthine	2.50
Succinate	2.50
Choline	1.00
Inosine	1.00
Uracil	2.00
Uridine	1.25

After waiting an hour for the cells to adapt, the cultures were infected with the GFP baculovirus construct at an MOI of 5. In all cases, the addition of baculovirus stock corresponded to less than 10% volume addition. During the course of the infection, the cells were tracked for three days. During this period, the cell density and cell viability were measured daily via the cell counter. The samples were further analyzed by flow cytometry and ^{1}H-NMR spectroscopy in accordance with the procedure outlined in the general methods section.

Section 5.2 – Results – GFP Baselines

In this first experiment, the goal was to establish the fluorescence and metabolism baselines for infected cells. Cells were infected at both low cell-densities and high cell-densities to examine the overall impact that the cell-density effect would have on the expected level of fluorescence. Because it has been well reported that the cell-density effect can be mitigated through various media replacement or feeding strategies, this condition was also covered in this baseline experiment. Flasks either received media replacement (MR) or no treatment (no MR) prior to infection. The cell-density effect was demonstrated – low density cultures had an average cell fluorescence nearly double that of high cell-density cultures. However, media replacement did not appear to have a major effect in this experiment. At high cell-densities, media replacement only caused a very slight increase in average fluorescence; at low cell-densities, media replacement actually caused a slight drop in average fluorescence.

Section 5.2.1 – Results – Low Cell Density Infection Results

The cell density profiles for the MR condition and non-MR condition of low cell-density infections are shown below in Figure 27. The densities of viable cells alone are shown as well as the total cell densities for comparison.

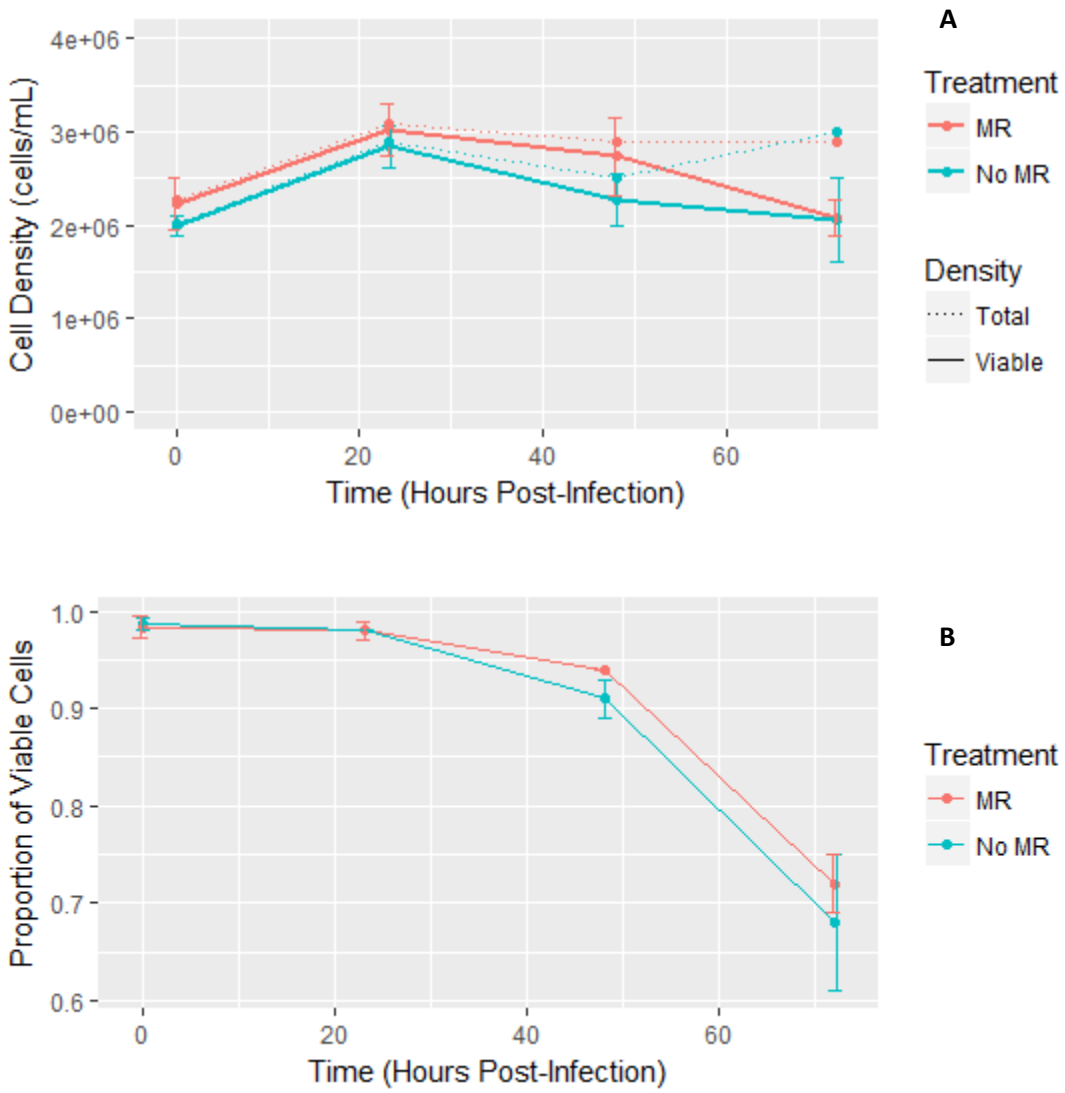

Figure 27: Progression of low cell-density infection. **A)** Total cell density and viable cell density over the course of infection. **B)** Viability over the course of infection. (n = 3 and error bars = 1σ. MR indicates that the cells receaved a full media replacement treatment immediately prior to infection with the baculovirus construct. No MR did not receive this treatment, and was infected as normal)

Figure 27A shows that the cells were infected at or just above 2 x 10^6 cells/mL and that the infection proceeded as has been previously observed. Cells experienced less than one doubling, confirming the expectation that the infection is synchronous. The media replacement strategy does not

appear to have any noteworthy effect on the viable cell density as shown by the overlapping error bars at 24 and 48 hpi, and by the equal cell density at 72 hpi. The cell viability alone is plotted in Figure 27B, and demonstrates that the viability of both conditions also progressed in a nearly identical manner. As expected from past infections, the viability dropped to roughly 95% after 48 hours, then down to 70% after 72 hours.

Section 5.2.2 – Results – High Cell Density Infection Results

The data from a set of high cell-density infections are shown in Figures 28A and B. Additionally, two separate non-infected controls were included with this experiment. The first was a flask subjected to batch growth conditions (i.e. with no additions for the duration of the culture) while the second was subjected to a media replacement in a manner identical to the infected flasks.

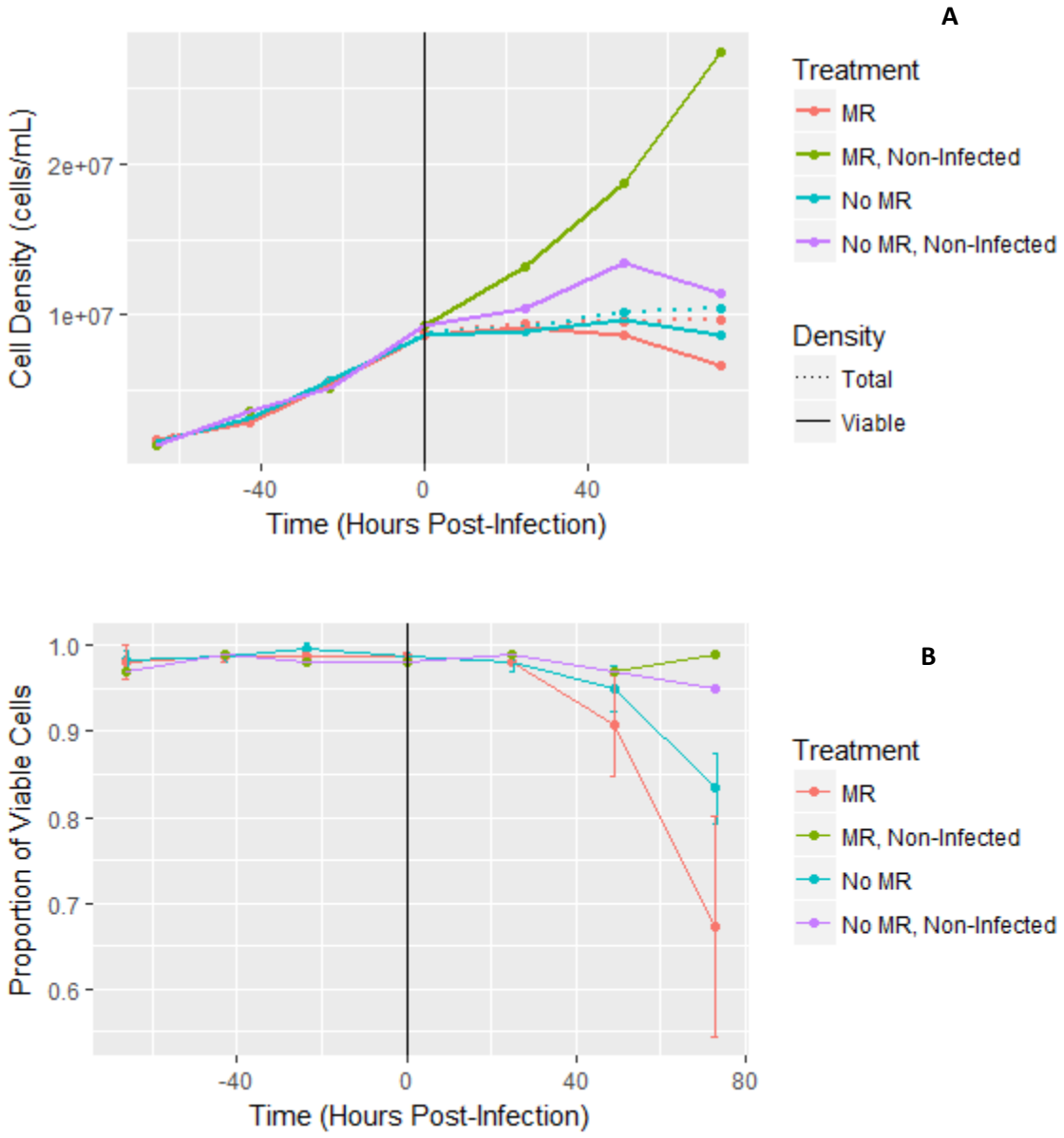

Figure 28: Progression of high cell-density infection. **A)** Total cell density and viable cell density over the course of infection. **B)** Viability over the course of infection. (n = 3 and error bars = 1σ. Two control flasks of non-infected cells were tracked alongside the infections to provide a into the synchronicity of the infection and the cessation of cell growth. MR indicates that the cells receaved a full media replacement treatment immediately prior to infection with the baculovirus construct. No MR did not receive this treatment, and was infected as normal. The vertical line indicates the time at which the cells were infected with the baculovirus)

In Figure 28A, the growth of control cultures are shown in addition to the growth profiles of the high cell-density infections. As was the case in the low cell-density infection, cell growth effectively ceased after introducing the baculovirus. The cell density achieved under both infection conditions at high cell-density were lower than what was achieved in the control cultures; the infected cultures only achieved a maximum peak cell density of 10 x 10^6 cells/mL as opposed to the 14 x 10^6 cells/mL maximum density in the uninfected control without media replacement, or the 27 x 10^6 cells/mL maximum density achieved in the uninfected control with media replacement. This effectively confirms that the infection is still occurring synchronously in the high cell-density conditions.

Shown in Figure 28B, the viability of the cultures varied more than was the case in the low cell-density infections. The MR control culture maintained a viability of 99% at the final time point whereas the "no MR" control was slightly lower at 95%. In the infected cultures, the "no MR" condition dropped to 80% viability at the final time point. On the other hand, the viability of the infected culture with MR dropped the lowest, down to 70% viability. It is interesting to note that this latter value was very similar to the viability trend observed in the low cell-density infections. This suggests that in the case of a high cell-density infection, MR allows the infection to proceed more efficiently.

Section 5.2.3 – Results – Fluorescence Results

To better establish the efficacy of protein production under different infection conditions, the cells described in the above sections were tracked via flow cytometry. For each sample, the cells were first gated in the FSC vs. SSC channels to remove debris. Afterwards, the "healthy cells" and "compromised cells" gates established in Chapter 4 were drawn in to gate the bulk of the remaining detected events. In the following figures, these two populations will be referred to as "Live Cells" and "Dead Cells" respectively. As a further criterion for analysis, the events in these two gates were further gated in the FL1 channel to exclude any events with an FL1 value of less than 0.5 in order to separate out

any non-infected or non-fluorescent cells. In the following figures, these sub-populations will be referred to as "FL1+ Cells".

In order to present the results in a straightforward manner, these populations have been divided across the following four figures. Figures 29 and 30 will show the contribution of these different populations to the total cell count. In other words, the "Proportion of Cells Within Gate" value will be a measure of the number of cells satisfying the gating criteria divided by the total number of cells recorded. Following these plots, Figures 31 and 32 will show the geometric mean fluorescence of these same populations. In Figures 29 and 31, the "Live Cells" populations are shown for all four infection conditions, and the "Live FL1+ Cells" (i.e. "Live Cells" that additionally fulfill the criterion of having an FL1 value > 0.5) are presented alongside them. Similarly, the "Dead Cells" and "Dead FL1+ Cells" are presented in Figures 30 and 32. In each of these figures, the results of the low cell-density infections and high cell-density infections are presented side-by-side for ease of comparison.

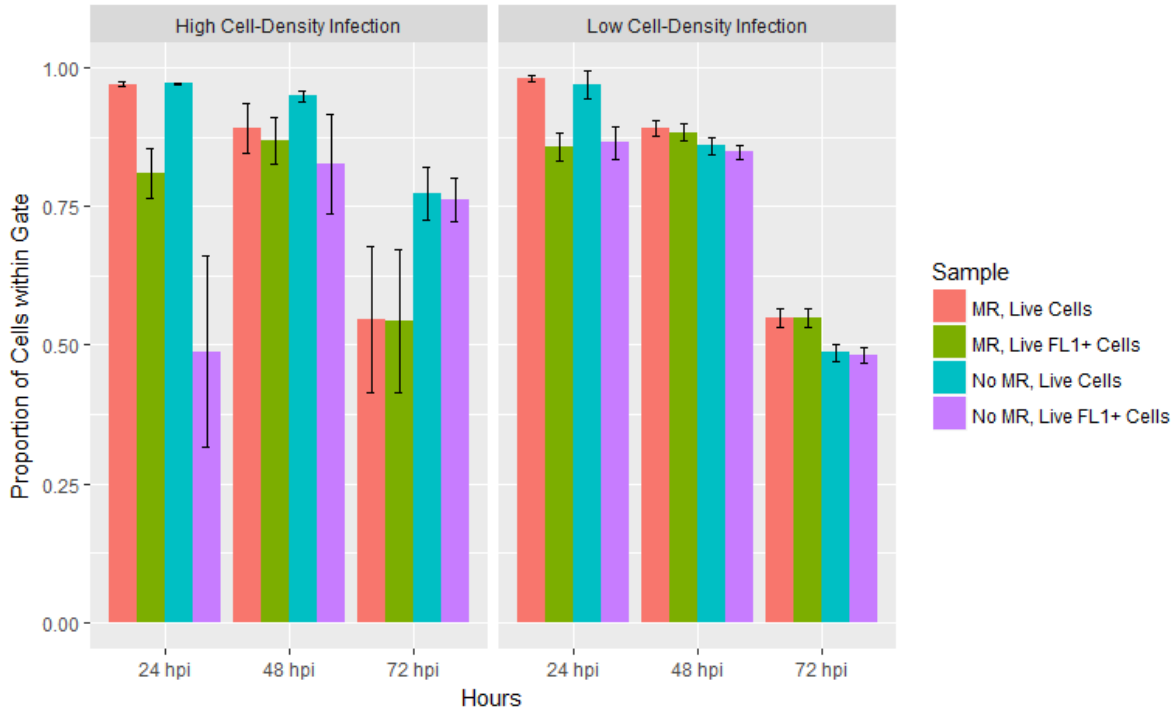

Figure 29: Proportion of cells counted that fall within the living cells gate. (n = 3 and error bars = 1σ)

This figure demonstrates the cell density effect in a distinct manner. Specifically, when comparing the low cell-density infection to the high cell-density infection, the appearance of fluorescence-expressing cells is drastically slowed. For an infection at a low cell-density, within the first 24 hours of infection, almost 90% of the living cells will express fluorescence above the baseline level used to distinguish them from non-infected cells. This is consistent regardless of whether or not the media is exchanged prior to infection, and the proportion increases to nearly 99% by 48 hpi. In the high cell-density infection however, only 50% of cells will express fluorescence within 24 hours if media replacement is not performed. If the media is replaced, then the proportion of fluorescent cells observed within 24 hours recovers to 84%, similar to the level seen in the low cell-density infection. At 48 hpi, 98% of the cells expressed fluorescence in the case of media replacement, but only 87% of cells expressed fluorescence if media replacement was not performed. Without media replacement, 99% fluorescence expression only appeared after 72 hpi.

Regardless of the conditions used in the infection, the proportion of cells appearing within the "Live Cells" gate decreased with time. The rate of this shift was quite similar for both of the low cell-density conditions as well as the high cell-density infection in which the media was exchanged. In line with the results shown in Figure 28B, the rate at which the cells in the high cell-density infection without media replacement moved from being alive to dead or compromised was much slower than the other three conditions. This observation is complemented with Figure 30 below, which shows the proportion of cells that fell within the gate for compromised cells.

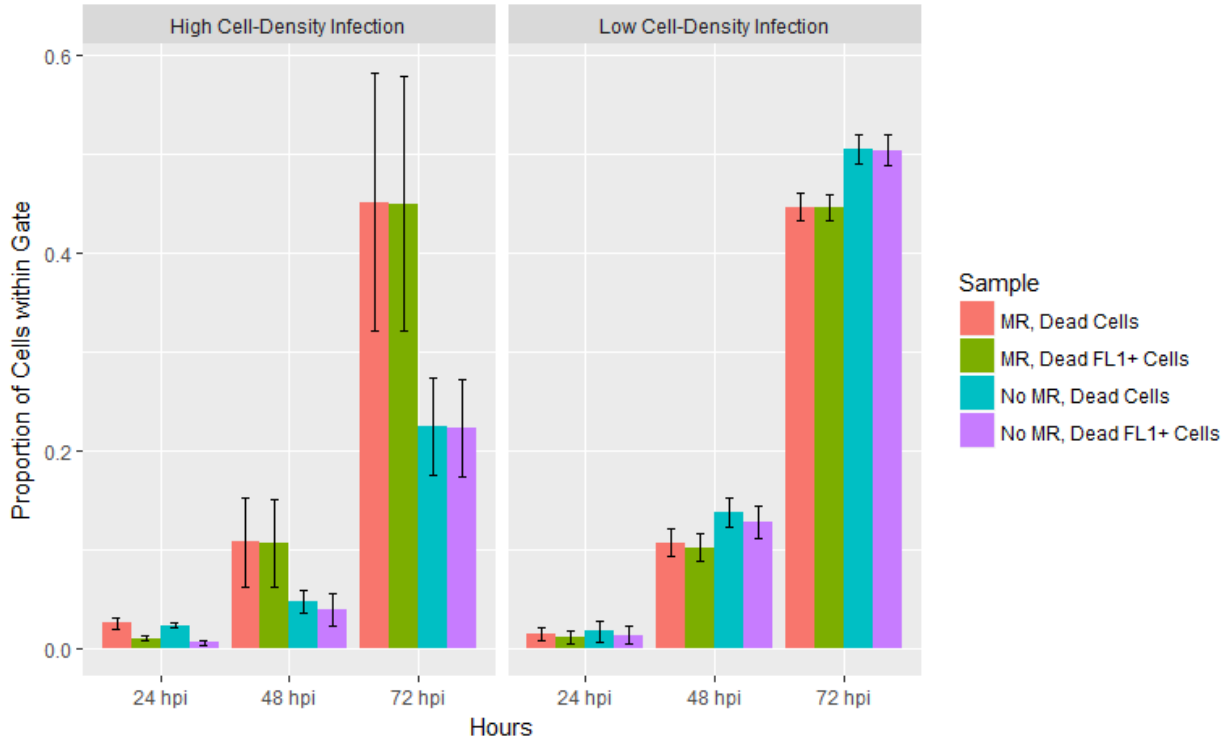

Figure 30: Fraction of cells counted that fall within the compromised cells gate. (n = 3 and error bars = 1σ)

The results in the Figure 30 show a great deal of similarity for most of the conditions. For the low cell-density infections, it appeared that the media replacement condition slightly slowed the death of the cells. At 72 hpi, only 45% of the cells were within the dead/compromised cells gate in the case of media replacement, whereas only 50% of the cells were within this gate without media replacement. In the case of the infection at high cell-densities, a low proportion of the dead cells exhibited fluorescence immediately after 24 hpi. Only 40% of the dead cells were fluorescent at 24 hpi in the case of media replacement, and only 23% of the dead cells were fluorescent at 24 hpi without media replacement. Both cases are notably worse than the 75% fluorescence expression in the dead cells of the low cell-density infection at this same time point. However, after 48 hpi, nearly all cells were fluorescent under all experimental conditions.

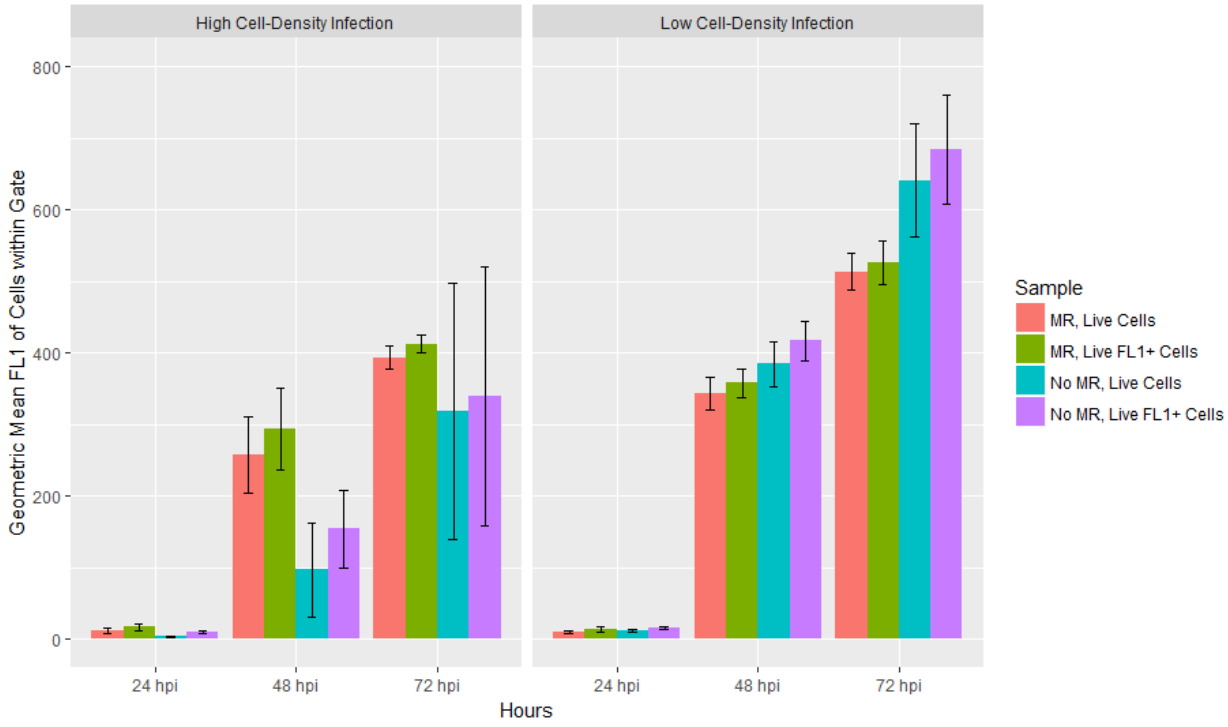

Figure 31: Geometric mean fluorescence of cells counted that fall within the living cells gate. (n = 3 and error bars = 1σ)

Figure 31 shows the mean fluorescence generated in all conditions. Despite the sub-90% fluorescence expression presented in Figure 29, at 24 hpi the overall amount of fluorescence generated was low enough that it had little effect. At 48 and 72 hpi, excluding the events with an FL1 value below 0.5 did not have a significant effect on the reported mean fluorescence (i.e. comparing the "Live Cells" bars to their respective "Live FL1+" bars, the effect was negligible). However, it did have a small effect when testing for significant differences in the means of the different conditions.

A 2-tailed T-test was used on the "Live FL1+ Cells" data in Figure 31, and it suggested that there were significant differences between the mean fluorescence of different conditions. Specifically, at 48 hpi there was a significant difference between 1) the low density no MR and MR conditions, 2) the high density no MR and MR conditions, 3) the low density no MR and high density MR conditions, 4) the low

density no MR and high density no MR conditions, and also 5) the low density MR and high density no MR conditions ($p < 0.05$). Repeating this analysis for the results at 72 hpi, there was a significant difference between 1) the low density no MR and MR conditions, 2) the low density MR and high density MR conditions, 3) the low density no MR and high density MR conditions, and 4) the low density no MR and high density no MR conditions ($p < 0.05$).

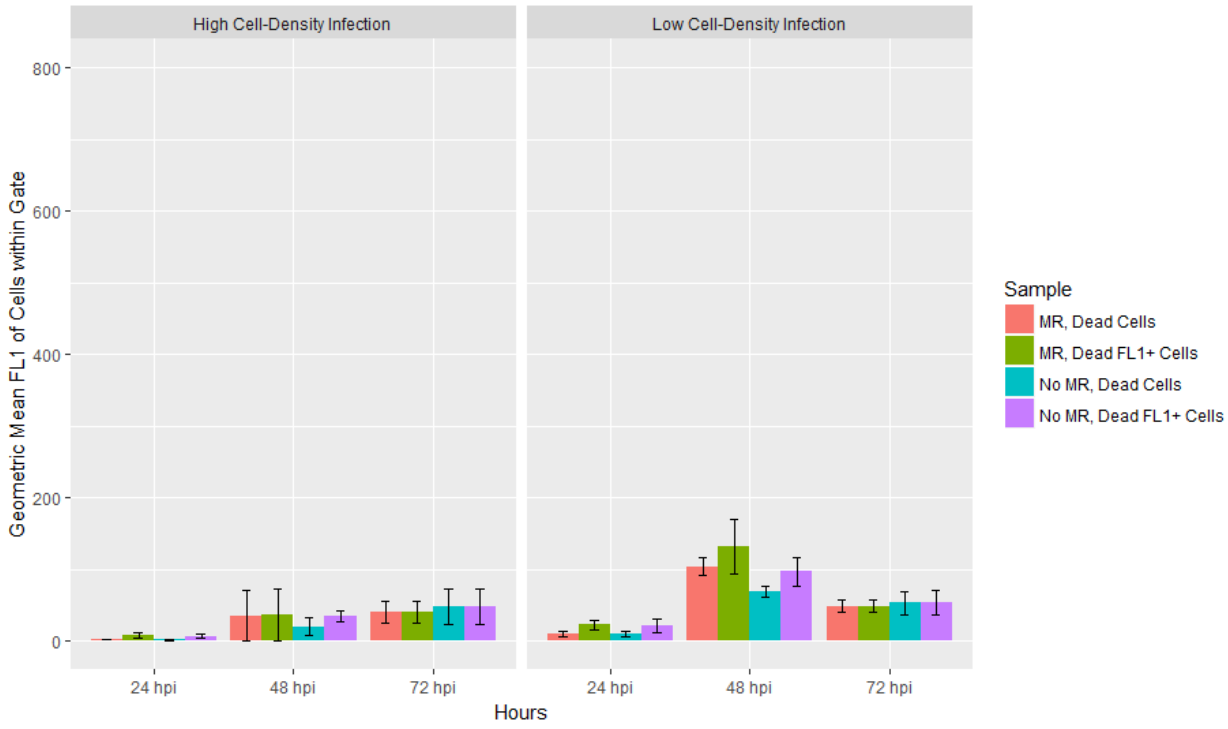

Figure 32: Geometric mean fluorescence of cells counted that fall within the compromised cells gate. (n = 3 and error bars = 1σ)

In Figure 32, some slight differences were observed in the average fluorescence of the dead cells at 48 hpi in the low cell-density infection. However, this distinction disappeared at 72 hpi. This difference was likely due to a small inclusion of actual live cells within the "compromised cells" gate, boosting the average fluorescence at this time point. Later, once a greater number of actual dead cells were present however, the small numbers of live cells that fell within this gate were likely not enough to shift the average as much as at 48 hpi. Besides this point, there does not appear to anything else

interesting about the analysis of the dead cells, so this will be excluded from the future analysis in this section.

Section 5.3 – Results – Placket-Burman-based Metabolite Additions

Section 5.3.1 – Results – Prior Experiments Examining Key Compounds

Eight compounds were initially identified in Chapter 4 as being potentially of interest. In a high cell-density batch culture infection, the ^{1}H-NMR profiling reveals these same eight compounds as being of note, either increasing substantially or being nearly fully depleted. These compounds of interest are shown below in Figure 33.

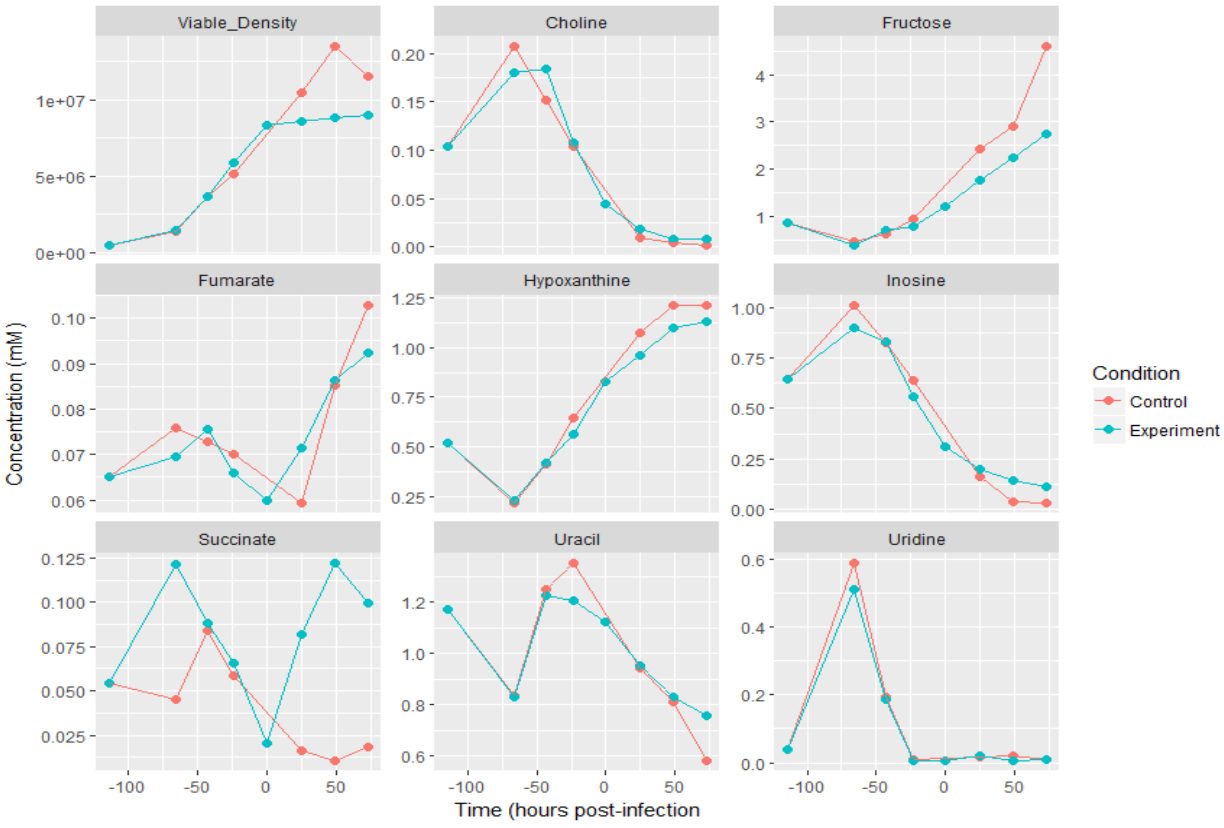

Figure 33: ^{1}H-NMR profiles of selected compounds in a high cell-density infection.

Choline, uracil, uridine, and inosine are seen to be depleted while fructose, fumarate, hypoxanthine, and succinate all accumulate to varying degrees. Of particular interest is the succinate as it appears to only accumulate during the infection condition. Otherwise, in the absence of infection, the succinate concentration remains low.

Section 5.3.2 – Results of Metabolite Additions

All data from this experiment were analyzed using ANOVA as described in an analysis by Miller (Miller, 2013). Interestingly, there appear to be many statistically significant associations between specific compounds and cellular changes over time. Of these, succinate has the most dominant effect in the majority of the tested conditions. Each of the parameters will be reported on in the next several figures, and the overall statistical results are highlighted in Table 3 below. In this table, there are five parameters assessed: "Total Cell-Density", "Viable Cell-Density", "Viability", "FL1-H +", and "Mean FL1-H". As has been the case in previous figures, Total Cell-Density describes the combined cell-density with both live and dead cells included in the count. Viability is the percentage of cells found to be alive at the time of counting, and Viable Cell-Density is the Total Cell-Density multiplied by the Viability to report only the cell-density of living cells. FL1-H + is used to denote the fraction of cells living cells expressing an FL1-H value of 0.5 or higher. Lastly, Mean FL1-H is the geometric mean fluorescence value of the cells assessed by the flow cytometer. As discussed in the previous chapter, this fluorescence only includes cells with the healthy morphology, separated from compromised cells in the FSC vs. SSC gate.

Table 4: Compiled List of ANOVA Significance Values (p-values): Significance of Metabolite Spikes on Reporters of Infection Progress and Quality. Statistical significance was calculated for each metabolite at each of the time points for five different reporters of the quality of the infection. "Density" is the total cell density achieved at that time in the culture. "Viable Dens." is the viable cell density achieved at that time in the culture. "Viability" is the percentage of viable, healthy cells at that time in culture. "FL1-H+" is the expression of fluorescence in the cell population, or in other words the percentage of cells in the culture that expressed fluorescence above baseline levels (FL1 > 0.5) at that time in culture. "Mean FL1-H) is the geometric mean fluorescence of the cells at that time in culture. Cells that were found to be statistically significant ($p < 0.05$) have been highlighted in green.

Condition	Time	Fructose	Fumarate	Hypoxan.	Succinate	Choline	Inosine	Uracil	Uridine
Density	24 hpi	0.802	0.261	0.760	0.520	0.760	0.618	0.245	0.546
Density	48 hpi	0.970	0.910	0.092	0.051	0.610	0.727	0.785	0.450
Density	72 hpi	0.886	0.092	0.430	0.016	0.798	0.329	0.320	0.044
Viable Dens	24 hpi	0.621	0.223	0.827	0.427	0.663	0.357	0.210	0.498
Viable Dens	48 hpi	0.925	0.688	0.062	0.035	0.533	0.558	0.856	0.507
Viable Dens	72 hpi	0.229	0.016	0.489	0.001	0.059	0.151	0.021	0.022
Viability	24 hpi	0.308	0.710	0.474	0.710	0.710	0.092	0.710	1.000
Viability	48 hpi	0.444	0.133	0.444	0.444	0.789	0.239	0.444	0.239
Viability	72 hpi	0.187	0.187	0.699	0.016	0.049	0.845	0.049	1.000
FL1-H +	24hpi	0.457	0.237	0.819	0.028	0.791	0.877	0.134	0.519
FL1-H +	48hpi	0.593	0.318	0.789	0.002	0.549	0.663	0.291	0.830
FL1-H +	72hpi	0.929	0.318	0.410	0.011	0.712	0.636	0.641	0.889
Mean FL1-H	24hpi	0.235	0.257	0.879	0.107	0.813	0.510	0.209	0.621
Mean FL1-H	48hpi	0.955	0.243	0.813	0.085	0.592	0.917	0.168	0.451
Mean FL1-H	72hpi	0.376	0.418	0.516	0.017	0.791	0.799	0.143	0.641

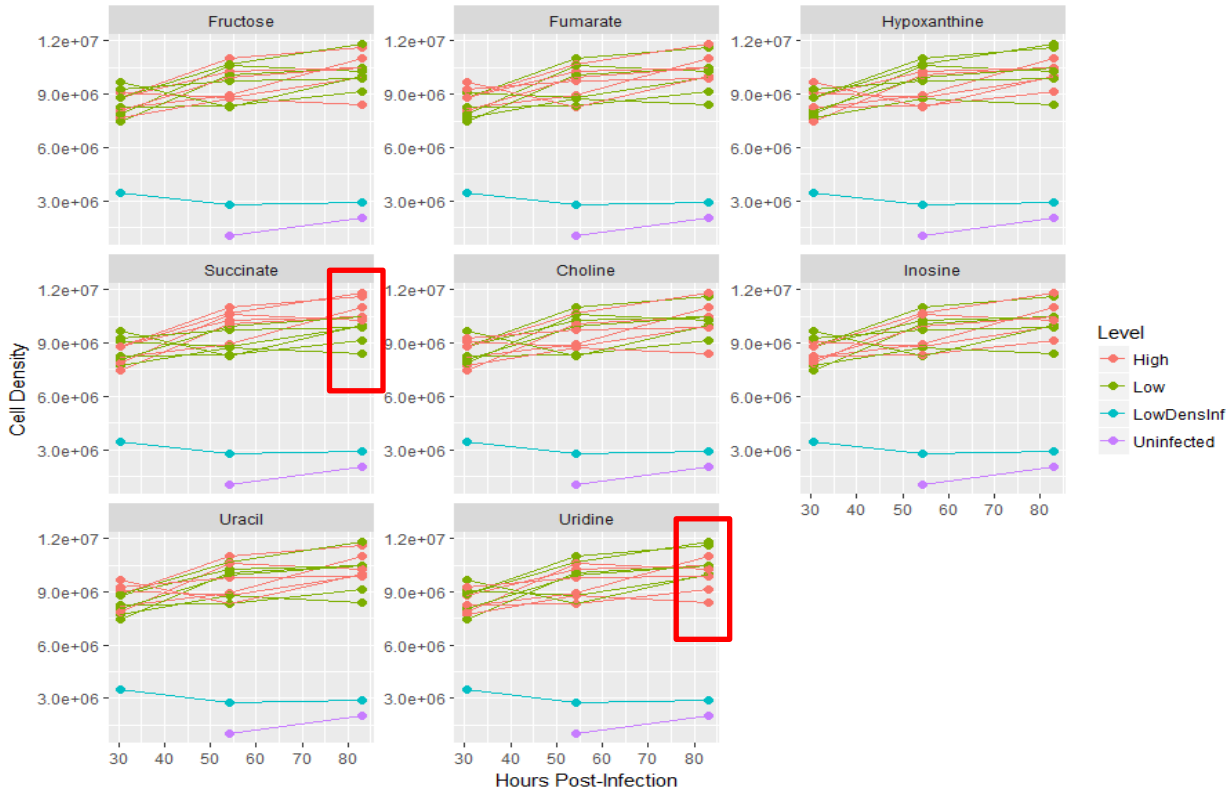

Figure 34: Total Cell Density during Placket-Burman (Each plot is separated to focus on a different metabolite. Each line represents one "run" of the Placket-Burman Design, color-coded to show whether the focussed metabolite was at a high level (red) or a low level (green) in that run. A red box has been drawn around the statistically significant points.)

As shown in Figure 34, after infection, the cell cultures all performed similarly with regards to the total cell-density. The cells appear to have essentially ceased growing within the first 24 hours, suggesting that a successful synchronous infection was achieved. Overall, the metabolite spikes did not seem to have a major effect on the cell-density change over time. Running the statistical analysis on this set of data, only succinate ($p = 0.015$) and uridine ($p = 0.044$) were statistically significant at 72 hpi. Interestingly, however, their effects are opposite; addition of succinate increases the maximum cell density achieved while uridine reduces the maximum cell density achieved. This may relate to the compounds decreasing or increasing the efficacy of the infection, respectively, since an effective synchronous infection should lead to cessation of cell division.

The analysis in Table 3 revealed that there were numerous compounds affecting the viable cell density to a statistically significant degree. However, there is also a strong possibility that this is due to the compounding of separate effects on both the total cell-density and the viability, the two of which were used to calculate the viable cell-density. This plot failed to reveal visually-noticeable effects, and has therefore been excluded.

As a complement to the analysis above, Figure 35 shows the viability of the infected cultures. In this figure, there is a much more evident separation of the different Placket-Burman conditions. On the third day of the infection, the infection is causing some of the cultures to die much more quickly than others. Carrying out the statistical analysis of the results, it was found that there were three metabolites with a significant effect at this time point. Specifically, succinate ($p = 0.016$), choline ($p = 0.049$), and uracil ($p = 0.049$) all significantly reduce the amount of cell death at 72 hours post-infection. None of the compounds added were significant at either 24 or 48 hours post-infection.

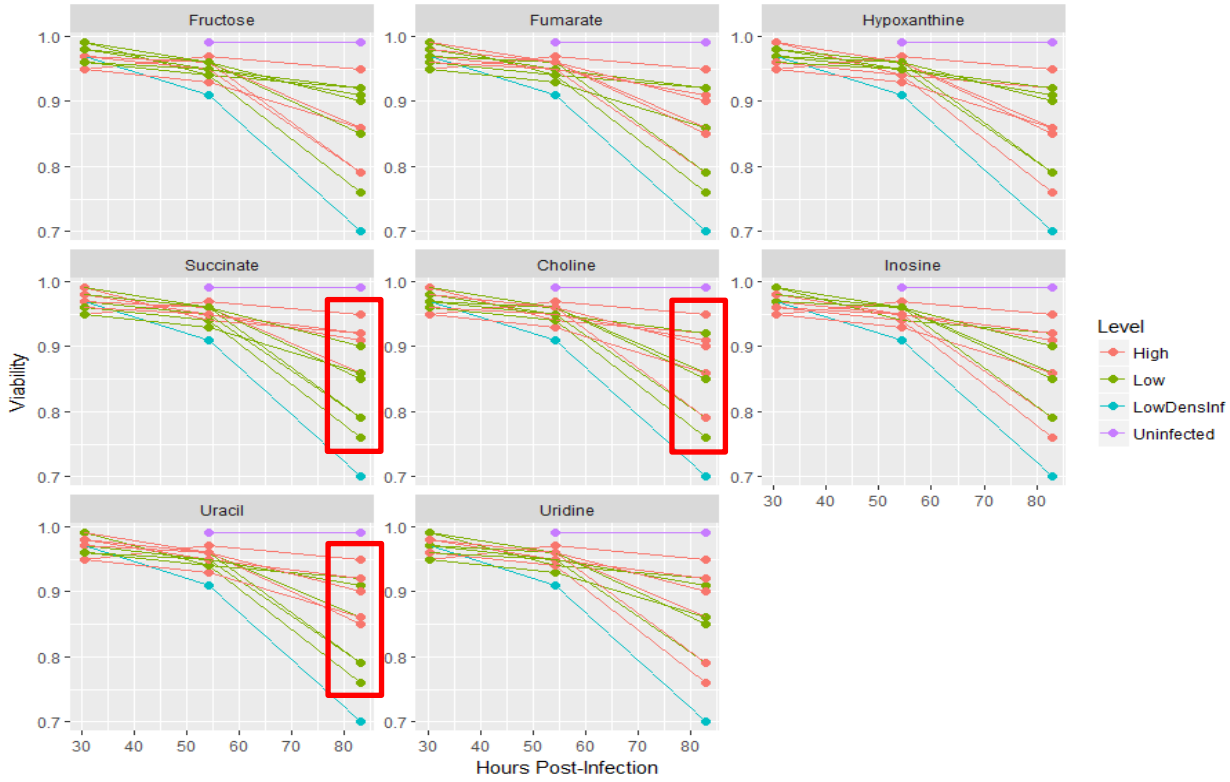

Figure 35: Cell Viability during Placket-Burman (Each plot is separated to focus on a different metabolite. Each line represents one "run" of the Placket-Burman Design, color-coded to show whether the focussed metabolite was at a high level (red) or a low level (green) in that run. A red box has been drawn around the statistically significant points.)

To provide insight into the productivity of the cell, the results of the flow cytometry analysis are presented below. To start the analysis (as described in Chapter 4), all samples were gated first in the FSC vs. SSC domain to remove events corresponding to debris. The remaining events corresponding to cells were then separated into living and dead cells in this domain, and then filtered in the FL1 channel to exclude those with a value below 0.5. Below in Figure 36A, the overall percentage of cells that remained within the "Live Cells" gate are shown. The subset of the cells within this gate and also had an FL1 value over 0.5 are shown below in Figure 36B. The complementary plot showing the proportions for the "Dead Cell" populations are illustrated below in Figure 37A and B. The data from a control, low cell-density infection are shown as well, as an additional point of comparison.

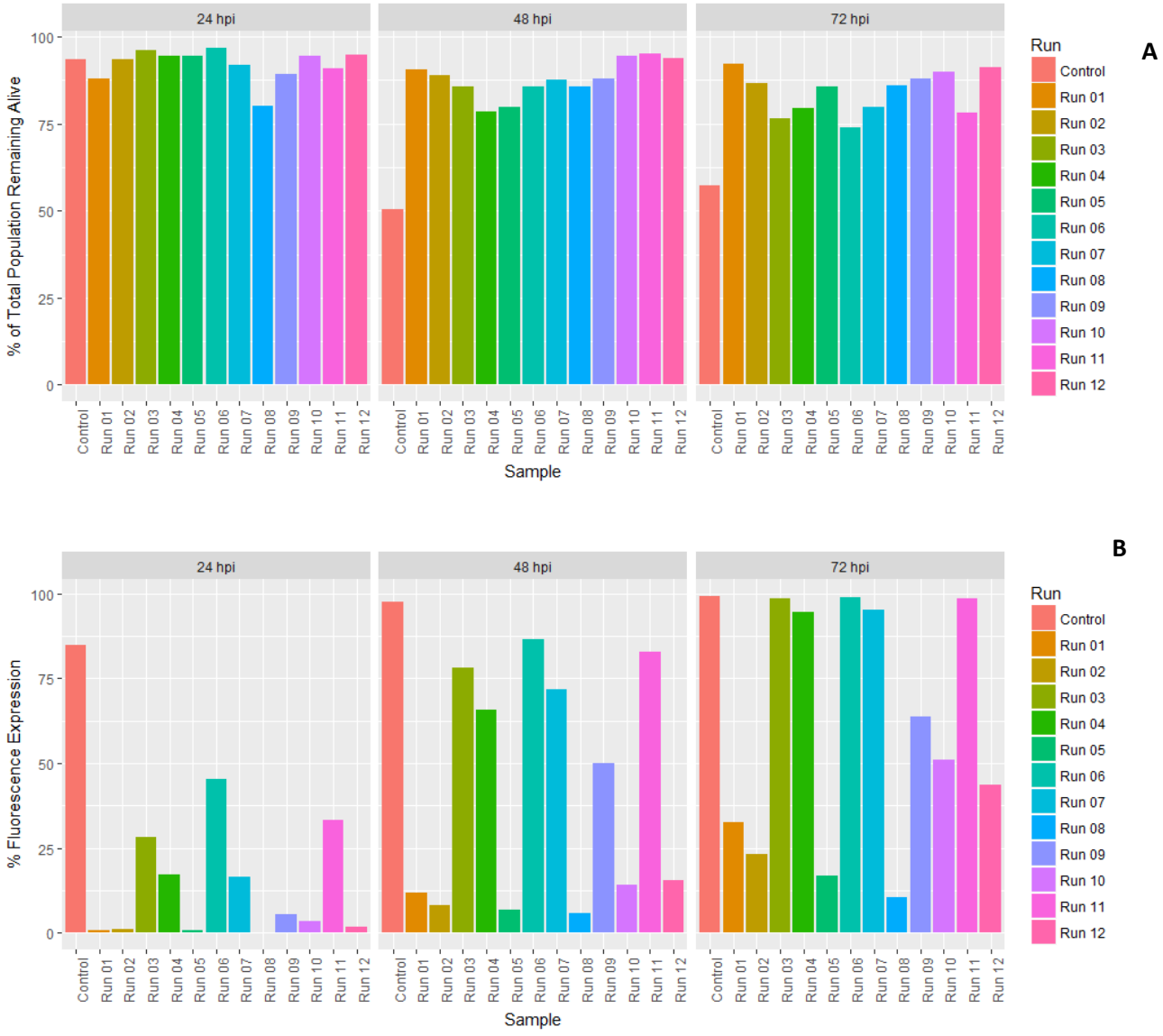

Figure 36: Distribution of Live-gated cells from Placket-Burman experiment. **A)** Overall proportion of cells found within the "Live Cells" gate at various time points for each set of Placket-Burman conditions **B)** The expression of fluorescence of each run. (The control was a low cell-density infection run simultaneously, and infected at 2 x 10^6 cells/mL. Fluorescence expression was defined as the percentage of living cells that had an FL1 value > 0.5.)

A

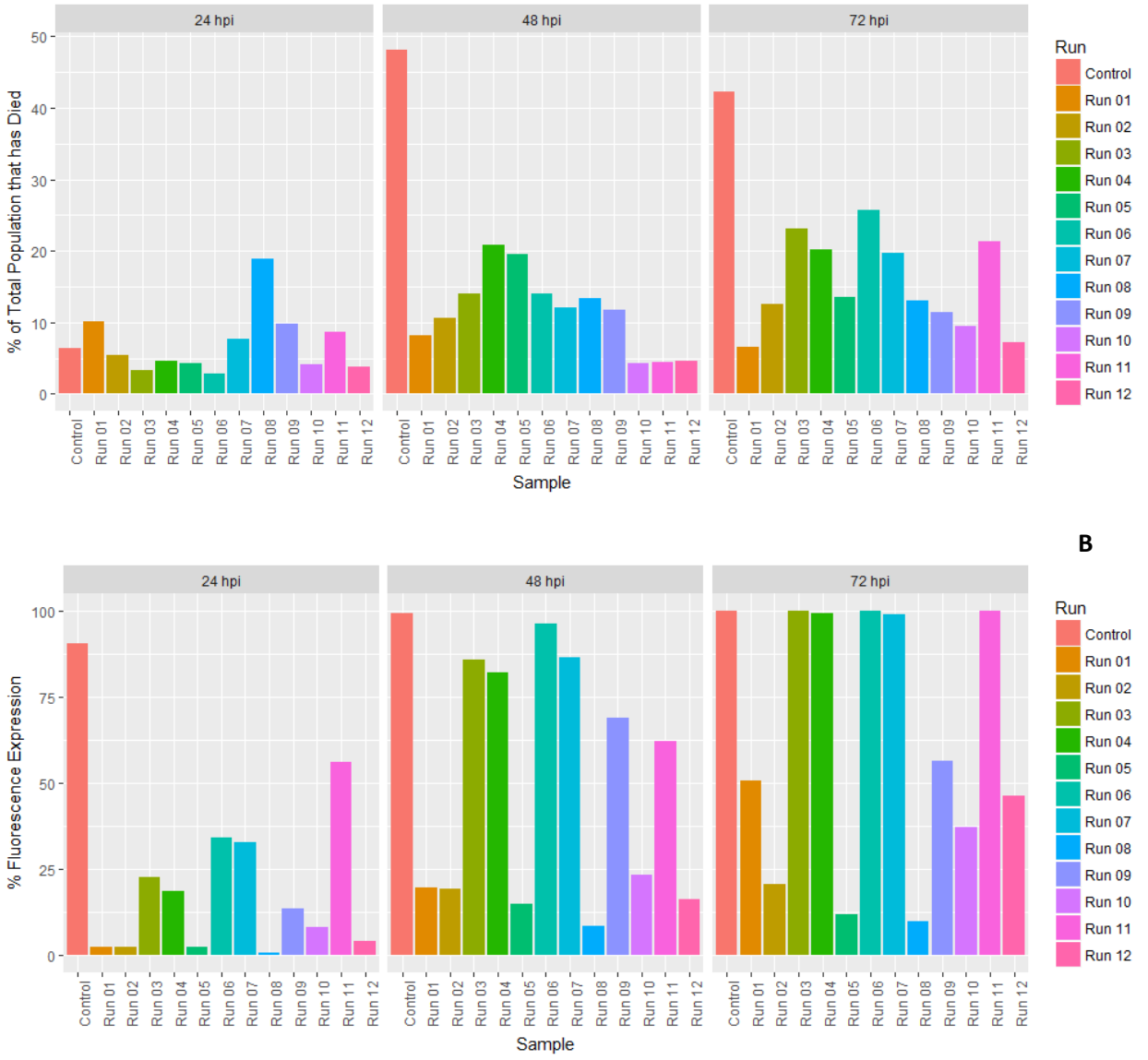

Figure 37: Distribution of Dead-gated cells from Placket-Burman experiment **A)** Overall proportion of dead cells found at various time points for each set of Placket-Burman conditions **B)** The expression of fluorescence of each run. (The control was a low cell-density infection run simultaneously, and infected at 2 x 10^6 cells/mL. Fluorescence expression was defined as the percentage of living cells that had an FL1 value > 0.5.)

An interesting common point about these two figures is that the runs 3, 4, 6, 7, and 11 appear to have performed extremely well compared to the rest of the runs. As was revealed in the baseline experiments in Figures 29 and 30, an effective infection should see near 100% fluorescence expression

within 48 hours of the onset of infection. By comparison, for an ineffective infection (i.e. High cell-density without media replacement), the efficacy is noticeably lowered. In Figure 29, at 48 hpi, this condition corresponded to roughly 87% fluorescence expression for the living cells. In Figure 36B above, the 5 runs noted performed similarly (albeit slightly worse), with the expression of fluorescence falling in the range of 66% to 86% after 48 hours. At 72 hpi, these 5 runs were in the range of 95%-99% fluorescence expression. In contrast, for the 7 other experimental conditions that were run, fluorescence expression was only in the range of 6%-15% after 48 hours, and was only up to 10%-51% at 72 hours. The expression of fluorescence above baseline levels was slightly more prevalent amongst the dead cells shown in Figure 37, but overall the same trend persisted; the 5 runs noted had extremely high levels of fluorescence expression when compared to the other 7 runs. In all cases, the analysis in Table 4 attributed succinate as the only statistically significant compound having an effect on the expression of fluorescence. However, it was founds to be statistically significant at all time points ($p = 0.028$, 0.002, and 0.011 at 24, 48, and 72 hpi respectively). As for the actual magnitude of the fluorescence produced by the cells, the geometric mean FL1 values for living cells are shown below in Figure 38.

Figure 38: Geometric mean fluorescence of gated cells from Placket-Burman experiment. **A)** Geometric mean fluorescence of all live cells **B)** Geometric mean fluorescence of all live, fluorescence expressing cells(The control was a low cell-density infection run simultaneously, infected at 2 x 10^6 cells/mL. Fluorescence expression was defined as the percentage of living cells that had an FL1 value > 0.5.)

The same 5 runs noted in Figures 36 and 37 stand out once again in Figure 38. Interestingly, when only cells with an FL1 value > 0.5 are considered, the geometric mean FL1 is far higher than the case where all living cells are considered. This indicates that even under extremely unfavourable conditions (for instance, in runs 1 and 2) there was still a subset of cells that were able to produce the GFP protein rather well, coming close to the values achieved under the conditions that were not unfavourable

(for instance, run 4). Specifically, in runs 1, 2, and 4, the geometric mean FL1 value is close to 30 for the "Live FL1+ Cells" population. However, the key difference is that this subset of cells was extremely small for runs 1 and 2, and is completely covered up by a much larger population of non-productive cells. This difference gave runs 1 and 2 mean FL1 values close to 0 at 48 hpi when all living cells were considered, as opposed to the value of 10 achieved in run 4. This gap between the productive and non-productive experimental conditions only widened further at 72 hpi.

Carrying out the analysis on this Placket-Burman experiment, as reported in Table 4, the only compound that had a significant effect on the geometric mean fluorescence was succinate. Further, it is only at the 72 hour time point that its effect was significant ($p = 0.017$); at the 24 and 48 hour time points, nothing was found to have a significant effect.

The ^{1}H-NMR spectra have not been shown here, but the common point linking the 6 most poorly performing runs was that they had peak clusters shifted horizontally from their expected location. This was interpreted as a large pH shift. Because it is known that Sf9 cells perform poorly outside of their standard pH range, a minor experiment was carried out wherein cells were infected at 8×10^{6} cells/mL, and the cells were given either a succinate addition, a pH adjustment (HCl if no succinate addition, or NaOH if succinate addition), or both. Two flasks were subjected to each condition, and flow cytometry was performed at 72 hpi. These results are shown in Figure 39.

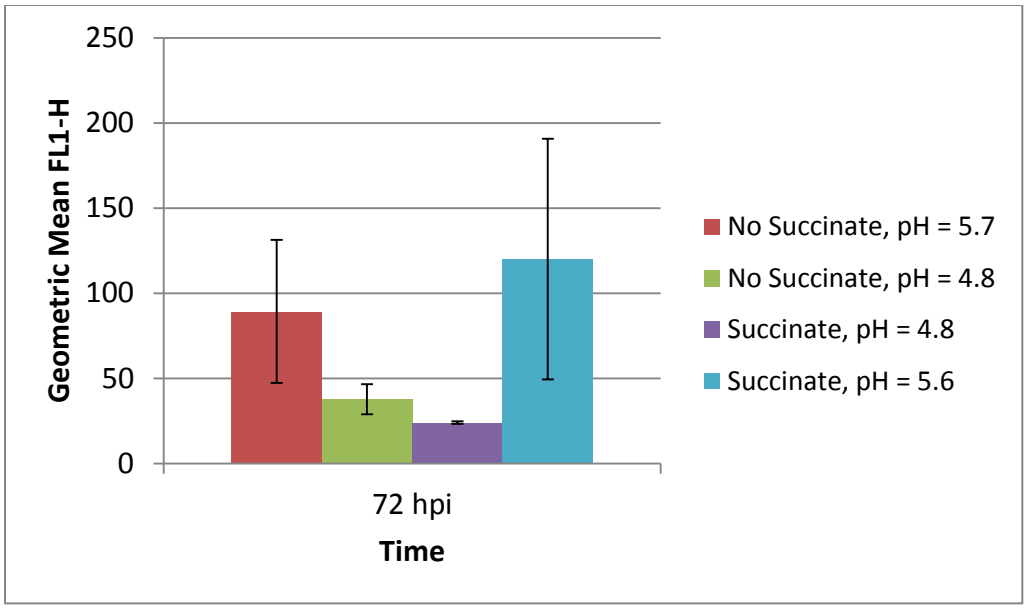

Figure 39: Geometric mean fluorescence of infection after pH adjusted succinate or saline additions (n = 2 and error bars = 1σ)

In Figure 39, the two conditions with high pH (5.7) were both able to achieve a mean FL1 value of roughly 100. When the pH was dropped to 4.8, however, the average fluorescence was reduced by 60-80%.

Section 5.4 – Discussion

Section 5.4.1 – Establishing the Cell Density Effect

As was established in Chapter 4, the cells can be sorted into separate populations based on their characteristic appearance by flow cytometry. When the healthy-looking population alone is separated and analyzed, differences appear that indicate it should not be considered lumped together with any dead or compromised cells. As such, when analyzing the results of the experiment, this provided a strong incentive to apply the new gating scheme developed. By applying this schema, the cell-density effect was demonstrated in Figures 27 through 30. It was revealed that either with or without media replacement,

the geometric mean fluorescence is significantly higher in the low cell density population than in the high cell-density population. Oddly, carrying out a media replacement significantly lowered the mean fluorescence at low cell-densities. There is mention in the literature that a full media replacement is actually less effective at improving the productivity of the culture than a partial media replacement (Ikonomou et al., 2004). Sf9 cells produce some insulin-associated proteins related to cell growth and proliferation, so it has been suggested that the benefits of partial media replacement may be due to the presence of these or other autocrine signalling factors (Ikonomou et al., 2004). Applying this reasoning in conjunction with the ^{1}H-NMR data generated in this thesis, it could be theorized that replacing the media at low cell-densities may end up removing these signalling molecules without also providing a benefit of replacing depleted compounds. In other words, because it is too early in the culture for anything to be fully depleted yet, there is no net beneficial effect. Consider the ^{1}H-NMR data presented in Chapter 4 regarding the preparation of the baculovirus stocks. The Appendix Figure B1 shows that almost none of the profiled compounds were depleted, with uridine being the one exception. Succinate and maltose were also reduced to roughly one-third of their original concentrations, and choline and inosine were reduced to roughly half of their original concentrations. So, while these 5 compounds could be replaced by media replacement, it would seem that this early into culture the benefits that they may provide are outweighed by the loss of some other currently unidentified molecules.

Contrary to the low cell-density infection analysis, due to the high FL1 variability in one flask of the "high density, no MR" condition, it is difficult to draw significant conclusions at high cell-densities at the 72 hour time point. The 48 hpi time point, however, does suggest that the media replacement strategy led to an improvement of the culture productivity. It would seem reasonable to assume that if the infection were repeated, a similar distinction should appear between the MR and no-MR conditions at 72 hpi.

It is important to note that the original intent of this first experiment was to establish the baselines and afterwards assess if an improvement in protein production could be achieved by supplementing the

growth media. However, it revealed that there is less of a difference in the average fluorescence between a low cell-density (i.e. efficient producer) and high cell-density (i.e. inefficient producer) culture than originally expected. Based on the literature about the overall productivity and yield of a culture, it has been well established that a high cell-density infection is much less effective than a low density infection. In Sf9 cells, one report found the specific productivity of β-gal protein to drop by 95% between their lowest and highest -cell densities tested (Huynh et al., 2013). For comparison to the conditions tested in my thesis, in cultures infected between a cell-density of 2×10^6 cells/mL they observed a roughly 15-fold higher specific production of β-gal protein than in cultures infected at 8×10^6 cells/mL and a roughly 2-fold higher specific production of viral DNA (Huynh et al., 2013). In a similar study in Hi-5 cells, when moving from low cell-density infections to high cell-density infections, they observed a 97% decrease in β-gal protein and an 85% decrease in viral DNA production (Huynh et al., 2014). In another report, Sf9 cells infected around 2×10^6 cells/mL were found to have a specific productivity of β-gal roughly 6-fold higher than when infected around 8×10^6 cells/mL, and a roughly 2-fold higher specific viral titre (Radford et al., 1997). In this same study, both cell-specific yields were decreased even further when moving to higher infection densities (Radford et al., 1997).

Meanwhile, in the baseline experiment of this thesis, it has been established that the fluorescence is roughly halved at high cell-density. Considering that prior reports found substantially higher reductions in cell-specific protein production at high cell-densities, it suggests that there may be a non-linear relation between the fluorescence of the cell and the actual yield of GFP in each cell. It is highly likely that this would be due to interference or quenching of the signal. One report studying GFP production found this to be the case when using a fluorescence spectrophotometer to analyze populations of *Escherichia coli*, and were consequently forced to establish a calibration fitting curve (Zhang et al., 2010). The amount of GFP produced should be measured and its correlation to the emitted fluorescence needs to be established. Until that is completed, it is merely an assumption that the fluorescence is reflective of the physical quantity of GFP formed. With this in mind, it was decided that in the Placket-

Burman experiment, the goal would instead be to compare the average fluorescence achieved to the two high cell-density values found here and see if they improve or fall under different conditions.

Section 5.4.2 - Effects of Metabolite Additions

To summarize the results of the Placket-Burman experiment, several of the tested compounds were found to have significant effects on one or more of the parameters analyzed. Succinate and uridine both had significant effects on final cell density, with succinate slightly increasing cell density and uridine slightly decreasing the final cell density. Succinate, choline, and uracil all significantly reduced the amount of cell death at 72 hours post-infection. As well, succinate significantly reduced the number of cells capable of producing fluorescence at all time points, and at the final time point it was revealed to significantly reduce the mean fluorescence of the cells that were able to produce detectable levels.

Overall, while half of the tested compounds had statistically significant effects, none came close to the effect that succinate had. Furthermore, as is shown in Figure 38, none of these spikes of metabolites were capable of pushing the productivity of the cells to levels anywhere close to what is achievable in a low cell-density infection. On the contrary, it appeared that, when compared to the baselines established in the first half of this chapter, the metabolite additions in the Placket-Burman experiment only had negative effects, overall.

In Figures 36, 37, and 38, only the runs 3, 4, 6, 7, and 11 performed on the level of a standard high cell-density infection. For the remainder of the runs, nearly all of the parameters examined were observed to suffer. For runs 3, 4, 6, 7, and 11, succinate was the only compound that was not fed in their metabolite additions. Interestingly, run 9 also did not have any succinate added, but did not perform nearly as well as these other 5 runs. While it is not reflected in the analysis of the data, this seems to suggest that perhaps one or more other component were also having a smaller negative effect on the quality of the infections. So, with the data as it is, it is difficult to make any meaningful conclusions about the compounds tested besides succinate. The performance of one flask (run 9) appeared to suffer

from some combination of compounds, but succinate had too great of an effect overall, likely hiding any effects that may have been attributable to other compounds. Figure 39 suggests very strongly that the effects seen in Figures 36 through 38 were largely meaningless from the perspective determining the effect that succinate had on the performance of the cultures. However, because the pHs of the cultures from the Placket-Burman design-based experiment were not measured after the experiment was concluded, it is uncertain how far outside of the tolerable pH window they were. A similar concern can be applied to all of the metabolite additions. While only those that received succinate performed extremely poorly, there was a high degree of variation between that performed at an acceptable level. It is uncertain if that was due to the actual effects of the metabolites that were added in those respective spikes, or if that too was due to pH changes caused by the spikes (albeit with a smaller overall shift in the pH). Run 9, for instance, performed almost as poorly as the six runs that received succinate additions (and thus had low pH values), suggesting that the combination of metabolites that it received may have also taken it just slightly below the tolerable range of pH and hindered its performance.

In order to fix this issue, two different things are required. Firstly, the experiment would need to be rerun. Either succinate would need to be removed from the design entirely, or the root cause of its effect would need to be addressed, i.e. the pH would have to be adjusted after each of the metabolite additions in the experiment. Secondly, because this first round of Placket-Burman testing has suggested that the tested additives failed to have any positive effects (even in the absence of succinate), more emphasis must be placed on determining the magnitude of the negative effects. To this end, it would be reasonable to take the complementary design to what was used in this experiment. That is, in each run, the compounds that were added and that were not added should be reversed. In this manner, run 1 would become much more useful. In its present form, run 1 was a flask into which each of the 8 compounds were added. In the complementary design, this flask would have none of the compounds added, and as such this would provide a much more reliable point of comparison for the basic high cell-density infection.

Chapter 6 – Conclusions and Recommendations

Section 6.1 – Conclusions

Daily media replacements were found to be a highly effective method of improving the overall cell growth achieved in Sf9 cultures. Carrying out this media replacement increased the maximum cell density achievable in culture from 12 x 10^6 cells/mL up to 44 x 10^6 cells/mL. A decrease in the total cell growth rate was seen when the culture exceeded 15 x 10^6 cells/mL, but this was unable to be solved by increasing the frequency of media exchange. Oxygen limitations also did not seem to be the cause for this decrease in cell growth rate, as a set of flasks deprived of oxygen were seen to grow at a similar rate and to a similar density as a control culture despite a 3.6-fold difference in dissolved oxygen levels.

^{1}H-NMR analysis of the spent media over the course of these two experiments revealed that 43 of the compounds were measureable and that 8 were of specific interest due to their lack of study in the literature. Fructose, fumarate, hypoxanthine, and succinate all accumulated in the culture while choline, inosine, uracil, and uridine were depleted. Succinate in particular was unique in that it appeared in the case of oxygen deprivation and extremely high cell densities, and was otherwise consumed. Succinate also acted as a better marker for oxygen deprivation than the standard molecule of interest in other systems, lactate

In order to pursue the goal of improving cell productivity, flow cytometry was utilized as a means of tracking the accumulation of fluorescent proteins post-infection. When the infected cells were all considered together, the results indicated that the average fluorescence of the culture decreased by roughly 20% between48 hpi and 72 hpi. Propidium iodide staining revealed that dead cells have a much lower average fluorescence than living cells, and the two populations should therefore be separated. When these two populations were considered individually, the average fluorescence of living cells increased by roughly 60% between 48 hpi and 72 hpi.

Baselines were established by comparing infections at low and high cell densities of 2 and 8 x 10^6 cells/mL, respectively. After infection, cell viability dropped faster in the low cell density infection than the high cell density infection (70% vs. 80% at 72 hpi). Media replacement restored this to similar levels, however. Fluorescence expression was also only 50% in the high cell density condition after 24 hours, compared to the 80% expression in the low cell density condition. Media replacement also restored this to the desired level. Comparing the average fluorescence achieved by the cells, the low cell density infection averaged an FL1 value of over 600. The high cell density infection was only able to achieve a value of roughly 300, roughly half as effective as the low cell density infection. However, media replacement improved this to roughly 400, a 33% improvement. Oddly, media replacement decreased the effectiveness of the low cell density infection, reducing the average FL1 by roughly 20% to 500. Overall, the 50% difference in average fluorescence with and without the cell density effect taking place suggests that fluorescent proteins are not an ideal product of interest in that they do not directly seem to reflect the total product concentration. Instead, a concentration calibration curve should be necessary to correlate the level of fluorescence with actual concentration and increase the accuracy of the measure; in its base form, the methodology used here is useful for comparing the relative levels of fluorescent protein accumulation, not the absolute levels of accumulation.

Spike additions of the 8 compounds of interest immediately prior to infection failed to elicit an improvement in the production of fluorescent proteins. In the best-case scenario, the average fluorescence level was roughly 50% of what the control, low density infection reached. This was comparable to the trend that was observed for the high cell density infection without media replacement in the baseline experiment. Unexpectedly, in the flasks where succinate was added, the cells were effectively prevented from accumulating any fluorescent protein and the average fluorescence of the cells was near 0. It was suspected that this effect was largely due to the lack of monitoring of the pH levels however, and that if they were balanced after the spike additions then the results would differ greatly.

Section 6.2 – Recommendations

The experiments described in this thesis provided some useful information, but there is still ample opportunity to explore further in the direction that these experiments have covered. To better understand some of the key phenomena taking place, the following three sets of future experiments would be recommended.

Some aspects of the metabolism deserve further attention. It was noted in the metabolic studies that there were a multitude of nucleic acid derivatives that seemed to be of interest. Further, in considering these nucleic acid derivatives, it was noticed that the pairs would typically experience a drop in the level of one and a corresponding increase in the level of the other (uracil and uridine as one pair, hypoxanthine and inosine as another). The difference between the two compounds in a pair was a single ribose ring, and the direction of the shift points towards the cleaving off of this ribose ring as the culture progresses. Therefore, it would be worthwhile to explore whether this activity is specific to these nucleic acid compounds, if it is more simply a case of the cells having an overactive glycolysis pathway that sees the ribose ring as an additional energy source, or even if there was just enzymatic activity in the media that was driving this conversion without any beneficial drive by the cells.

In a similar vein, the second question that came up regarding metabolic activity was: what is the significance of fructose to the culture? It was hypothesized that the accumulation of fructose may have been as a result of a bottleneck in the glycolysis pathway, with fructose accumulation being a result of the fructose-phosphate compounds being shunted out of the cell to support the continued consumption of the (excess) glucose in the media. It is critical to note that, in order to explore this theory, ^{1}H-NMR is only partially useful. It is unable to detect phosphate groups, so with this method it would be unknown whether or not the measured fructose is phosphorylated. It could be interesting to see if the transport of fructose out of the cell could somehow be blocked. Alternatively, could this glycolytic activity and appearance of fructose be a result of free-floating enzymes in the media? Because it has been previously

demonstrated in the literature that Sf9 cells can only sustain growth in a limited fashion when supplied with only fructose, it is curious that there would be any benefit for the cells to allow it to simply accumulate in the media and be wasted.

Lastly, a third key recommendation would be to re-run the Placket-Burman metabolite addition experiment. It was found that succinate was overwhelmingly impactful on the efficacy of the infection. However, the succinate additions may have caused an excessive shift in the pH of the culture. If the pH of the culture was the factor that was causing the poor performance of the infection as opposed to the succinate concentration itself, the result of the experiment would need to be rejected. Therefore, it is recommended that the entire Placket-Burman experiment be performed again. However, in this retrial, it is crucial that the pH of each of the metabolite spikes be monitored and adjusted as necessary. Only by doing this could there be confidence in the result that is generated. Additionally, in this redo of the experiment, it would also be recommended that the complementary Placket-Burman design (i.e. each of the conditions flipped) be used instead. This would likely be more useful since it would give a direct comparison to the baseline (no addition) as one of the test conditions as opposed to the currently implemented design where instead all 8 components were added in the spike (i.e. run 1).

Section 6.3 – Closing Remarks

The work done in this thesis provides a useful look at how we may better analyze flow cytometry data in a number of different contexts, and provides some insight into potential limitations in our culture conditions. The ^{1}H-NMR data is also quite interesting as it provides a rather effective look at how the metabolite fluxes may occur under conditions of both rich and depleted growth media.

With respect to the three hypotheses posed at the start of the thesis, there has been a mixed degree of success. The first hypothesis was that key compounds related to growth limitations could be found. A set of 8 compounds were found, and their concentration profiles did trend in a manner that suggested that

they have some use in culture growth limitations, particularly because the depleted compounds all tended to be fully consumed quickly relative to the sugars and amino acids. However, because exploring the cell density effect was deemed to be of greater importance, their effect on cell growth was not studied farther, independent of one another.

The second hypothesis saw a much greater level of focus and success, however. An effective method for the measurement and tracking of fluorescent protein production was established for Sf9 cells, and with this method, a steady accumulation of these proteins was consistently observed. There was one minor concern with this method however, and that was that the accuracy of the reported fluorescence as it correlates with protein concentration was left unknown. As such, the method developed will serve as an effective qualitative tool for assessing the efficacy of the infection conditions, but it is less effective for quantifying the magnitude of any difference between protein concentrations under different production conditions.

The third hypothesis started off well, but the conclusion to the hypothesis was never fully realized. The methodology developed for measuring the fluorescent protein fluorescence was able to show clear differences in baseline conditions, firmly establishing the cell density effect. However, the Placket-Burman design used to test the 8 compounds of interest fell short of the intended goal. Succinate was misconstrued as being highly detrimental towards specific productivity, but further testing established that this was erroneously caused by pH change in the metabolite spikes. The design still holds merit and can be used to farther test this third hypothesis (that these 8 compounds are related to the cause of the cell density effect), but that was not something that could be achieved at the time of the writing of this thesis. As such, the work described still has gaps before it can be considered complete. However, hopefully, this body of work may contribute to furthering our understanding of BEVS as a useful and effective production platform, and allow for the cell density effect to eventually be overcome.

References

Agathos, S. N., Jeong, Y. -H, & Venkat, K. (1990). Growth Kinetics of Free and Immobilized Insect Cell Cultures. *Annals of the New York Academy of Sciences*, *589*(1), 372–398. https://doi.org/10.1111/j.1749-6632.1990.tb24259.x

Ahn, J. H., Jang, Y. S., & Lee, S. Y. (2016). Production of succinic acid by metabolically engineered microorganisms. *Current Opinion in Biotechnology*, *42*, 54–66. https://doi.org/10.1016/j.copbio.2016.02.034

Bedard, C., Kamen, A., Tom, R., & Massie, B. (1994). Maximization of recombinant protein yield in the insect cell/baculovirus system by one-time addition of nutrients to high-density batch cultures. *Cytotechnology*, *15*(1–3), 129–138. https://doi.org/10.1007/BF00762387

Bédard, C., Tom, R., & Kamen, A. (1993). Growth, Nutrient Consumption, and End-Product Accumulation in Sf-9 and BTI-EAA Insect Cell Cultures: Insights into Growth Limitation and Metabolism. *Biotechnology Progress*, *9*(6), 615–624. https://doi.org/10.1021/bp00024a008

Bernal, V., Carinhas, N., Yokomizo, A. Y., Carrondo, M. J. T., & Alves, P. M. (2009). Cell density effect in the baculovirus-insect cells system: A quantitative analysis of energetic metabolism. *Biotechnology and Bioengineering*, *104*(1), 162–180. https://doi.org/10.1002/bit.22364

Bernal, V., Monteiro, F., Carinhas, N., Ambrósio, R., & Alves, P. M. (2010). An integrated analysis of enzyme activities, cofactor pools and metabolic fluxes in baculovirus-infected Spodoptera frugiperda Sf9 cells. *Journal of Biotechnology*, *150*(3), 332–342. https://doi.org/10.1016/j.jbiotec.2010.09.958

Bhatia, R., Jesionowski, G., Ferrance, J., & Ataai, M. M. (1997). Insect cell physiology. *Cytotechnology*. https://doi.org/10.1023/A:1007985208221

Bock, A., Schulze-Horsel, J., Schwarzer, J., Rapp, E., Genzel, Y., & Reichl, U. (2011). High-density microcarrier cell cultures for influenza virus production. *Biotechnology Progress*, *27*(1), 241–250. https://doi.org/10.1002/btpr.539

Butler, M. (2005). Animal cell cultures: Recent achievements and perspectives in the production of biopharmaceuticals. *Applied Microbiology and Biotechnology*, *68*(3), 283–291. https://doi.org/10.1007/s00253-005-1980-8

Chan, L. C., Greenfield, P. F., & Reid, S. (1998). Optimising fed-batch production of recombinant proteins using the baculovirus expression vector system. *Biotechnology and Bioengineering*, *59*(2), 178–188. Retrieved from http://www.ncbi.nlm.nih.gov/pubmed/10099329

Clincke, M. F., Mölleryd, C., Samani, P. K., Lindskog, E., Fäldt, E., Walsh, K., & Chotteau, V. (2013). Very high density of Chinese hamster ovary cells in perfusion by alternating tangential flow or tangential flow filtration in WAVE bioreactor™-part II: Applications for antibody production and cryopreservation. *Biotechnology Progress*, *29*(3), 768–777. https://doi.org/10.1002/btpr.1703

Clincke, M. F., Molleryd, C., Zhang, Y., Lindskog, E., Walsh, K., & Chotteau, V. (2013). Very high density of CHO cells in perfusion by ATF or TFF in WAVE bioreactor: Part I: Effect of the cell density on the process. *Biotechnology Progress*, *29*(3), 754–767. https://doi.org/10.1002/btpr.1704

Deitch, A., Law, H., & White, R. D. (1982). A Stable Propidium Iodide Staining Procedure for Flow

Cytometry. *The Journal of Histochemistry and Cytochemistry*, *30*(9), 967–972. https://doi.org/0022-1554/82/09096706$02.75

Demain, A. L., & Vaishnav, P. (2011). Production of Recombinant Proteins by Microbes and Higher Organisms. *Comprehensive Biotechnology, Second Edition*, *3*(3), 333–345. https://doi.org/10.1016/B978-0-08-088504-9.00542-0

Doverskog, M., Han, L., & Häggström, L. (1998). Cystine/cysteine metabolism in cultured Sf9 cells: influence of cell physiology on biosynthesis, amino acid uptake and growth. *Cytotechnology*, *26*(2), 91–102. https://doi.org/10.1023/A:1007963003607

Drews, M., Doverskog, M., & Lars, O. (2000). Pathways of glutamine metabolism in Spodoptera frugiperda (Sf9) insect cells : evidence for the presence of the nitrogen assimilation system , and a metabolic switch by 1 H / 15 N. *Journal of Biotechnology*, *78*, 23–37.

Elias, C. B., Zeiser, A., Bédard, C., & Kamen, A. A. (2000). Enhanced growth of Sf-9 cells to a maximum density of 5.2 x 107 cells per mL and production of β-galactosidase at high cell density by fed batch culture. *Biotechnology and Bioengineering*, *68*(4), 381–388. https://doi.org/10.1002/(SICI)1097-0290(20000520)68:4<381::AID-BIT3>3.0.CO;2-D

George, S., Jauhar, A. M., Mackenzie, J., Kielich, S., & Aucoin, M. G. (2015). Temporal characterization of protein production levels from baculovirus vectors coding for GFP and RFP genes under non-conventional promoter control. *Biotechnology and Bioengineering*, *112*(9), 1822–1831. https://doi.org/10.1002/bit.25600

Grace, T. D. (1962). Establishment of four strains of cells from insect tissues grown in vitro. *Nature*, *195*, 788–789. https://doi.org/10.1038/195788a0

Haas, R., Cucchi, D., Smith, J., Pucino, V., Macdougall, C. E., & Mauro, C. (2016). Intermediates of Metabolism: From Bystanders to Signalling Molecules. *Trends in Biochemical Sciences*, *41*(5), 460–471. https://doi.org/10.1016/j.tibs.2016.02.003

Hink, W. F. (1970). Established insect cell line from the cabbage looper, Trichoplusia ni. *Nature*, *226*(5244), 466–467. https://doi.org/10.1038/226466b0

Huynh, H. T., Tran, T. T. B., Chan, L. C. L., Nielsen, L. K., & Reid, S. (2013). Decline in baculovirus-expressed recombinant protein production with increasing cell density is strongly correlated to impairment of virus replication and mRNA expression. *Applied Microbiology and Biotechnology*, *97*(12), 5245–5257. https://doi.org/10.1007/s00253-013-4835-8

Huynh, H. T., Tran, T. T. B., Chan, L. C. L., Nielsen, L. K., & Reid, S. (2014). Effect of the peak cell density of recombinant AcMNPV-infected Hi5 cells on baculovirus yields. *Applied Microbiology and Biotechnology*, *99*(4), 1687–1700. https://doi.org/10.1007/s00253-014-6260-z

Ikonomou, L., Bastin, G., Schneider, Y. J., & Agathos, S. N. (2004). Effect of Partial Medium Replacement on Cell Growth and Protein Production for the High-Fivetrade mark insect cell line. *Cytotechnology*, *44*(1–2), 67–76. https://doi.org/10.1023/B:CYTO.0000043413.53044.fa

Ikonomou, L., Schneider, Y. J., & Agathos, S. N. (2003). Insect cell culture for industrial production of recombinant proteins. *Applied Microbiology and Biotechnology*, *62*(1), 1–20. https://doi.org/10.1007/s00253-003-1223-9

Jäger, V., & Kobold, A. (1995). Propagation ofSpodoptera frugiperda cells (Sf9) and production of

recombinant proteins with the baculovirus expression system using improved spinner flasks with membrane aeration. *Biotechnology Techniques*, *9*(6), 435–440. https://doi.org/10.1007/BF00160832

Jardin, B. A., Montes, J., Lanthier, S., Tran, R., & Elias, C. (2006). High Cell Density Fed Batch and Perfusion Processes for Stable Non-Viral Expression of Secreted Alkaline Phosphatase (SEAP) Using Insect Cells: Comparison to a Batch Sf-9-BEV System. *Biotechnology and Bioengineering*, *97*(2), 332–345. https://doi.org/10.1002/bit

Klöppinger, M., Fertig, G., Fraune, E., & Miltenburger, H. G. (1990). Multistage production of Autographa californica nuclear polyhedrosis virus in insect cell cultures. *Cytotechnology*, *4*(3), 271–8. https://doi.org/10.1007/BF00563787

Kretzmer, G. (2002). Industrial processes with animal cells. *Applied Microbiology and Biotechnology*, *59*(2–3), 135–142. https://doi.org/10.1007/s00253-002-0991-y

Kwang, T. W., Zeng, X., & Wang, S. (2016). Manufacturing of AcMNPV baculovirus vectors to enable gene therapy trials. *Molecular Therapy - Methods and Clinical Development*, *3*(September 2015), 15050. https://doi.org/10.1038/mtm.2015.50

Maranga, L., Brazao, T. F., & Carrondo, M. J. T. (2003). Virus-like particle production at low multiplicities of infection with the baculovirus insect cell system. *Biotechnology and Bioengineering*, *84*(2), 245–253. https://doi.org/10.1002/bit.10773

Mena, J. A., Aucoin, M. G., Montes, J., Chahal, P. S., & Kamen, A. A. (2010). Improving adeno-associated vector yield in high density insect cell cultures. *The Journal of Gene Medicine*, *12*(2), 157–167. https://doi.org/10.1002/jgm.1420

Mendonça, R. Z., Palomares, L. A., & Ramírez, O. T. (1999). An insight into insect cell metabolism through selective nutrient manipulation. *Journal of Biotechnology*, *72*(1–2), 61–75. https://doi.org/10.1016/S0168-1656(99)00094-2

Miller, J. N. (2013). Experimental design and optimisation (4): Plackett–Burman designs. *Analytical Methods*, *5*(8), 1901. https://doi.org/10.1039/c3ay90020g

Monteiro, F., Bernal, V., Saelens, X., Lozano, A. B., Bernal, C., Sevilla, A., … Alves, P. M. (2014). Metabolic profiling of insect cell lines: Unveiling cell line determinants behind system's productivity. *Biotechnology and Bioengineering*, *111*(4), 816–828. https://doi.org/10.1002/bit.25142

Mulukutla, B. C., Kale, J., Kalomeris, T., Jacobs, M., & Hiller, G. W. (2017). Identification and control of novel growth inhibitors in fed-batch cultures of Chinese hamster ovary cells. *Biotechnology and Bioengineering*, *114*(8), 1779–1790. https://doi.org/10.1002/bit.26313

Petiot, E., Cuperlovic-Culf, M., Shen, C. F., & Kamen, A. (2015). Influence of HEK293 metabolism on the production of viral vectors and vaccine. *Vaccine*, *33*(44), 5974–5981. https://doi.org/10.1016/j.vaccine.2015.05.097

Plagemaen, P. G. W. (1971). Choline metabolism and membrane formation in rat hepatoma cells grown in suspension uptake by simple diffusion and lack of direct exchange with phosphatidylcholine, *12*, 715–724.

Plagemann, P. G. W. (1969). CHOLINE METABOLISM AND MEMBRANE FORMATION IN RAT HEPATOMA CELLS GROWN IN SUSPENSION CULTURE II . Phosphatidylcholine Synthesis during Growth Cycle and Fluctuation of Mitochondrial Density. *The Journal of Cell Biology*,

42(14), 766–782.

Pohlscheidt, M., Langer, U., Minuth, T., Bödeker, B., Apeler, H., Hörlein, H. D., … Reichl, U. (2008). Development and optimisation of a procedure for the production of Parapoxvirus ovis by large-scale microcarrier cell culture in a non-animal, non-human and non-plant-derived medium. *Vaccine*, *26*(12), 1552–1565. https://doi.org/10.1016/j.vaccine.2008.01.032

Radford, K. M., Reid, S., & Greenfield, P. F. (1997). Substrate limitation in the Baculovirus Expression Vector System. *Biotechnology and Bioengineering*, *56*(1), 32–44. https://doi.org/10.1002/(SICI)1097-0290(19971005)56:1<32::AID-BIT4>3.0.CO;2-W

Rodrigues, A. F., Formas-Oliveira, A. S., Bandeira, V. S., Alves, P. M., Hu, W. S., & Coroadinha, A. S. (2013). Metabolic pathways recruited in the production of a recombinant enveloped virus: Mining targets for process and cell engineering. *Metabolic Engineering*, *20*, 131–145. https://doi.org/10.1016/j.ymben.2013.10.001

Rosinski, M., Reid, S., & Nielsen, L. K. (2000). Osmolarity effects on observed insect cell size after baculovirus infection are avoided using growth medium for sample dilution. *Biotechnology Progress*, *16*(5), 782–785. https://doi.org/10.1021/bp000083n

Sander, L., & Harrysson, *Æ*. A. (2007). Using cell size kinetics to determine optimal harvest time for Spodoptera frugiperda and Trichoplusia ni BTI-TN-5B1-4 cells infected with a baculovirus expression vector system expressing enhanced green fluorescent protein. *Cytotechnology*, 35–48. https://doi.org/10.1007/s10616-007-9064-5

Sandhu, K. S., Naciri, M., & Al-Rubeai, M. (2007). Prediction of recombinant protein production in an insect cell-baculovirus system using a flow cytometric technique. *Journal of Immunological Methods*, *325*(1–2), 104–113. https://doi.org/10.1016/j.jim.2007.06.005

Scott, R. I., Blanchard, J. H., & Ferguson, C. H. R. (1992). Spodoptera frugiperdaEffects of oxygen on recombinant protein production by suspension cultures of Spodoptera frugiperda (Sf-9) insect cells. *Enzyme and Microbial Technology*, *14*(10), 798–804.

Shabram, P., & Aguilar-Cordova, E. (2000). Multiplicity of Infection / Multiplicity of Confusion. *Molecular Therapy*, *2*(5), 420–421. https://doi.org/10.1006/mthe.2000.0212

Shcherbo, D., Murphy, C., Ermakova, G., Solovieva, E., Chepurnykh, T., Shcheglov, A., … Chudakov, D. (2010). Far-red fluorescent tags for protein imaging in living tissues. *Biochem Journal*, *418*(3), 567–574. https://doi.org/10.1042/BJ20081949.Far-red

Sokolenko, S., Blondeel, E. J. M., Azlah, N., George, B., Schulze, S., Chang, D., & Aucoin, M. G. (2014). Profiling convoluted single-dimension proton NMR spectra: A plackett-burman approach for assessing quantification error of metabolites in complex mixtures with application to cell culture. *Analytical Chemistry*, *86*(7), 3330–3337. https://doi.org/10.1021/ac4033966

Sokolenko, S., McKay, R., Blondeel, E. J. M., Lewis, M. J., Chang, D., George, B., & Aucoin, M. G. (2013). Understanding the variability of compound quantification from targeted profiling metabolomics of 1D-1H-NMR spectra in synthetic mixtures and urine with additional insights on choice of pulse sequences and robotic sampling. *Metabolomics*, *9*(4), 887–903. https://doi.org/10.1007/s11306-013-0503-3

Tapia, F., Vázquez-Ramírez, D., Genzel, Y., & Reichl, U. (2016). Bioreactors for high cell density and continuous multi-stage cultivations: options for process intensification in cell culture-based viral

vaccine production. *Applied Microbiology and Biotechnology*, *100*(5), 2121–2132. https://doi.org/10.1007/s00253-015-7267-9

Wang, M. Y., Kwong, S., & Bentley, W. E. (1993). Effects of oxygen/glucose/glutamine feeding on insect cell baculovirus protein expression: A study on epoxide hydrolase production. *Biotechnology Progress*, *9*(4), 355–361. https://doi.org/10.1021/bp00022a002

Weiss, S. A., Smith, G. C., Kalter, S. S., & Vaughn, J. L. (1981). Improved Method for the Production of Insect Cell Cultures in Large Volume, *17*(6), 30.

Weljie, A. M., Newton, J., Mercier, P., Carlson, E., & Slupsky, C. M. (2006). Targeted pofiling: Quantitative analysis of1H NMR metabolomics data. *Analytical Chemistry*, *78*(13), 4430–4442. https://doi.org/10.1021/ac060209g

Wilson, E., Id, M. O., Kyes, N., Mayfield, D., Wilson, C., Sabatka, D., … Sutlief, A. L. (2018). Using Fluorescence Intensity of Enhanced Green Fluorescent Protein to Quantify Pseudomonas aeruginosa, (2), 1–14. https://doi.org/10.3390/chemosensors6020021

Wong, T. K., Nielsen, L. K., Greenfield, P. F., & Reid, S. (1994). Relationship between oxygen uptake rate and time of infection of Sf9 insect cells infected with a recombinant baculovirus. *Cytotechnology*, *15*(1–3), 157–167.

Wyatt, S. S. (1956). CULTURE IN VITRO OF TISSUE FROM THE SILKWORM, BOMBYX MORI L. *The Journal of General Physiology*, *39*(6), 841–852. https://doi.org/10.1085/jgp.39.6.841

Zhang, K., Li, X., Ma, Y., Zou, S., Yang, L., & Zhang, M. (2010). A curve fitting method of quantifying green fluorescent protein expression level in Escherichia coli. *Journal of Microbiological Methods*, *80*(2), 172–177. https://doi.org/10.1016/j.mimet.2009.12.003

Appendices

Appendix A – Growth Profiles

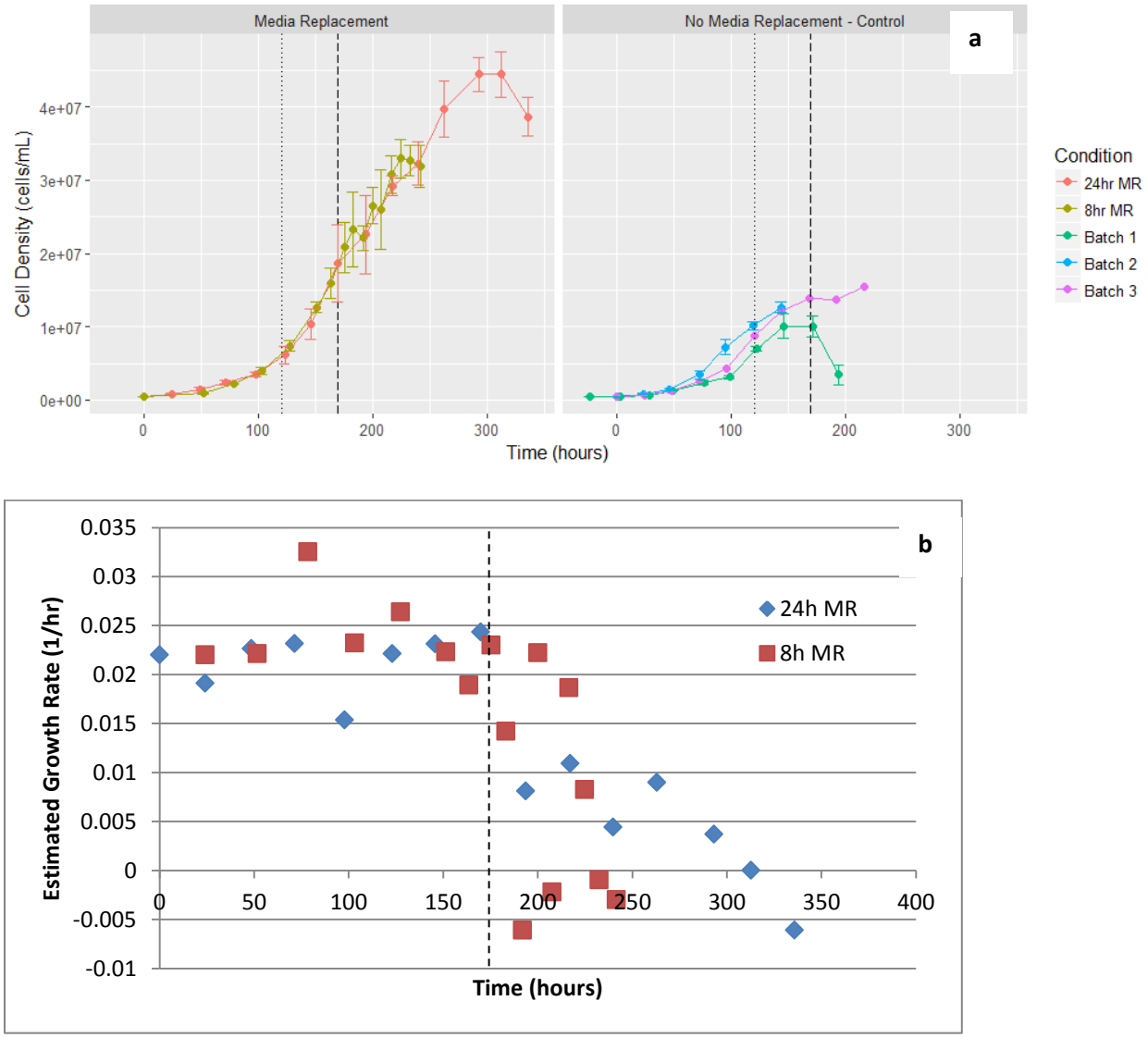

Figure A1: a) Non-log scale presentation of cell density of high cell density culture described in section 3.2. **b)** Average cell growth rate for every time interval for the high cell density culture. The value was calculated for each time period as $\mu = \frac{\ln(CD_2/CD_1)}{(t_2 - t_1)}$ where CD is the viable cell density at a certain time and t is that time in hours. The first time point (t = 0) was assumed to be a growth rate of 0.022 h^{-1}, based on a relatively consistent average across previous maintenance cultures. The dotted vertical line has been drawn in in accordance with the drop in growth rate.

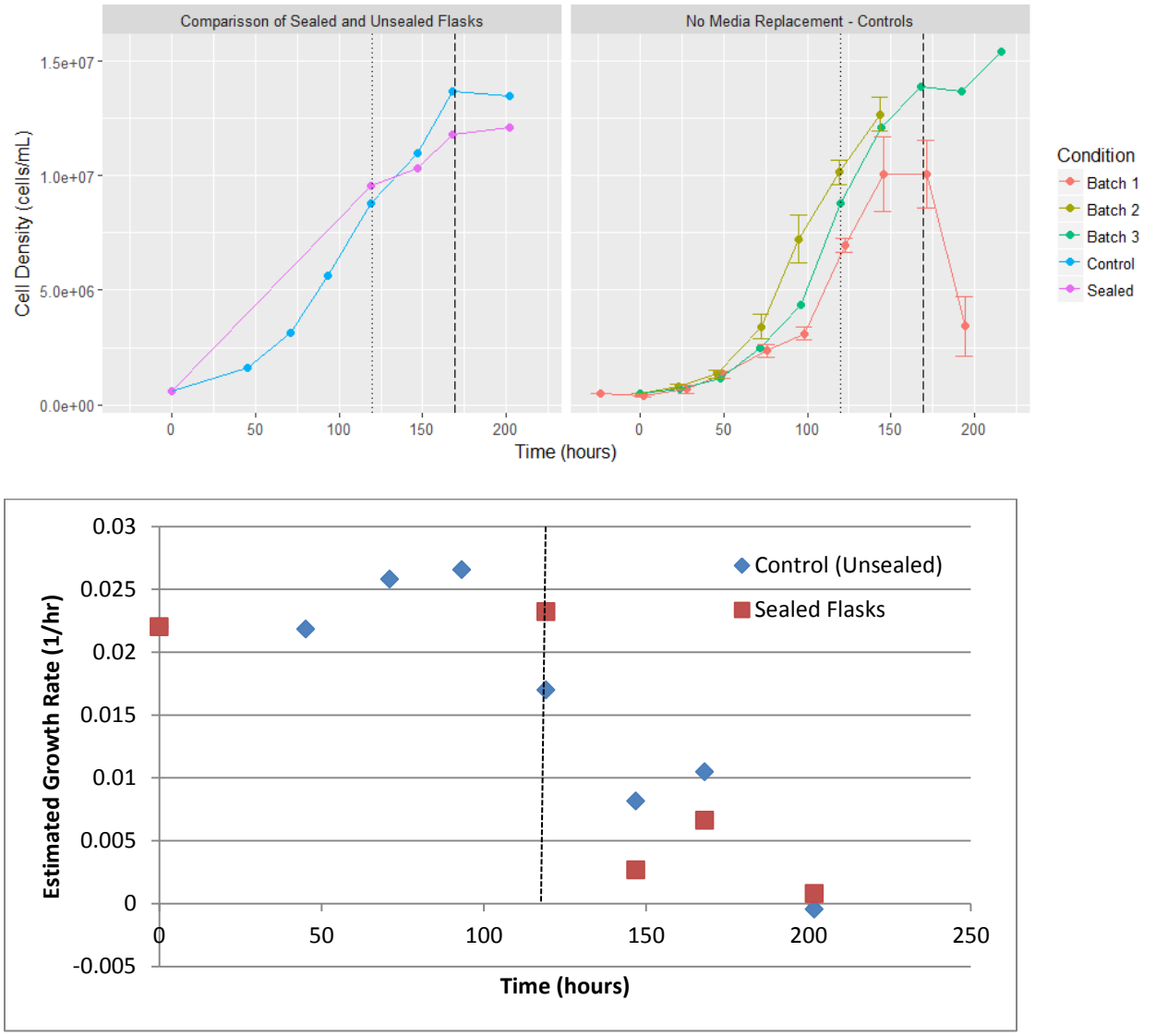

Figure A2: a) Non-log scale presentation of cell density of sealed flask culture described in section 3.2. **b)** Average growth rate of cultures in sealed-flask experiment. There are no error bars here, as each entry for the sealed flasks corresponded to one flask (no replicates). The value was calculated for each time period as $\mu = \frac{\ln(CD_2/CD_1)}{(t_2 - t_1)}$ where CD is the viable cell density at a certain time and t is that time in hours. The first time point (t = 0) was assumed to be a growth rate of 0.022 h^{-1}, based on a relatively consistent average across previous maintenance cultures. Because the sealed flasks were necessarily sacrificed after opening, the previous cell density value used was the one measured for the previously sacrificed flask.

Appendix B – Full Set of compounds profiled for media replacement experiment

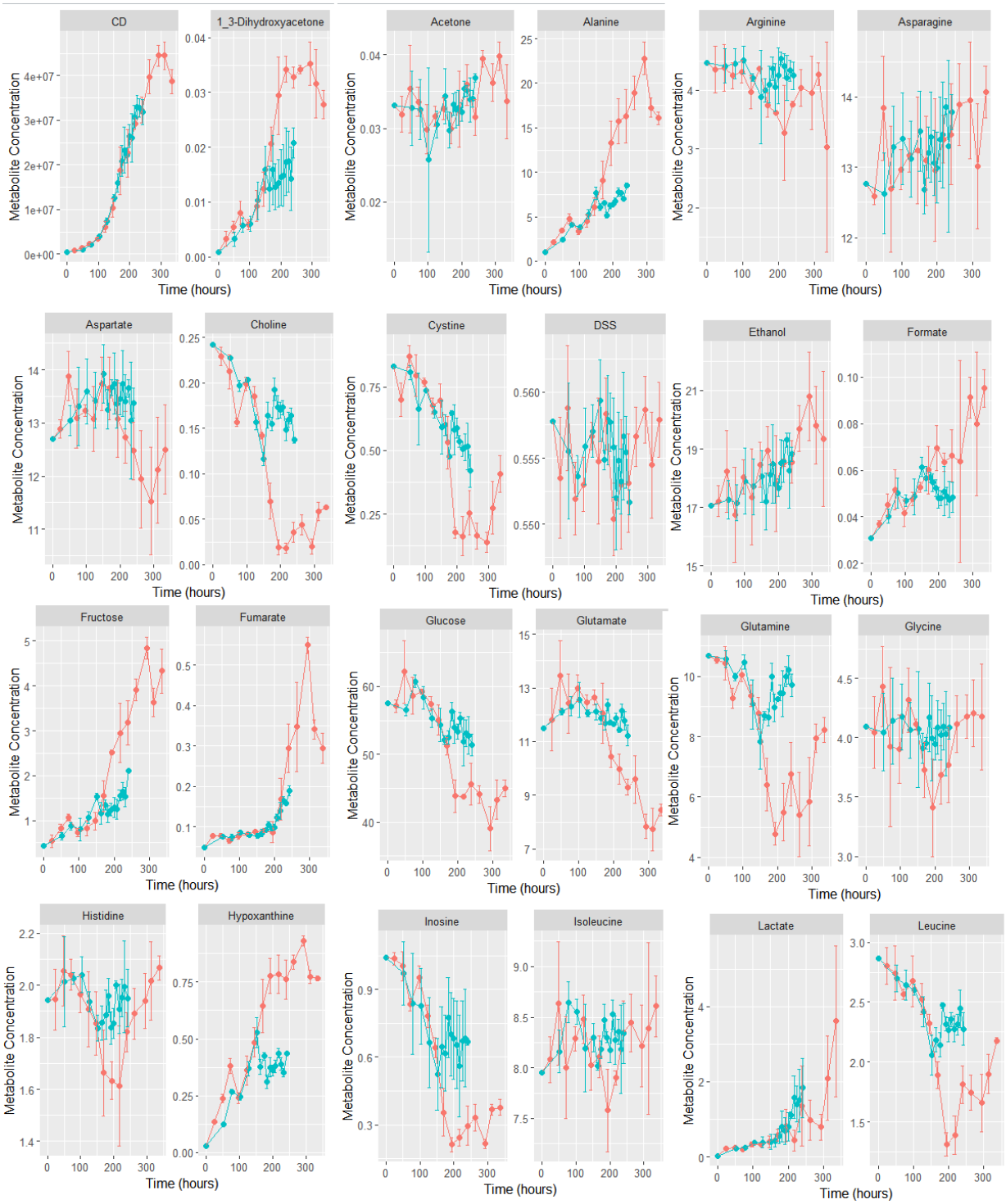

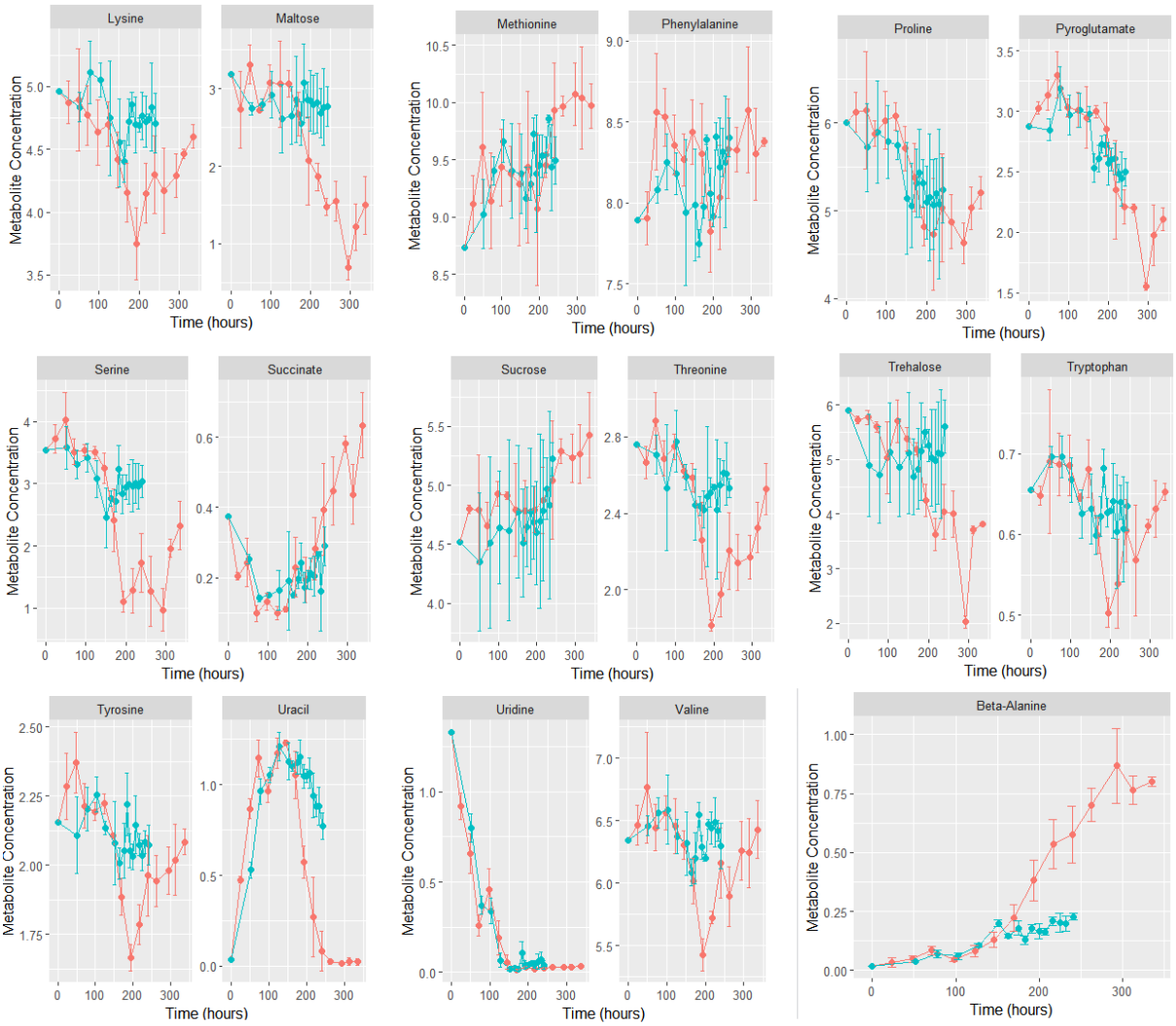

Figure B1: All metabolic profiles of consumption patterns of metabolites in high cell-density media replacement culture

Appendix C – Media Replacement Methodology

Methods – Centrifugation Experiment

As described in Section 2.3, the cells for this experiment were seeded into four 125 mL shake flasks. Each flask was identically seeded to yield 25 mL culture volumes at 0.6 x 10^6 cells/mL. Once the cells were confirmed to be growing exponentially, they were subjected to different treatment conditions. One flask was designated as the control, and the others were set to receive centrifugation at 100, 500, or 1000 RCF respectively.

The cells were counted at the initial time point to get their starting densities and viabilities, and NMR samples were taken for assessment of the initial metabolite concentrations. The content of each flask was then transferred to a separate 50 mL Falcon tube and centrifuged at its designated speed setting. Cell counts were taken for the supernatant of the Falcon tube after centrifugation to get a measure of the cells that were not effectively pelleted at that centrifugation speed. NMR samples were also taken at this point to see if there were any compounds that were released by the cells that may be a signal of cellular damage due to the centrifugation. The media in each flask was then replaced by following the same procedure used in the high cell-density experiments, and the flasks were returned to the incubator to resume growth.

Cell counts were performed on the re-suspended cell culture to ensure that there was no loss in cell density when the media was removed (i.e. due to pipetting too close to the pellet and removing cells in that manner) and to check that the cells were not noticeably harmed by their dissociation from the pellet (as could be evidenced by a drop in viability). NMR samples were also collected at this point. The flasks were tracked over the following seven days via cell counts, and NMR samples were also collected at each of these time points.

Results – Media Replacement Methodology

Overall, the strategy described in the previous section seemed to be effective in achieving very high cell densities for Sf9 cultures. However, a concern with the results of this experiment was that the cells were only counted prior to the media exchange. As such, there was no way to determine if cells were lost when the spent media was removed. Hypothetically, in the event that large portions of the cell population were lost after each media exchange, this would result in an apparent loss in the cell growth rate due to the lowered starting density. To address this issue, the experiment described herein was performed.

Cells were subjected to different centrifugation conditions once the control flask reached 3 x 10^6 cells/mL. In Figure C1, the immediate result of the centrifugation is shown. Each condition had only one

flask, so the error bars here are the standard deviation of the two counts taken per sample. Thus they indicate the variation in the counting of cell density rather than variation of cell density itself. "Initial Count" is the cell density before centrifugation, "Centrifuge Supernatant" is the cell density in the spent media after centrifugation, and "Media Replaced" is the cell density after the cells are resuspended in the new media. Despite being seeded from the same flask, the different cultures grew with a high degree of variation in the days leading up to the experiment. This may have been due to poor pipetting when transferring the cells between tubes. Alternatively, this may have been due to the different amounts of time required to resuspend the cell pellets from each of the different tubes. These were done one at a time, so there was a notable amount of time between the first and the last flasks being returned to the incubator post-centrifugation treatment. This makes comparing the conditions rather difficult when presented based solely on cell density, and as such Figure C1 shows the densities normalized versus each flask's initial cell density prior to centrifugation.

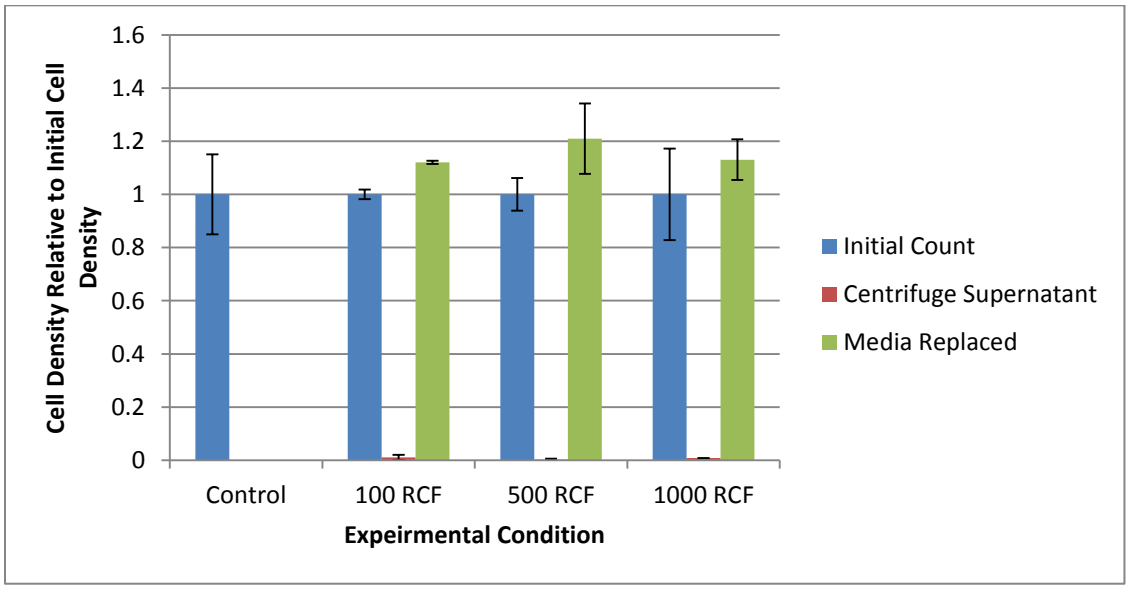

Figure C1: Cell density of samples – Normalized versus initial cell density in flask (In contrast to earlier experiments, only one flask was seeded after each of the centrifugation conditions. Because there were

no triplicates used, the error bars are equal to the standard deviation on the cell counts themselves, instead. That is, the cell density was recorded twice for each sample, once per half of the hemocytometer, and these two counts were used in the calculation of the standard deviation.)

The cell density in the centrifuge supernatant was roughly 1% of the initial cell density in all experimental conditions, suggesting that even the lowest speed setting ensures near total separation of cells from the spent media. As for the samples taken after media replacement, based on the recorded cell density counts we cannot conclude that cells were being lost when removing the spent media. Instead, Figure C1 shows that, strangely, the cell density appears to increase after the media replacement for all three conditions. The degree of variation in counts for both the 500 and 1000 RCF conditions suggests that this is likely just due to the inherent variability of the hemocytometer loading, and suggests that the density is in fact likely to be unchanged after media replacement.

The viability of the cells remained at nearly 100% under all conditions tested, indicating that the centrifugation is likely not causing extensive damage to the cells. Immediately after centrifugation, considering only the viability recorded in the first count after centrifugation, there is no noteworthy loss in cell viability. Given that the viability of cells tends to drop as they sit on the hemocytometer, only the viability of the first count is a reliable measure.

In Figure C2 below, the growth profiles of the cultures for each condition have been plotted post-centrifugation. As each flask had a different cell density at the time of centrifugation, it is difficult to make a direct comparison of the conditions. Therefore, each culture has been shifted in the time domain to better align with one another

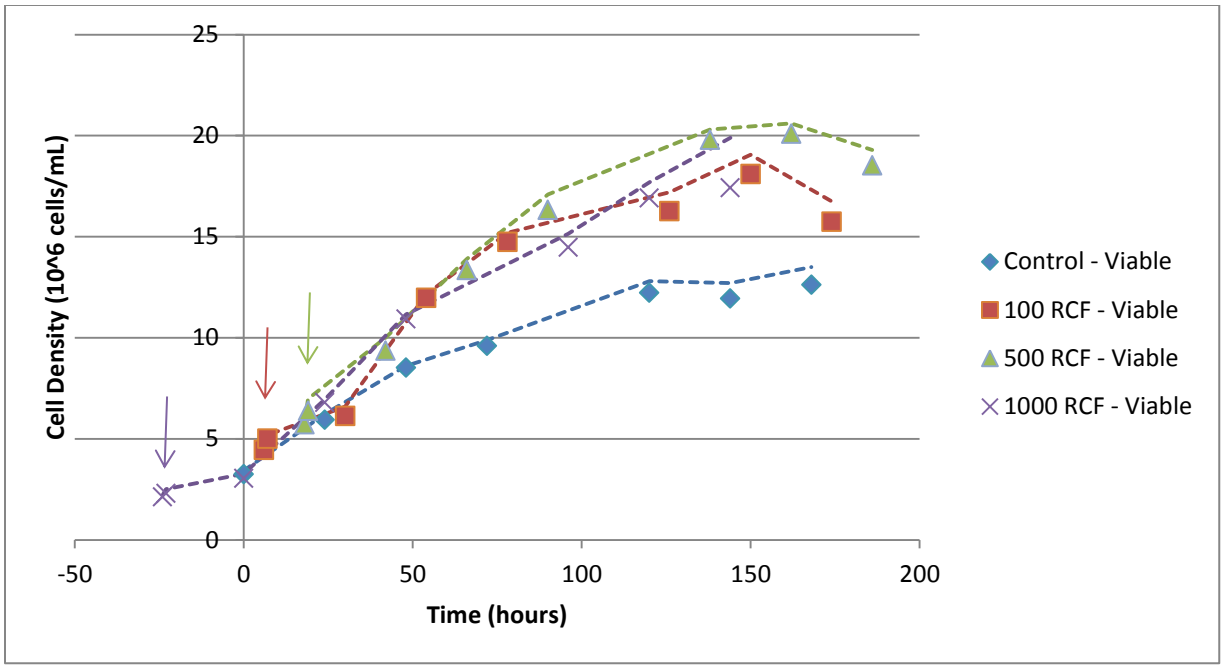

Figure C2: Growth profiles of cells under each centrifugation condition (individually time-shifted to allow curves to better align. 100 RCF shifted +6 hours, 500 RCF shifted +18 hours, 1000 RCF shifted -24 hours. Dotted lines correspond to the total cell density of that condition, while markers represent the viable cell density. Arrows denote point of centrifugation/media exchange, with same color assignment as in the legend)

After manipulating the time domain, the three profiles for the experimental conditions all aligned well. This again provides evidence that even at the highest centrifugation setting tested, there did not appear to be lasting damage to the cells, at least not in a manner that would affect their growth. All three grew much more than the control flask and reached roughly 20 x 10^6 cells/mL at their peak, but this is to be expected since the media was replaced in each of these flasks while the control received nothing to help boost its growth.

In conclusion, regarding the methodology used in this experiment, the centrifugation tests suggest that the current procedure used for replacing the media is safe for the cells. A low centrifugation speed of 100 RCF is sufficient to fully pellet the cells out of suspension. There does not seem to be a loss of cells when the supernatant is removed after centrifugation, and the subsequent resuspension does not appear to

inflict lasting damage on the cells. At higher centrifuge speeds, no damage is observed either, and cells can achieve their maximum cell density seemingly without major problems. Therefore, this method is deemed appropriate for carrying out the media replacement procedure when pushing the culture towards high cell densities.

Appendix D – Full set of NMR profiles for baculovirus stocks

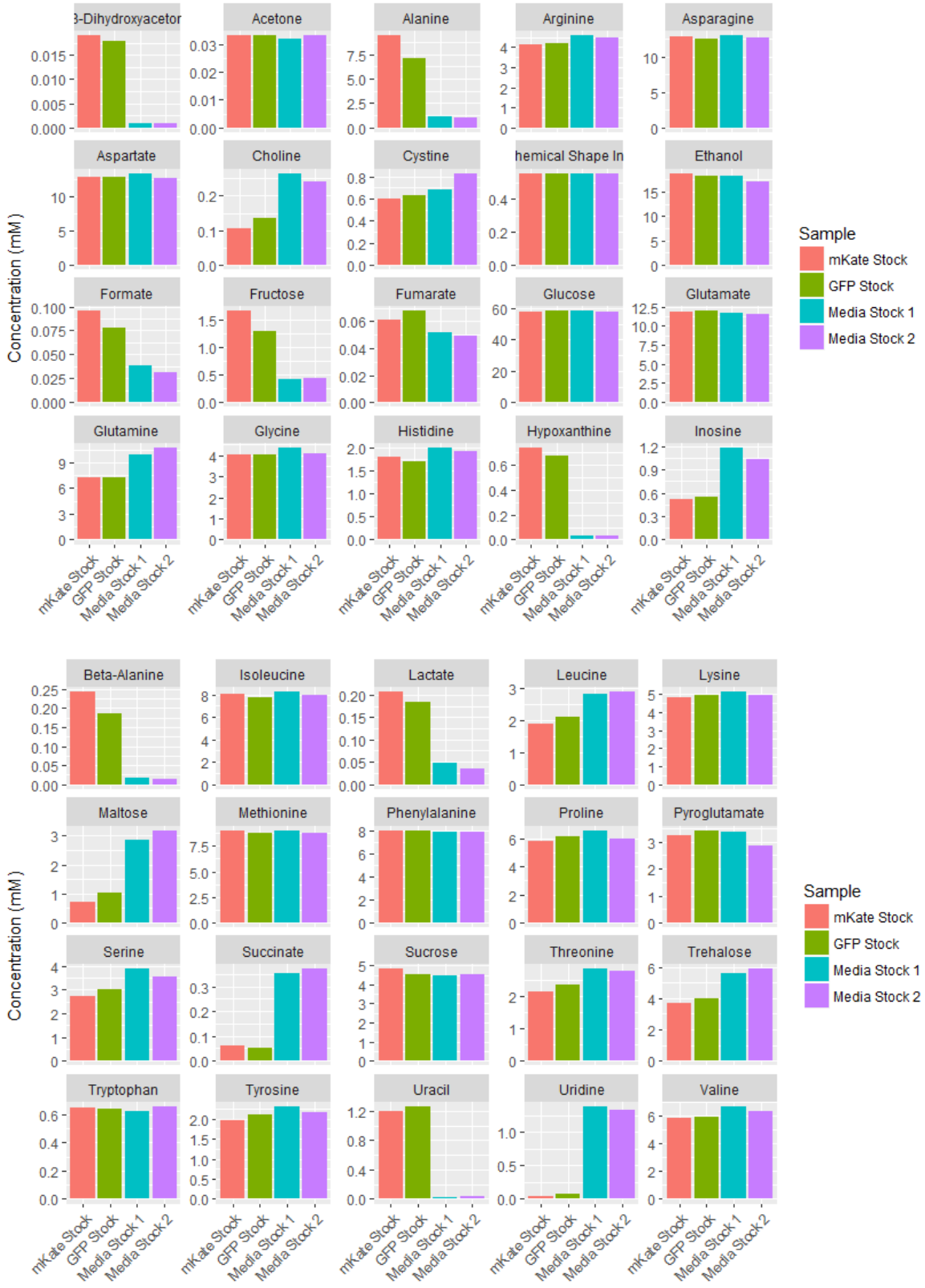

Figure D1: Complete Metabolic Profiling of Baculovirus Stocks

Appendix E – Freeze-killed cells versus standard, end of infection cycle

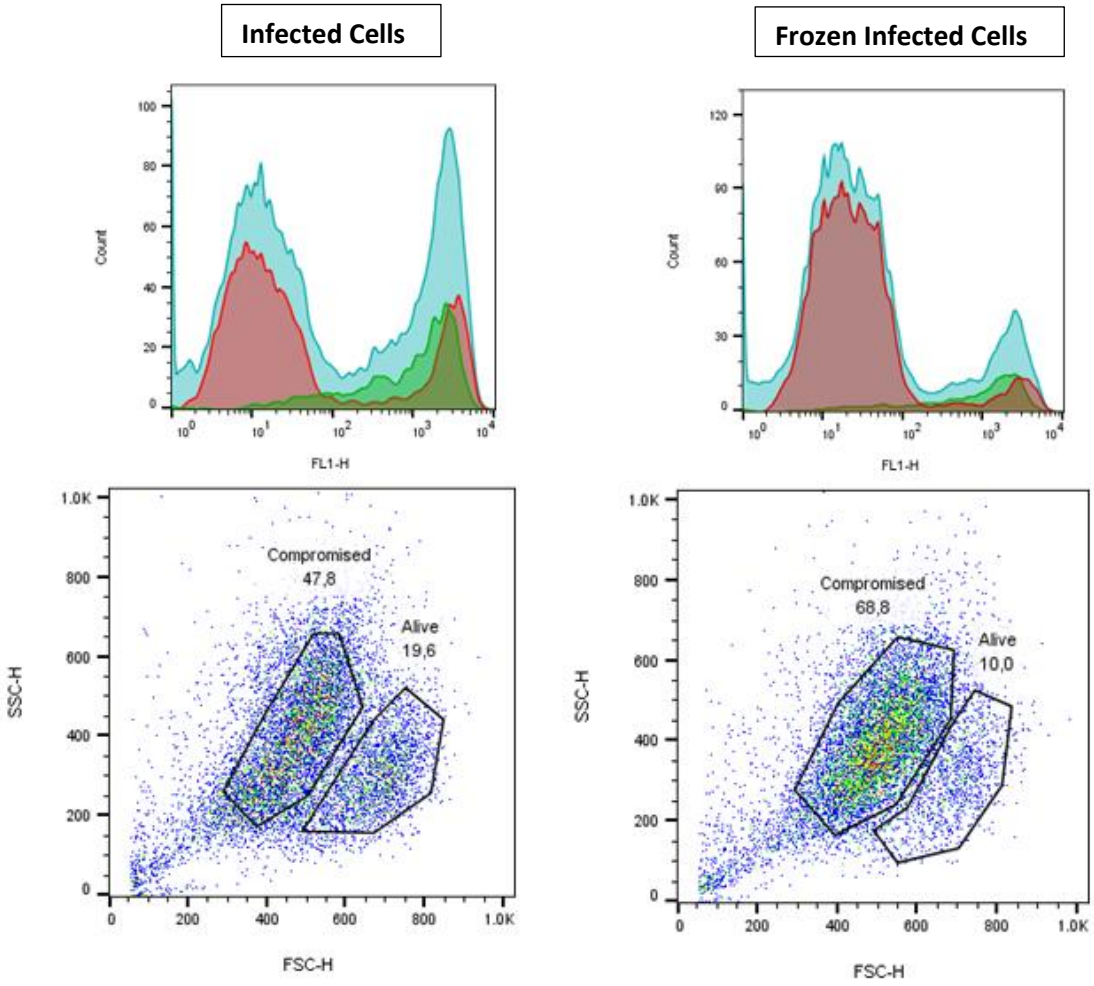

Figure E1: FL1 Distribution for Infected and Freeze-Lysed Infected Cells

Appendix F – Propidium Iodide Troubleshooting

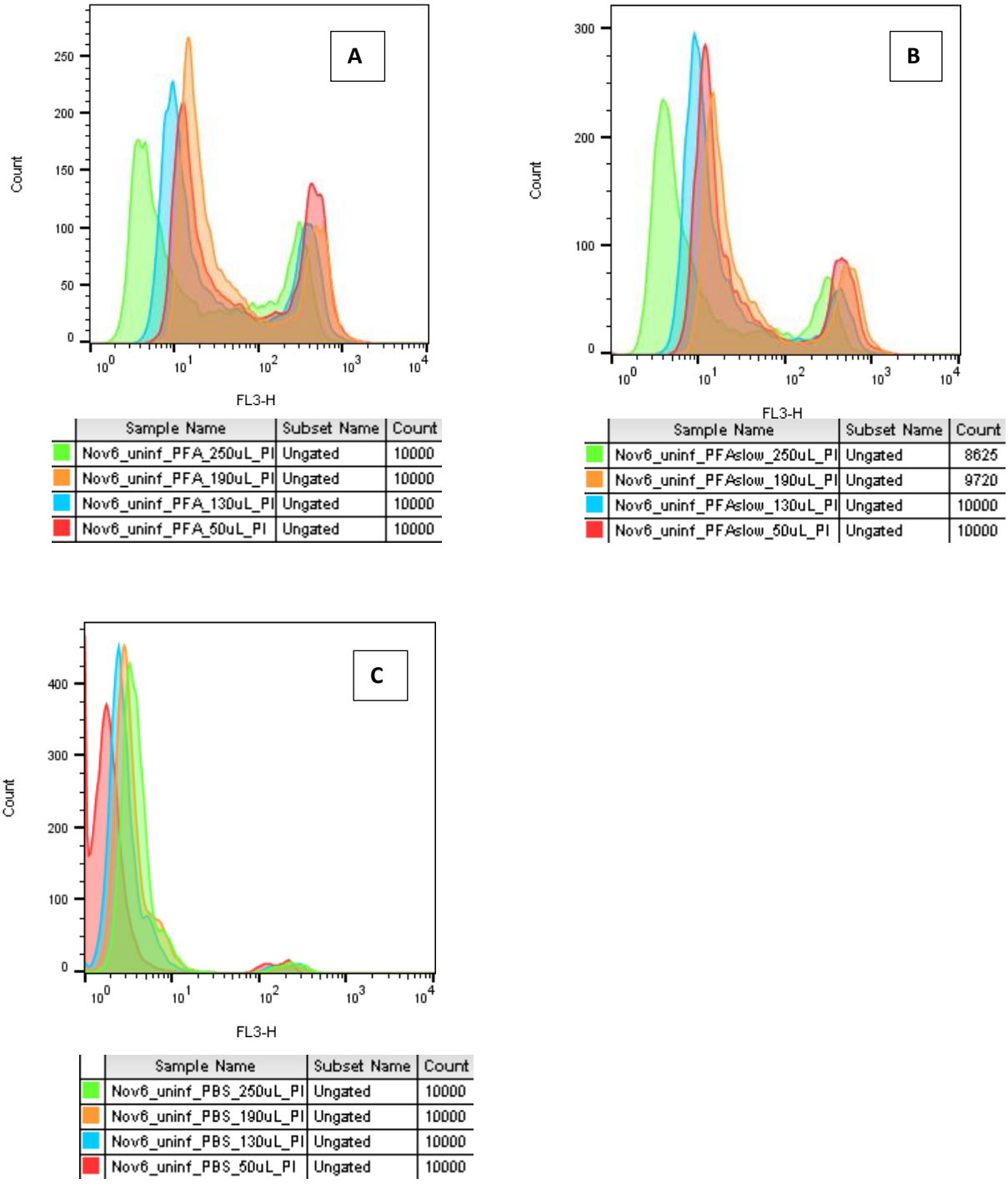

	Sample Name	Subset Name	Count
	Nov6_uninf_PFA_250uL_PI	Ungated	10000
	Nov6_uninf_PFA_190uL_PI	Ungated	10000
	Nov6_uninf_PFA_130uL_PI	Ungated	10000
	Nov6_uninf_PFA_50uL_PI	Ungated	10000

	Sample Name	Subset Name	Count
	Nov6_uninf_PFAslow_250uL_PI	Ungated	8625
	Nov6_uninf_PFAslow_190uL_PI	Ungated	9720
	Nov6_uninf_PFAslow_130uL_PI	Ungated	10000
	Nov6_uninf_PFAslow_50uL_PI	Ungated	10000

	Sample Name	Subset Name	Count
	Nov6_uninf_PBS_250uL_PI	Ungated	10000
	Nov6_uninf_PBS_190uL_PI	Ungated	10000
	Nov6_uninf_PBS_130uL_PI	Ungated	10000
	Nov6_uninf_PBS_50uL_PI	Ungated	10000

Figure F1: FL3 Histograms of samples testing concentration of PI addition. A) PI added to samples prepared as normal. B) PI added to samples prepared carefully, with cells resuspended slowly in PFA. C) PI added to samples without the PFA fixative step.

Appendix G – Overall productivity of population, and cell-density effect

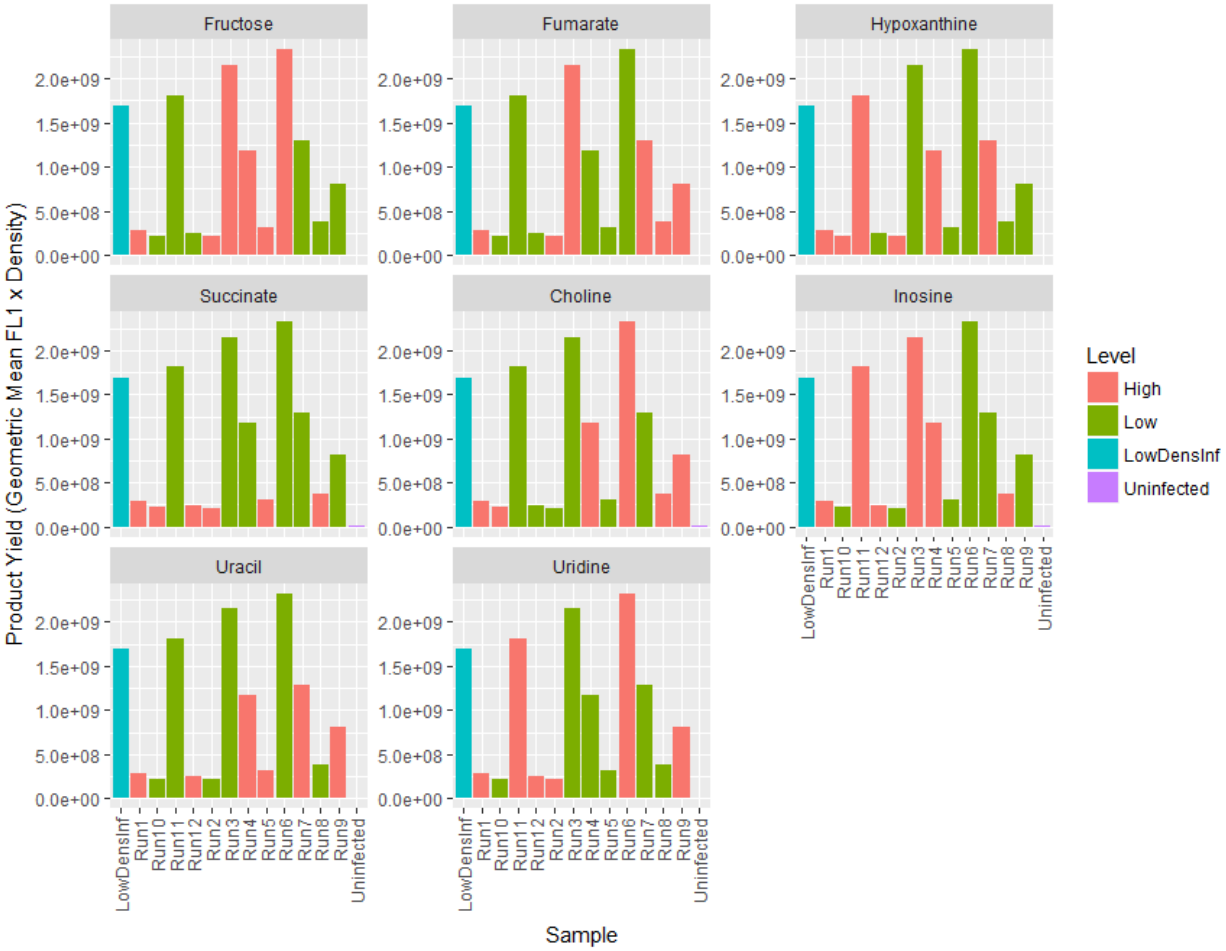

Just as an example of why (FL1) x (population) doesn't quite work out. This case makes it look like the cell-density effect is negligible, when in reality the literature suggests its effect is really quite drastic.

(Wilson et al., 2018), regarding comment on using (mean fluorescence) x (number of cells) to predict total fluorescence. Paper tried this with bacteria, and found that fluorescence plotted versus colony forming units/mL was non-linear (logarithmic). Within a 1 order of magnitude cell concentration window, it is *almost* linear, having an R-value of 0.93. So, not exactly linear, but not bad.